



SURFACE OXIDATION STUDY OF URANIUM DIOXIDE UNDER WET AND DRY
CONDITIONS

THESIS

Gary T. Brett, Major, USA

AFIT/GNE/ENP/05-01

DEPARTMENT OF THE AIR FORCE
AIR UNIVERSITY

AIR FORCE INSTITUTE OF TECHNOLOGY

Wright-Patterson Air Force Base, Ohio

APPROVED FOR PUBLIC RELEASE; DISTRIBUTION UNLIMITED

The views expressed in this thesis are those of the author and do not reflect the official policy or position of the United States Air Force, Department of Defense, or the United States Government.

AFIT/GNE/ENP/05-01

SURFACE OXIDATION STUDY OF URANIUM DIOXIDE UNDER WET AND DRY
CONDITIONS

THESIS

Presented to the Faculty

Department of Physics

Graduate School of Engineering and Management

Air Force Institute of Technology

Air University

Air Education and Training Command

In Partial Fulfillment of the Requirements for the
Degree of Master of Science (Nuclear Science)

Gary T. Brett, BA

Major, USA

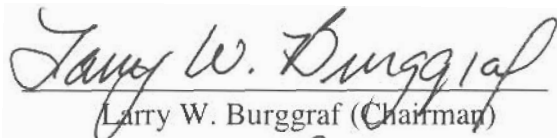
March 2005

APPROVED FOR PUBLIC RELEASE; DISTRIBUTION UNLIMITED

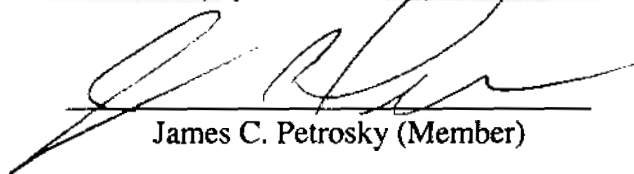
SURFACE OXIDATION STUDY OF URANIUM DIOXIDE UNDER WET AND DRY CONDITIONS

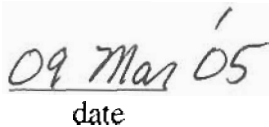
Gary T. Brett, BA
Major, USA

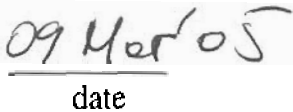
Approved:

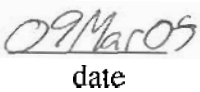

Larry W. Burggraf (Chairman)


Anthony I. Khaskelis (Member)


James C. Petrosky (Member)


date


date


date

Abstract

The surface oxidation of pressed uranium dioxide (UO_2) powder under controlled environmental conditions and the oxidation and reduction of pressed uranium trioxide (UO_3) powder are presented.

This is a continuing research project in the investigation of the oxidation of UO_2 powder using Photoluminescence (PL) Spectroscopy. UO_2 particles exposed to the ambient atmosphere will oxidize into a number of chemical complexes (specifically hydrates, hydroxides, and carbonates). During certain of these oxidation processes, the uranium ion can lose two of its electrons and change from uranous ($\text{U}^{\text{IV}+}$) to uranyl ($\text{U}^{\text{VI}+}$). This research is an attempt to monitor and control the oxidation of UO_2 as well as the development of the uranyl ion from the uranous ion and model their behavior under both wet and dry atmospheric conditions.

Two UO_2 samples were created by pressing UO_2 powder into a tungsten screen and were then subjected to a pure, dry oxygen environment and a wet oxygen environment at temperatures below $200\text{ }^\circ\text{C}$. The UO_2 oxidation was periodically monitored with *in-situ* PL spectroscopy. Using this analysis method, I was not able to successfully distinguish between the different uranium oxide compounds as they were formed under the different weathering conditions enforced at this temperature.

Acknowledgments

I would like to express my sincere appreciation to my faculty advisor, Doctor Larry W. Burggraf, and Doctors Khaskelis and Petrosky for their guidance and support throughout the course of this thesis effort. Their insight and experience was certainly appreciated. I would also like to thank my wife for her support and latitude, as well as her enduring patience, provided to me in during this endeavor.

Gary T. Brett

Table of Contents

	Page
Abstract	iv
Acknowledgments	v
List of Figures	ix
List of Tables	xiii
I. Introduction	1
Background	1
Problem Statement	2
Research Objectives	4
Scope	5
II. Theory	7
Chapter Overview	7
Uranium Oxides	7
Oxidation of Uranium Dioxide	8
Structures of the UO_3 Phases	11
Photoluminescence Spectroscopy	14
Chemical Kinetics	16
Oxidation Modeling	25
Brunauer-Emmett-Teller Surface Area Measurement Method	26
III. Methodology	32
Chapter Overview	32
Standards and Samples	33
Oxidation and Weathering Apparatus	35
Photoluminescence Spectroscopy	37
Surface Analysis	42
IV. Analysis and Results	45
Chapter Overview	45
Photoluminescence Measurements	45
UO_3 Oxidation and Reduction	54
Ambient Environmental Oxidation of UO_3	54
UO_3 Vacuum and Temperature Reduction, and Re-oxidation in dry Oxygen	65
UO_2 Dry Oxidation	76
UO_2 Wet Oxidation	85
Surface analysis	97

V. Conclusions and Recommendations	101
Chapter Overview.....	101
Conclusions of Research	101
Recommendations for Action.....	102
Future Research	102
Appendix A. Equipment	105
A-1. Glove Box	106
A-2. Hydraulic Press and Dies	107
A-3. Vacuum System.....	109
A-4. Water Vapor System	113
A-5. Hansen Cell	113
A-6. Photoluminescence Spectrometer	116
Appendix B. Glove Box Operation.....	119
Appendix C. Sample Preparation.....	125
C-1. Preparing the tungsten screen.....	126
C-2. Cleaning the Pressing Dies.....	127
C-3. Pressing Uranium Oxide Powders into Samples	128
Appendix D. Vacuum System Operation.....	132
D-1. Pumping Down the Vacuum System.	132
D-2. Oxygen Introduction into the Hansen Cell.....	135
Appendix E. Temperature Controller Operation	137
E-1. Initial Set-up of the Temperature Controller.	138
E-2. Operation of the Temperature Controller.	140
Appendix F. Sample Mounting.....	141
Appendix G. Procedures for Photoluminescence Measurements	145
G-1. Initial calibration	145
G-2. Sample runs	153
Appendix H. Procedures for Introducing Water Vapor	157
Appendix I. Procedures for Surface Analysis Measurements	160
I-1. Calibration	161
I-2. Analysis Set-up.....	162
I-3. Sample Analysis	163
I-4. File Names	164

Bibliography	165
--------------------	-----

List of Figures

	Page
1. Three step phase transition of UO_2 to UO_3	9
2. Diatomic Jablonski Diagram.....	15
3. Zero-Order Reaction.....	21
4. First-Order Reaction.....	23
5. Second-Order Reaction.....	24
6. Cross-section of a sample particle for surface analysis.....	29
7. Cross-section of particle at approximately 30% saturation.....	30
8. Cross-section of particle at 70% and 100% saturation.....	31
9. Lamp-corrected, front-face, PL emission scan of UO_3 sample T101L.....	47
10. Lamp-corrected, front-face PL emission scan of UO_3 sample T101K.....	48
11. Lamp-corrected, front-face PL emission scan of UO_3 sample T101L.....	48
12. PL emission scan comparison of UO_3 samples T101K and T101L.....	49
13. PL emission scan of UO_2 sample T200A scanned from 660 to 740 nm.....	50
14. PL emission scan of UO_2 sample T200A scanned from 470 to 660 nm.....	50
15. PL emission scan of UO_2 sample T200B scanned from 660 to 740 nm.....	51
16. PL emission scan of UO_2 sample T200B scanned from 470 to 660 nm.....	51
17. Unsmoothed, red PL emission spectra.....	53
18. Initial PL emission scan comparison of UO_2 to UO_3	54
19. PL scan of UO_3 sample T101K after exposure for 26 hours at 28° C.....	56
20. Base line integration between 470 and 600 nm for UO_3 sample T101K.....	57

21. Base line integration between 470 and 600 nm for UO ₃ sample T101K.....	57
22. Lamp-corrected, front-face PL emission scan of UO ₃ sample T101K.....	59
23. Base line integration between 470 and 600 nm for UO ₃ sample T101K.....	59
24. Base line integration between 470 and 600 nm for UO ₃ sample T101K.....	60
25. Base line integration between 470 and 600 nm for UO ₃ sample T101K.....	60
26. Lamp-corrected, front-face PL emission scan of UO ₃ sample T101K.....	62
27. Lamp-corrected, front-face PL emission scan of UO ₃ sample T101K.....	63
28. Lamp-corrected, front-face PL emission scan of UO ₃ sample T101L.....	66
29. Base line integration between 470 and 600 nm for UO ₃ sample T101L.....	66
30. Base line integration between 470 and 600 nm for UO ₃ sample T101L.....	67
31. Lamp-corrected, front-face PL emission scan of UO ₃ sample T101L.....	69
32. Lamp-corrected, front-face PL emission scan of UO ₃ sample T101L.....	70
33. Lamp-corrected, front-face PL emission scan of UO ₃ sample T101L.....	71
34. Base line integration between 470 and 600 nm for UO ₃ sample T101L.....	71
35. Base line integration between 470 and 600 nm for UO ₃ sample T101L.....	73
36. Base line integration between 470 and 600 nm for UO ₃ sample T101K.....	73
37. PL emission scan of UO ₂ sample T200A scanned from 660 to 740 nm.....	77
38. PL emission scan of UO ₂ sample T200A scanned from 470 to 660 nm.....	77
39. Initial and final PL emission scans of UO ₂ sample T200A.....	79
40. Initial and final PL emission scans of UO ₂ sample T200A.....	80
41. Base line integration between 660 nm and 740 nm for UO ₂ sample T200A.....	81
42. Base line integration between 680 and 710 nm for UO ₂ sample T200A.....	81

43. Base line integration between 470 and 660 nm for UO ₂ sample T200A.....	82
44. PL emission scan of UO ₂ sample T200B scanned from 660 to 740 nm.....	86
45. PL emission scan of UO ₂ sample T200B scanned from 470 to 660 nm.....	86
46. PL scan comparison of UO ₂ T200B scanned from 660 nm to 740 nm.....	88
47. PL scan comparison of UO ₂ T200B scanned from 470 nm to 660 nm.....	88
48. Base line integration, 660 nm and 740 nm for UO ₂ sample T200B.....	90
49. Peak area integration, 680 nm and 710 nm for UO ₂ sample T200B.....	90
50. Base line integration, 470 nm and 660 nm for UO ₂ sample T200B.....	92
51. Peak area integration, 496 nm and 524 nm for UO ₂ sample T200B.....	92
52. Final PL emission comparison of T200A and T200B.....	93
53. 25-Point BET comparison of all UO ₂ powder measurements.....	99
54. Plas-Labs TM 818-GB Glove Box.....	106
55. Carver® hydraulic press.....	108
56. Custom pressing dies for sample creation.....	109
57. Photo and drawing of lower vacuum system.....	110
58. Photo and drawing of upper vacuum system.....	110
59. Photo of the Varian the Multi-Gauge controller.....	112
60. System used to introduce water vapor.....	113
61. Hansen Cell schematic and Photo.....	115
62. A diagram of the FL3-22 setup.....	116
63. FL3-22 with Hansen Cell in T-Box Sample Compartment Module.....	118
64. NOVA-1000 High Speed Gas Sorption Analyzer.....	119

65. Glove box.....	121
66. Drawing of lower vacuum system.....	132
67. Drawing of upper vacuum system.....	133
68. Lake Shore temperature controller.....	138
69. Sample holder and spanner wrench.....	141
70. Hansen cell.....	142
71. DataMax Excitation Acquisition dialog box.....	146
72. Xenon lamp spectrum.....	148
73. DataMax Visual Setup screen.....	149
74. Grating calibration dialog box.....	149
75. DataMax Emission Acquisition dialog box.....	151
76. Water Raman spectrum.....	152
77. DataMax Phosphorimeter emission acquisition dialog screen.....	155
78. Apparatus for water vapor introduction.....	157
79. Schematic of NOVA-1000, High Speed Gas Sorption Analyzer.....	160

List of Tables

	Page
1. UO ₃ Properties Summary.....	13
2. Uranium oxide certificate information.....	33
3. List of prepared uranium oxide samples.....	35
4. Parameters for uranium oxide PL measurements.	46
5. UO ₃ sample T101K upon exposure to ambient atmospheric conditions	64
6. UO ₃ Reduction and Oxidation Data Table of Sample T101L	75
7. UO ₂ Dry Oxidation Data Table.....	83
8. UO ₂ Wet Oxidation Data Table	95
9. BET surface area results and comparison.....	98
10. BET volume and density results and comparison.....	100
11. Vacuum System Materials Listing.....	112
12. Hansen Cell Assembly Equipment Listing.....	114
13. FL3-22 Component Listing.....	117
14. Equipment and materials used in operation of glove box.....	122
15. Equipment and materials used for tungsten screen preparation.....	125
16. Equipment and materials used to clean the pressing dies.	127
17. Materials and equipment used to prepare uranium oxide samples.	128
18. Excitation calibration parameters.	147
19. Settings for emission monochromator calibration.	151
20. Photoluminescence experiment file names.....	154

21. Parameters for uranium oxide photoluminescence measurements.	156
---	-----

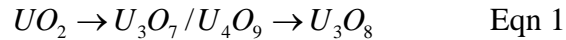
SURFACE OXIDATION STUDY OF URANIUM DIOXIDE UNDER WET AND DRY CONDITIONS

I. Introduction

Background

When exposed to normal atmospheric conditions, particulates of uranium dioxide (UO_2) powder can react and oxidize to form a multitude of surface complexes (i.e. hydroxides, hydrates, and carbonates). These various chemical processes change and erode the UO_2 particulates. The primary focus of this research is a measurement of the surface oxidation of pressed UO_2 powder under both wet and dry conditions in a pure oxygen environment utilizing *in-situ* photoluminescence (PL) spectroscopy.

UO_2 powder will oxidize and transition to U_3O_8 via the two-step reaction below [McEachern, 1998].



U_3O_8 can eventually oxidize and transition into uranium trioxide (UO_3) at high partial pressures of oxygen. The most important genuine stable phases of uranium oxides are UO_2 , U_4O_9 , U_3O_8 , and UO_3 . Numerous studies have been conducted to determine the transitions undergone by the UO_2 as it phase transitions to amorphous UO_3 , its equilibrium state in an oxidizing environment [Schueneman, 2001], [Rand, 1999], [Holmes, 1998], and [Hoekstra, 1961].

Initially, the surface oxidation of UO_2 to $\text{U}_3\text{O}_7/\text{U}_4\text{O}_9$ to U_3O_8 proceeds with a very low surface activation barrier until the UO_2 surface is covered with a layer of $\text{U}_3\text{O}_7/\text{U}_4\text{O}_9$. The continued oxidation then slows down to a rate defined by oxygen diffusion into the particle until covered by a layer of U_3O_8 . Depending on the oxygen composition of the ambient atmosphere, the layer of U_3O_8 may prevent the continued diffusion of O_2 and the formation of amorphous UO_3 . The outer layer of oxidized UO_2 could fall-off, or spall, as a function of the volumetric increase of the U_3O_8 molecule compared to the UO_2 molecule [McEachern, 1998]. This has the effect of increasing the surface area exposed to the oxidizing environment. The oxidation of UO_2 and formation of UO_3 under set environmental conditions proceed at a rate that remains to be determined. If a baseline for the partial pressure of oxygen in the ambient atmosphere, the moisture content of the air, and the initial condition of the oxides present in the reactor fuel at the time of release can be determined, then a method will exist for dating recovered UO_2 particles based on the condition of surface oxidation.

Problem Statement

UO_2 is the most common form of the uranium metal used as fuel in practically all Boiling-water Reactors (BWR), Pressure-tube Graphite Reactors (PTGR), Pressurized-water Reactors (PWR), Pressurized-heavy-water Reactors (PHWR), and, when mixed with plutonium dioxide (PuO_2), Liquid-metal Fast-breeder Reactors (LMFBR) in the world [Knief, 1992]. During its use, reprocessing, and disposal, small particulates of

UO₂ could escape into the atmosphere and be inhaled or ingested by personnel in the vicinity. As such, minute particles of UO₂ pose a serious health hazard.

In the form used by nuclear reactors, UO₂ is a stable ceramic that has a very high melting point, around 2800° C, which is required for use as a reactor fuel. The UO₂ particle adopts the fluorite structure, which has a face-centered cubic geometrical composition. The crystal ionic radius of uranium is 0.97 Å (Angstroms) for U^{IV+} and 0.80 Å for U^{VI+} whereas for oxygen, it is 1.32 Å for O²⁺ [CRC, 61st Edition]. The UO₂ molecule forms an interstitial alloy.

Uranium is generally, but not always, found in the form of some mineral, of which, close to 100 species have been identified. After mining, the uranium ore is then milled and chemically concentrated as U₃O₈ commonly referred to as “yellow cake”. The U₃O₈ is then further refined to remove additional impurities and converted to gaseous uranium hexafluoride (UF₆), which is then separated by its isotope’s atomic weight; one isotope has an atomic weight of 235.0439 and the other, which has an atomic weight of 238.0508 [CRC, 61st Edition] (²³⁵U versus ²³⁸U). The UF₆ is then chemically converted into UO₂ and enriched according to reactor type and destination. The fuel is then made into pellets and placed into zircalloy tubes and pressurized with an inert gas and welded shut to contain any fission fragments and to prevent any chemical reactions between the fuel and the reactor’s coolant and/or moderator. Sealing the tubes into fuel rods prevents oxidation of the fuel pellets. UO₂ does not react directly with water and therefore would not be affected by leakage of the cladding material in water-cooled reactors [Benedict, et al., 1981].

After the reactor fuel has been used, it is either stored at a designated radioactive materials storage area or it can be reprocessed for further use [Knief, 1992]. Since only about one-third of the useful uranium is actually used during its productive lifetime in a reactor [Benedict, et al., 1981], a significant amount of useful UO_2 will remain in the “spent” fuel rods. It is this remaining useful UO_2 that is reprocessed for further use as reactor fuel in some countries.

During the construction of nuclear reactor fuel rods, reprocessing of the fuel rods for continued use, or during short and/or long term storage, we have the possibility of minute particles of UO_2 to escape. UO_2 in particulate form is a hazardous, radioactive material capable of being inhaled. UO_2 is also able to enter into the human body through the eyes and pores of the skin via the fingers and subsequent touching. If we can accurately determine the oxidation of the UO_2 particles encountered, we can then date the time of suspected leakage and from this, the suspected site of contamination.

Research Objectives

The objective of this research was to use PL spectroscopy to measure rates of oxidation of UO_2 in dry and wet oxidation conditions. The experiment consisted of preparing and weathering UO_2 samples in dry environments consisting of 760 torr pure oxygen and taking periodic PL measurements to search for changes in the sample's surface conditions. These procedures were duplicated for additional samples under a pure oxygen pressure of 700 torr with approximately 60 torr of water vapor present.

Again, PL measurements were taken at periodic, regular intervals to search for changes in the surface conditions of our samples.

Scope

The results of this analysis of UO_2 powder provided both qualitative and quantitative data for the chemical processes involved in its oxidation and vacuum reduction in dry and wet oxygen environments. Additionally, new qualitative and quantitative data was obtained for the room temperature oxygen reintegration following vacuum reduction of prepared UO_3 samples.

This thesis is a continuation of several projects initiated at the Air Force Institute of Technology. In 1997, Captain Matt Zickafoose designed and built a weathering station for small quantities of UO_2 powders mixed with diamond dust contained in small glass capillaries [Zickafoose, 1997]. Doctor DeLyle Eastwood and Major Jeff Martin continued this project and published data for changes in the photoluminescence spectra of the UO_2 samples weathered under different conditions [Eastwood, et al., 1998]. In 1999, Lieutenant Dennis Rand used Raman Spectroscopy, Photoluminescence, and Diffuse Reflectance Infrared Fourier Transform Spectroscopy to characterize the spectra of UO_2 powder samples, weathered under wet conditions [Rand, 1999]. In 2000, Major Richard Schueneman used *in-situ* Photoluminescence, X-Ray Photoelectron Spectroscopy, and Secondary Ion Mass Spectroscopy to detect oxidation on the surface of UO_2 particles and analyze the changes of UO_3 particles as they are reduced in a high vacuum. In 2001, Major Schueneman, along with Doctors Khaskelis, Eastwood, van Ooij, and Burggraf,

published a newly discovered peak from a red photoluminescence emission spectra at 695 ± 2 nm for octahedral $\text{U}^{\text{VI}+}$ on dry oxidized UO_2 at temperatures below 200°C [Schueneman, et al., 2001].

This research continues the published data of Schueneman, et al. by utilizing *in-situ* PL Spectroscopy in an attempt to repeat and characterize this red PL emission spectrum as a function of time. I will expose pressed UO_2 powder to varying atmospheric conditions of oxygen, water vapor, and temperature and monitor the development of UO_3 on the particle surface as it occurs. The results of this analysis should give us additional insight into the development of the uranyl ion from the uranous ion and the time rate of oxidation of UO_2 particles under these environmental conditions.

Further research is planned for thermal desorption studies of UO_2 under ultra-high vacuum and varying atmospheric conditions of oxygen, carbon dioxide, temperature, and moisture content. Additionally, X-Ray Powder Diffraction Spectroscopy will be used to look at the surfaces of the individual particles in an attempt to measure the changes in surface composition that might otherwise be too minute to be accurately measured using PL spectroscopy.

II. Theory

Chapter Overview

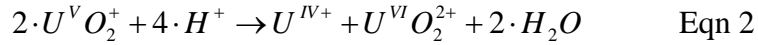
The purpose of this chapter is to provide the background theory of the uranium oxide samples utilized and the experimental procedures used. Additionally, it will cover previous experimental analysis and results and how they correlate to this research.

Uranium Oxides

Uranium dioxide (UO_2) is the most common composition of uranium when used as reactor fuel around the world. It is a stable ceramic that can be heated almost to its melting point, around 2760°C [Benedict, et al., 1981,], without serious mechanical deterioration and is brown in color. It does not react directly with water, so that it is not affected by leakage of cladding in water-cooled reactors [Benedict, et al., 1981]. UO_2 can also be produced by reduction of UO_3 by H_2 .

U_3O_8 occurs naturally as the mineral pitchblende and is black in color. It can be made by oxidizing UO_2 or by heating UO_3 . Uranium trioxide (UO_3) is a yellow-orange mineral and is stable in an oxygen environment.

Uranium ions may occur as trivalent $\text{U}^{\text{III}+}$, the tetravalent uranous ion $\text{U}^{\text{IV}+}$, pentavalent U^{VO_2+} , or the hexavalent uranyl ion $\text{U}^{\text{VI}+}\text{O}_2^{2+}$, in aqueous environments. However, $\text{U}^{\text{III}+}$ is unstable, reducing with H_2O to produce hydrogen, and U^{VO_2+} is also unstable, disproportionating into $\text{U}^{\text{IV}+}$ and $\text{U}^{\text{VI}+}\text{O}_2^{2+}$ [Benedict, et al., 1981] as shown in Equation 2 below:



Thus, only the uranous, U^{IV+} , and the uranyl ions, $U^{VI}O_2^{2+}$, are of practical interest for this research. These are stable aqueous ions and of these free ions, only uranyl (UO_2^{2+}) is known to exhibit phosphorescence.

Oxidation of Uranium Dioxide

The preponderance of nuclear chemistry is overshadowed by the ability of UO_2 to accommodate oxygen up to the stoichiometric composition UO_3 . Between these two extremes lies some twenty or so phases that have been reported to date [Allen and Holmes, 1987], many of which are polymorphic [Swissa, et al., 1990].

Uranium oxide can exist in many different stoichiometric and non-stoichiometric forms. Depending on the partial pressure of oxygen, it will be found in one of the following four stable forms: UO_2 , U_4O_9 , U_3O_8 , and UO_3 [Blackburn, et al. 1958]. UO_2 is the only stable oxide in a reducing environment and UO_3 is the only stable oxide in an oxidizing environment. The uranium atoms in the oxide compounds are ionic with valence states ranging from U^{IV+} through U^{VI+} . The U^{V+} ions are also metastable in oxides and generally disproportionate into U^{IV+} and U^{VI+} . Uranium dioxide has a face centered cubic crystal structure, is highly reactive, and oxidizes rapidly at low temperatures in air. The initial rate of oxidation is dependent upon the particle size [Anderson et al., 1952] and the partial pressure of oxygen [Hoekstra, et al., 1961].

Surface oxidation of UO_2 is non-stoichiometric and occurs in three defined steps

[McEachern et al., 1998] as in Figure 1 below.

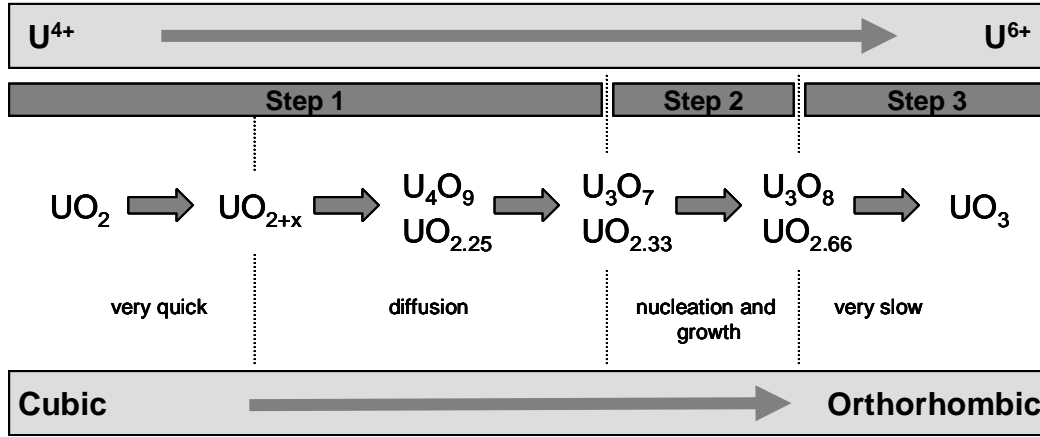


Figure 1. Three step phase transition of UO_2 to UO_3 .

As a stoichiometric oxide, UO_2 has a fluorite crystal structure in which the interstitial positions are centers of alternate cubes with oxygen atoms at the corners of each cube. This structure is oxygen deficient and the diffusion into the crystal lattice occurs rapidly upon exposure to an oxygen rich environment to form UO_{2+x} . In UO_{2+x} , the oxygen atoms are displaced to move from one to three interstitial oxygen positions and leave two vacancies resulting in a highly defected crystal structure. With sufficient energy and time, this defected structure will undergo a change in crystal structure to become either an intermediate oxide such as U_3O_8 or a stable oxide $\text{UO}_{3(s)}$.

Chemisorption of O_2 onto the UO_2 surface is the first oxidation step [McEachern et al., 1998], which results in the formation of UO_{2+x} on the particle surface. This step is complete when the surface of the UO_2 particle is covered with a layer of U_3O_7 (cubic crystal structure) or U_4O_9 (hexagonal crystal structure). The formation of U_4O_9 is

normally observed in irradiated fuel rod elements after exposure to an oxidizing environment. This may be a result of high levels of fission product impurities and changes to the crystal microstructure of the UO_2 particles from fission heating and lattice damage caused by neutron damage. The oxygen to uranium ratio is equal to 2.33 ($\text{UO}_{2.33}$) for unburned fuel and may be closer to 2.25 for irradiated fuel [Hoekstra, et al., 1961]. The oxidation rate to $\text{UO}_{2.33}$ appears to follow a parabolic curve for temperatures up to about 200 °C and there is little to no change in the rate for partial oxygen pressures from 160 torr to 760 torr [Blackburn, et al., 1958].

At any partial pressure of oxygen and temperature, U_3O_7 is unstable with respect to U_3O_8 and UO_3 [Taylor, et al., 1993] and the second step involves the continued oxidation to U_3O_8 . The oxidation rate for this step is much slower and has been shown to be a nucleation and growth controlled process [Blackburn, et al., 1958] due to crystal realignment [Taylor, et al., 1993] from a cubic crystal to a tetragonal crystal structure. Spallation of U_3O_8 from the surface of UO_2 fuel pellets has been observed in fuel rod elements as part of the crystal realignment and density change from 10.98-g/cm³ to 8.38-g/cm³ [McEachern et al., 1997].

The final step involves continued oxidation to $\text{UO}_{3(c)}$ and it will start before the second step is complete. From previous research we know that UO_3 exists in six different phases. Additionally, it has three different crystal structures cubic, hexagonal, or orthorhombic, where the alpha phase of UO_3 (denoted $\alpha\text{-UO}_3$) demonstrates a crystal structure similar to U_3O_8 . The $\alpha\text{-UO}_3$ may form a metastable oxidation product [Taylor, et al., 1993]. This final step involves changes in the crystal structure of the uranium

oxide. It is limited by the diffusion of oxygen through the layers of U_3O_8 covering the surface of the particle and diffusion of the uranium atoms in the crystal lattice [Taylor, et al., 1993]. The crystalline reorganization of the uranium-oxygen lattice is a kinetic barrier that must be overcome for any continued surface oxidation. Previous studies have found that UO_3 layers on the surface of UO_2 particles are amorphous (heavily defected) and will reach a thickness of 10 angstroms when the ambient temperature is in the range of 60 °C [Hoekstra, et al., 1961]. The end of oxidation on the surface of UO_2 particles and the completion of this step is the formation of gamma phase UO_3 ($\gamma\text{-UO}_3$) [McEachern, et al., 1997]. $\text{UO}_{3(c)}$ is the only known uranium oxide composed of uranium ions in the $\text{U}^{\text{VI}+}$ valence state and it is the only known form of uranium oxide with a phosphorescent emission.

Structures of the UO_3 Phases

Above the midpoint of the transition of UO_2 towards UO_3 (see Figure 1 above), the chemical transition is dominated by the stable orthorhombic structure of U_3O_8 [Allen et al., 1987]. In 1961, Hoekstra et al. presented evidence to show that the oxidized surface layer which forms on UO_2 at 25°C is amorphous UO_3 . As mentioned previously, the rate of formation of U_3O_8 from UO_2 is relatively quick with respect to the formation of UO_3 from U_3O_8 .

UO_3 can exist in multiple phases. In UO_3 phases the uranium atom may be coordinated to six, seven, or eight surrounding oxygen atoms, leading to at least six polymorphs [Allen et al., 1987] (see Table 1 below). One amorphous and six crystalline

modifications of UO_3 are known [Katz et al., 1986]. Only one of the UO_3 modifications, $\gamma\text{-UO}_3$, is stable at atmospheric pressure.

Air oxidation of UO_2 does not normally proceed beyond U_3O_8 [Taylor, et al., 1992]. We will attempt to overcome this barrier and accelerate the oxidation process in this research by using increased temperatures and high partial pressures of oxygen. The kinetic barrier to formation of $\gamma\text{-UO}_3$ from U_3O_8 is presumably related to the crystallographic re-organization involved: $\alpha\text{-U}_3\text{O}_8$ (the form stable up to $\sim 210^\circ\text{C}$) has a network structure of interlinked UO_7 polyhedra, whereas $\gamma\text{-UO}_3$ has been described as a uranyl uranate, $(\text{UO}^{2+}_2)(\text{UO}^{2-}_4)$ [Taylor, et al., 1992].

Another form of uranium trioxide, $\alpha\text{-UO}_3$, has a structure more closely related to U_3O_8 and might therefore be expected as a metastable oxidation product. Its formation from U_3O_8 would require the creation of vacancies in the uranium sub-lattice, however, and would therefore be constrained by the rate of uranium diffusion [Allen et al., 1987], which is very slow compared to oxygen diffusion (on the order of 8 orders of magnitude) [Kingery, et al., 1976].

The $\alpha\text{-UO}_3$ phase can be regarded as a uranium-deficient form of $\alpha\text{-U}_3\text{O}_8$. Introduction of oxygen into $\alpha\text{-U}_3\text{O}_8$ re-establishes an O:U ratio of 3:1. Approximately one-quarter of the oxygen atoms within the O-U-O-U-O chains are coordinated to one rather than two uranium atoms, shortening the U-O distance from 2.08 Å to 1.64 Å and giving the bond some ‘uranyl’ or double-bond character [Allen et al., 1987].

The structure of $\beta\text{-UO}_3$ contains three distinct types of uranium atom in a unit cell containing 10 uranium atoms: U(1) has a distorted octahedral coordination, U(2) and

U(3) each have six oxygen neighbors, and U(4) and U(5) are seven coordinate. Two of the oxygen atoms coordinated to U(2) and U(3) are considered to form a uranyl group, which has the usual O-U-O bond angle of 150° [Allen et al., 1987].

The structure of γ -UO₃ is pseudo-tetragonal with two distinct types of uranium atom: U(1) has a distorted octahedral coordination while U(2) has dodecahedral coordination. At room temperatures the shortest U-O distance is 1.796 Å which suggests the absence of pure uranyl bonds [Allen et al., 1987].

The δ -UO₃ phase adopts the ReO₃ structure in which UO₆ octahedral are linked together to form a framework of stoichiometric UO₃. All of the uranium atoms are in a regular octahedral coordination and there is no evidence for the presence of uranyl groups [Allen et al., 1987]. A summary of the UO₃ phase structure is presented in Table 1 below.

Table 1. UO₃ Properties Summary [Taylor, et al., 1992] [Allen et al., 1987].

Formula	Color	Symmetry	Lattice Parameters			Angle [deg]	Presence of 'Uranyl' Group
			a ₀	b ₀	c ₀		
A-UO ₃	Orange	Amorphous					Yes
α -UO ₃	Beige	Orthorhombic	6.84	43.45	4.157		Yes
β -UO ₃	Orange	Monoclinic	10.334	14.33	3.910	$\beta=99.03$	Yes
γ -UO ₃	Yellow	Orthorhombic	9.813	19.93	9.711		No
δ -UO ₃	Deep Red	Cubic	4.16	4.16	4.16		No
ϵ -UO ₃	Brick Red	Tri-clinic	4.002	3.841	4.165	$\alpha=98.10$ $\beta=90.20$ $\gamma=120.17$	No
η -UO ₃	Brown	Orthorhombic	7.511	5.466	5.224		No

Photoluminescence Spectroscopy

Upon striking matter, light can interact by either being absorbed or scattered; or it can be transmitted completely through the material without interacting at all. When a photon is absorbed, its energy is transferred to the atom or molecule in the absorption process. Every molecule's outer, or valence shell, electrons have a series of closely spaced energy levels. These electrons can go from a lower to a higher level by the absorption process if the quantum of light is of the same energy as the difference in energy between the two energy levels, as shown in Figure 2 below. The excited electrons will eventually fall back to its ground state and emit the difference in energy levels with a photon of equal energy. This is known as luminescence. Only a few molecules interact with light in this fashion and are raised to this higher excited state, thus being able to exhibit luminescence. UO_3 is currently the only known uranium oxide known to exhibit photoluminescence.

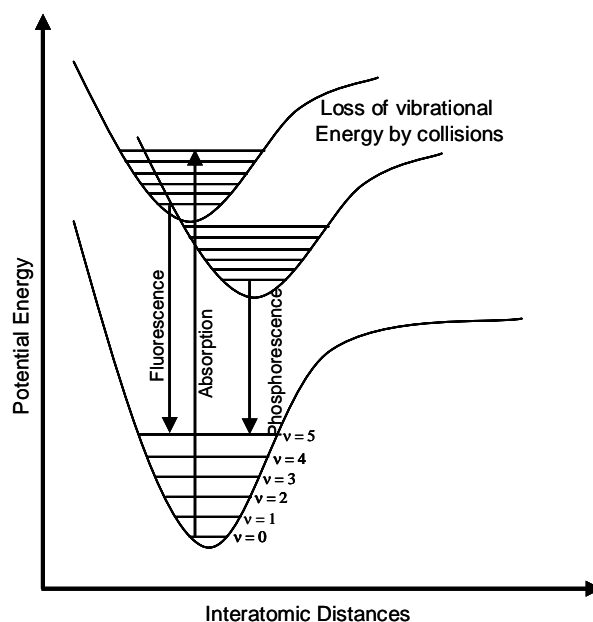


Figure 2. Diatomic Jablonski Diagram.

Between the main electronic states are the various vibrational levels of the molecule. These vibrational levels are where the excited electrons can lose energy in a molecule by collisions with other atoms in the molecule or other molecules.

Photoluminescence is a general term used to describe both phosphorescence and fluorescence and is a result of photon absorption and excitation of the outer shell electrons of a target material. Fluorescence is the term used to describe the short-lived luminescent properties of an element after being irradiated by energetic photons. The photon to outer shell electron energy transfer responsible for fluorescence does not result in a change of electron spin; therefore fluorescence is a very short-lived phenomenon. However, when there is a change in the electron's spin, the emitted radiation can endure for seconds. This phosphorescent effect is an increase of several orders of magnitude

over fluorescence. Generally, the wavelength of either fluorescence or phosphorescence emission has a longer wavelength than the incident radiation that caused the electronic excitation.

For this research, we will use a Fluorolog-3 with Phosphorimeter attachment manufactured by Jon Yvon (see Appendix A for a complete equipment description) to evaluate our UO_2 samples as they transition towards UO_3 for phosphorescence as our sample is exposed to various environmental conditions of oxygen, temperature, and humidity. Of the three photoluminescent modes available; emission, lifetime, and excitation, only photoluminescent emission scans will be conducted.

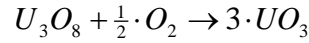
Chemical Kinetics

Chemical reactions convert substances with well-defined properties into materials with different properties. This research is an investigation into the chemical change of UO_2 towards UO_3 under different environmental conditions and the change of UO_3 towards U_3O_8 as a function of temperature and reduced partial pressures of oxygen. Chemical kinetics is concerned with the speed or rate in which chemical reactions occur [Brown et al., 1997]. The rates of these reactions can be affected by several factors:

- 1- The concentration of the reactants. The concentration of uranium oxide will remain fixed while the partial pressure of oxygen will be allowed to vary.

- 2- The temperature at which the reaction occurs. The rates of chemical reactions generally increase as temperature increases. These experiments will be conducted at elevated temperatures in an attempt to accelerate the chemical reactions.
- 3- The surface area of solid. The surface area will be made as large as possible using the techniques for sample preparation as discussed in Appendix C.

For illustration, the discussion of chemical reactions and kinetics will revolve around the reaction shown below, which is shown as Step-3 in the 3-Step chemical reaction of UO_2 towards UO_3 as shown in Figure 1:



The reaction rate is a measure of how quickly UO_3 is formed from the chemical reaction of U_3O_8 with oxygen and are usually measured as molarity per time. I will base the concentration increase or decrease of UO_3 on the integrated intensity of the PL emission spectrum taken during this research. I will use the assumption that the concentration of UO_3 is proportional to the value of the integrated PL emission spectra.

The rate of increase of UO_3 and the rate of decrease in U_3O_8 and O_2 , where the square brackets denote concentration, can be shown by:

$$\text{Increasing rate of } UO_3 \text{ formation} = \frac{d[UO_3]}{dt}$$

$$\text{Decreasing rate of } U_3O_8 \text{ formation} = \frac{-d[U_3O_8]}{dt}$$

$$\text{Decreasing rate of } O_2 \text{ formation} = \frac{-d[O_2]}{dt}$$

The conservation of mass, provided that all reactions are accounted for, tells us that the loss of U_3O_8 and O_2 must be equal to the increase in UO_3 . Additionally, the rate at which UO_3 is formed is controlled by the rate of loss of U_3O_8 and O_2 . From the reaction above, this can be described as:

$$\text{Rate} = \frac{1}{3} \cdot \frac{d[UO_3]}{dt} = \frac{-2}{1} \cdot \frac{d[O_2]}{dt} = \frac{-d[U_3O_8]}{dt}$$

Reaction rates generally diminish as the concentrations of reactants diminish. Likewise, rates generally increase as reactant concentrations increase [Brown et al., 1997]. The rate law, which shows how the rate of reaction depends on the concentration of reactants, is shown below. The constant k is the rate constant of the reaction.

$$\text{Rate} = k \cdot [U_3O_8][O_2]$$

The rate laws for most reactions have the general for:

$$\text{Rate} = k[\text{reactant 1}]^m[\text{reactant 2}]^n \dots$$

The exponents' m and n above are called reaction orders, and their sum is the overall reaction order. The reaction order does not necessarily correspond to the coefficients in the balanced equation. The values of the exponents are determined experimentally.

The rate of a reaction usually depends on concentration; the rate constant does not. Additionally, the rate constant and reaction rate are affected by temperature.

A rate law demonstrates how the rate of a reaction changes at a particular temperature as the concentrations of the reactants change. Rate laws can be converted into equations that tell us what the concentrations of the reactants or products are at any time during the course of a reaction.

Zero-Order Reactions

A zero-order reaction is one that occurs at a constant rate. This rate is independent of the concentration of the reactants. A zero-order reaction rate displayed graphically would be a straight line with no slope and is shown in Figure 3 below:

$$Rate = k \cdot [U_3O_8]^0 [O_2]^0 \quad \text{or} \quad Rate = k$$

The rate, or time rate of change of the reactant (using U_3O_8 as an example), is solved using differential equations. The zero-order rate law for the reaction above is written as:

$$-\frac{d[U_3O_8]}{dt} = k$$

Which, on integration of both sides, gives:

$$-[U_3O_8] = k \cdot t + \text{constant}$$

At the start of the reaction, when $t = 0$, $[U_3O_8]$ is the original concentration of reactant U_3O_8 , $[U_3O_8]_0$; the constant of integration must then be $-[U_3O_8]$. This gives the integrated rate law for a zero-order reaction.

$$[U_3O_8]_0 - [U_3O_8] = k \cdot t \quad \text{or} \quad [U_3O_8] = -k \cdot t + [U_3O_8]_0 \quad \text{Eqn 3}$$

The form of the integrated rate law shows that a zero-order reaction will give a straight-line plot if measured values of reactant concentration, $[U_3O_8]$, are plotted as a function of time. The slope of the line will be the apparent zero-order rate constant.

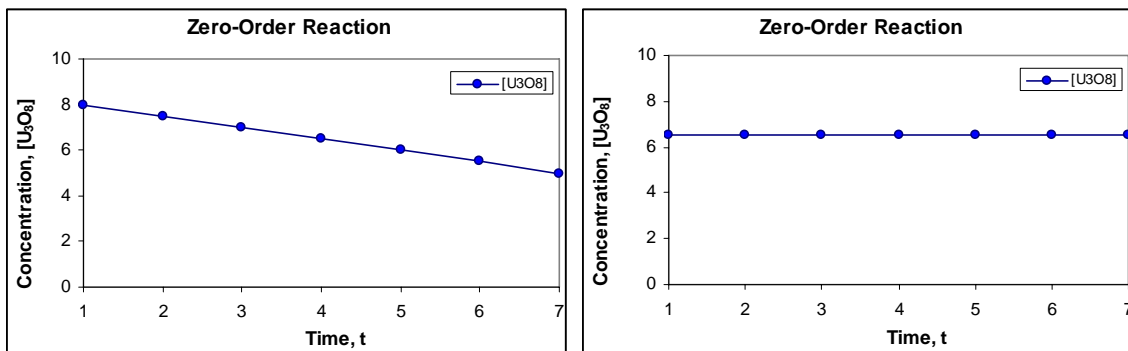


Figure 3. The figure on the left shows graphically a zero-order reaction whose rate changes over time and $k \neq 1$. The figure on the right also demonstrates a zero-order reaction whose rate is constant over time and $k = 1$. For zero-order reactions, the change is independent of the concentrations of the reactants.

A zero-order rate law for a chemical reaction means that the rate of the reaction is independent of the concentration of any reactant. A zero-order rate law can only be observed if the actual reactants cannot change as the reaction proceeds.

First-Order Reactions

A first order reaction is one whose rate depends on the concentration of a single reactant raised to the first power [Brown et al., 1997] or whose reactants exponents, when summed, equal one. For example, a first order reaction is described by:

$$Rate = k \cdot [U_3O_8][O_2]$$

However, if the concentration of one of the reactants is very large in comparison to the other, it becomes, in effect, constant. We will use the fact that the concentration of U₃O₈ is large when compared to O₂ for description of this rate kinetic. If the exponent

for the concentration of the other reactant is one, the rate law for the reaction is still first-order for both reactants.

$$Rate = k \cdot [O_2]$$

In this case, the rate law is solely a function of the concentration, or partial pressure, of oxygen, yet the reaction is still first-order for both $[U_3O_8]$ and $[O_2]$. Relating the initial concentration of $[O_2]_0$, to its concentration at any other time t , $[O_2]_t$:

$$\ln[O_2]_t - \ln[O_2]_0 = -k \cdot t \quad \text{or} \quad \ln \left[\frac{[O_2]_t}{[O_2]_0} \right] = -k \cdot t$$

Rearranging terms:

$$\ln[O_2]_t = -k \cdot t + \ln[O_2]_0 \quad \text{Eqn 4}$$

This equation has the form of the general equation for a straight line, $y = mx + b$, in which m is the slope and b is the y-intercept of the line. Thus, for a first order reaction, a graph of $\ln[O_2]_t$ versus time gives a straight line with a slope of $-k$ and a y-intercept of $\ln[O_2]_0$.

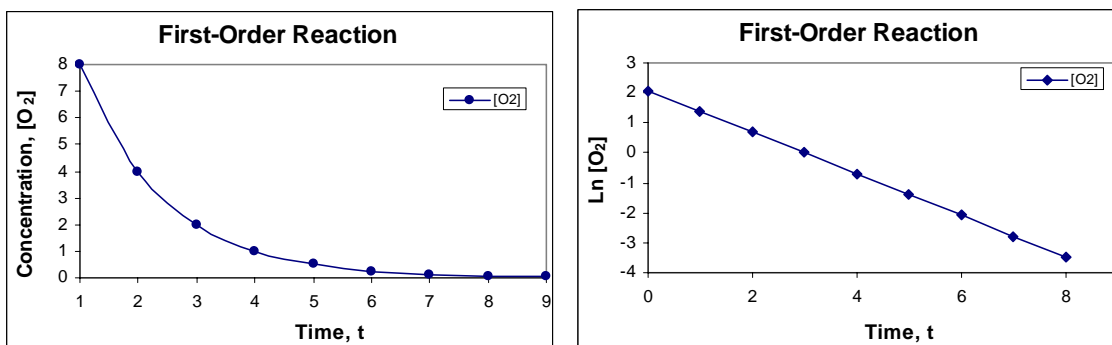


Figure 4. The figure on the left shows graphically a first-order reaction. The figure on the right demonstrates that when the natural logarithm of the concentration is plotted as a function of time, the plot is linear.

The linearity of the logarithmic plot establishes that the reaction is first-order.

Since the reaction of U_3O_8 with O_2 to UO_3 proceeds in both the forward and backwards direction, the equation can also be written for the vacuum reduction of UO_3 to U_3O_8 and O_2 as:

$$\ln[\text{UO}_3]_t = -k \cdot t + \ln[\text{UO}_3]_0$$

This is easier to see since the PL emission spectroscopy will show the increase or decrease of the UO_3 present as the reaction occurs in the forward or reverse direction.

Second-Order Reactions

A second order reaction is one whose rate depends on the reactant concentration raised to the second power or on the concentrations of two different reactants, each raised to the first power [Brown et al., 1997]. For a reaction that is second order, the rate law is given by:

$$\text{Rate} = k[U_3O_8][O_2] \quad \text{or, for example} \quad \text{Rate} = k[U_3O_8]^0[O_2]^2$$

Again, integrating both sides, this rate law is given by:

$$\frac{1}{[O_2]_t} = k \cdot t + \frac{1}{[O_2]_0}$$

This equation, like the one for first-order reactions, has the form of a straight line. If the reaction is second order, a plot of $1/[O_2]_t$ versus t will yield a straight line with a slope equal to k and a y-intercept of $1/[O_2]_0$.

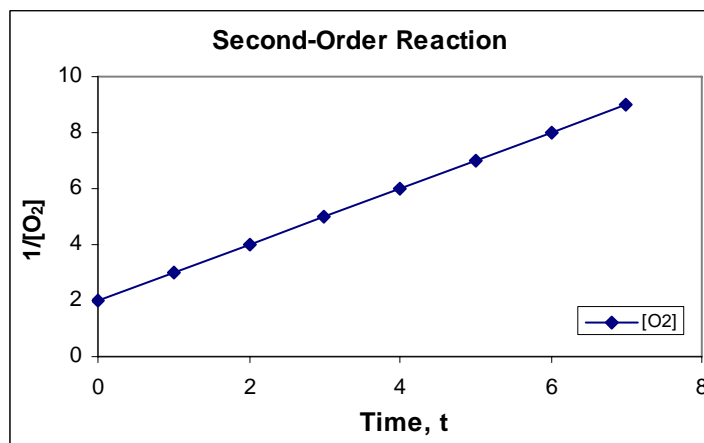


Figure 5. This figure demonstrates a second-order reaction plotted as the inverse of the concentration as a function of time. When plotted, the curve is linear.

Third-Order Reactions

Likewise, third order reactions are treated similarly. Rate laws of order higher than three in any one reactant are unknown, and third-order reactions are very rare. Rate laws of zero are also uncommon. Most chemical reactions follow either first-order or second-order rate laws [<http://www.psigate.ac.uk>, 2005].

Oxidation Modeling

Depending on the conditions involved in the chemical transition of UO_2 towards UO_3 , three relatively simple models have been used [Schueneman et al., 2003] to describe the rate limiting growth or reduction of an oxidized layer covering a UO_2 particle: first-order kinetics model, Fick's Law of diffusion, and a Cabrera-Mott diffusion model. As mentioned previously, zero-order reactions are rare but not unknown. We will see from the data collected in Chapter 4 that the ambient air oxidation and vacuum reduction of UO_3 can accurately be modeled using a zero-order kinetics model.

The kinetics of zero and first-order reactions are covered earlier in this chapter. If the chemical transition rate is in fact diffusion controlled, Fick's Law can be used to model the reaction kinetics, using appropriate boundary conditions. Fick's Law applied to an infinite slab surface describes the average oxidation thickness, x_{avg} , as a function of time, t , in accordance with the proportionality equation below:

$$x_{avg} \propto \sqrt{D \cdot t} \quad \text{Eqn 5}$$

Where D is the diffusion coefficient. If the diffusion of oxygen into the UO_2 particle is promoted by Coulombic gradients, a Cabrera-Mott model can be used. A Cabrera-Mott model is shown in the equation below:

$$\frac{1}{x} \cong \frac{1}{x_0} - k \cdot \ln(t) \quad \text{Eqn 6}$$

In the event diffusion is controlled by Coulombic gradients, impurities can also affect the charge distribution at the particles boundary, which will in turn, significantly enhance ion mobility. Diffusion, however, can be accelerated by several orders of magnitude for the cations present in excess. The surface-charge promoted cation mobility produce an inverse logarithmic oxide growth rate as shown in the equation above. The field-strengthened ionic transport initially enhances oxidation, but rapidly attenuates with oxide thickness.

Zero and first-order reaction kinetics as well as diffusion kinetics described by Fick's Law are the primary mathematical models used in this research.

Brunauer-Emmett-Teller Surface Area Measurement Method

As discussed in the previous section, the rates of reaction can be affected by the surface area of the reactants. As such, we have two sources of UO_2 available for this research. To determine the optimal source for oxidation, surface area measurements were taken. The surface area measurements taken and used in this research were obtained

using a NOVA (No Void Analysis) 1000, Gas Sorption Analyzer, Version 3.10 manufactured by the Quantachrome Corporation. The NOVA-1000 uses nitrogen gas (N₂) as the adsorbate and liquid nitrogen as the required coolant.

The following mathematical derivation and methodology were developed by the Quantachrome Corporation.

The Brunauer-Emmett-Teller (BET) method is one of the most widely used procedures for the determination of the surface area of solid materials and involves the use of the BET equation below [NOVA-1000, 1994].

$$\frac{1}{W((P_0/P)-1)} = \frac{1}{W_m C} + \frac{C-1}{W_m C} \left(\frac{P}{P_0} \right) \quad \text{Eqn 7}$$

Where W is the weight of gas adsorbed at a relative pressure P/P_o and W_m is the weight of the adsorbate constituting a monolayer of surface coverage. The term C is the BET constant and it is related to the energy of adsorption in the first adsorbed layer and consequently its value is an indication of the magnitude of the adsorbent/adsorbate interactions.

This research was conducted using the multipoint BET method. When using this method, the BET equation requires a linear plot of $1/(W (P_o/P) - 1)$ vs. P/P_o , which for this research, as well as most other solids, using N₂ as our adsorbate is restricted to a limited region of the adsorption isotherm, usually in the P/P_o range of 0.05 to 0.35.

The standard multipoint BET procedure requires a minimum of three points in the appropriate relative pressure range. The weight of a monolayer of adsorbate W_m can then be obtained from the slope s and intercept i of the BET plot. From the BET equation above:

$$s = \frac{C-1}{W_m C} \quad \text{And} \quad i = \frac{1}{W_m C}$$

Thus, the weight of a monolayer W_m can be obtained by combining the equations for the slope and the intercept as follows:

$$W_m = \frac{1}{s + i}$$

The second step in the application of the BET method is the calculation of the surface area. This requires knowledge of the molecular cross-sectional area A_{cs} of the adsorbate molecule. The total surface area S_t of the sample can be expressed as:

$$S_t = \frac{W_m N_A \cdot A_{cs}}{M} \quad \text{Eqn 8}$$

Where N_A is Avogadro's number (6.022×10^{23} molecules/mole) and M is the molecular weight of the adsorbate. N_2 is the most widely used gas for surface area determinations since it exhibits intermediate values for the C constant (50-250) on most solid surfaces, precluding either localized adsorption or behavior as a two-dimensional gas. Since it has already been established the C constant influences the value of the cross-sectional area of the adsorbate, the acceptable range of C constants for N_2 makes it possible to calculate its cross-sectional area from its bulk liquid properties. For the hexagonal close-packed N_2

monolayer at 77K, the cross-sectional area A_{cs} for N_2 is 16.2 Angstroms² [NOVA-1000, 1994].

The specific surface area S of the solid can be calculated from the total surface area S_t and the sample weight w , according to the following equation [NOVA-1000, 1994]:

$$S = \frac{S_t}{w} \quad \text{Eqn 9}$$

The following descriptions of the adsorption and particle size measurements were provided by the Quantachrome Website [www.Quantachrome.com, 2004].

Before performing gas sorption experiments, solid surfaces must be freed from contaminants such as water and oils. Surface cleaning, or degassing, is most often carried out by placing a sample of the solid in a glass cell and heating it under vacuum or flowing gas. Figure 6 below illustrates how a solid particle containing cracks and pores of different sizes and shapes may look after its pretreatment.

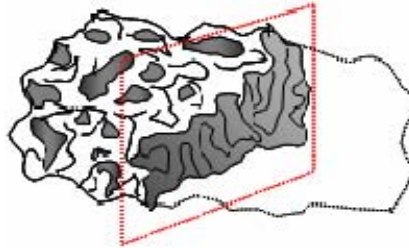


Figure 6. Cross-section of a sample particle for surface analysis [www.Quantachrome.com, 2004].

Once clean, the sample is brought to a constant temperature by means of an external bath. Then, small amounts of a gas (the N₂ adsorbate) are admitted in steps into the evacuated sample chamber. Figure 7 below demonstrates the cross-section of the sample particle with a monolayer of adsorbed molecules at approximately 30% saturation.

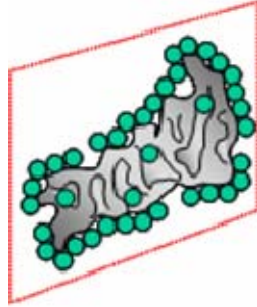


Figure 7. Cross-section of particle, approximately 30% saturation [www.Quantachrome.com, 2004].

Gas molecules that stick to the surface of the solid (adsorbent) are said to be adsorbed and tend to form a thin layer that covers the entire adsorbent surface. Based on the BET theory, one can estimate the number of molecules required to cover the adsorbent surface with a monolayer of adsorbed molecules, N_m .

Multiplying N_m by the cross-sectional area A_{cs} of an adsorbate molecule yields the sample's surface area.

$$S = N_m \cdot A_{cs} \quad \text{Eqn 10}$$

Continued addition of gas molecules beyond monolayer formation leads to the gradual stacking of multiple layers (see Figure 8 below). The first figure is the multilayer capillary condensation phase at approximately 70% saturation and the second is total pore volume filling at approximately 100% saturation.

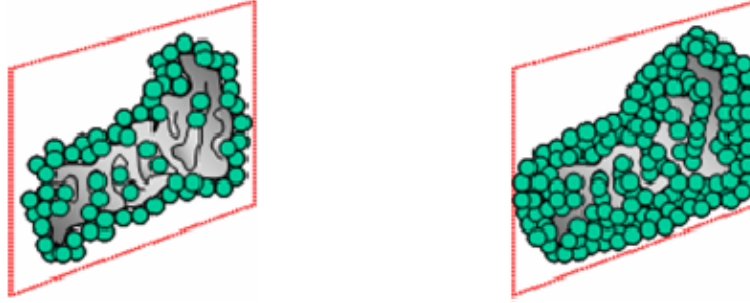


Figure 8. Cross-section of particle at 70% and 100% saturation [www.Quantachrome.com, 2004].

Monolayer formation occurs in parallel to capillary condensation. The latter process is adequately described by the Kelvin equation below [applet-magic.com, 2004], which quantifies the proportionality between residual (or equilibrium) gas pressure and the size of capillaries r capable of condensing gas within them.

$$\frac{P_v}{P_w} = \exp\left[\frac{-2\sigma}{r\rho_w R_v T}\right] \quad \text{Eqn 11}$$

Where P_v and P_w are the pressure of the water vapor and the water pressure, respectively, and σ is the surface tension of the water. The density of the water is ρ_w and R_v and T are the water vapor gas constant and temperature [applet-magic.com, 2004].

III. Methodology

Chapter Overview

This chapter provides a detailed overview of the experimental procedures used to conduct this research. The Appendices A through I provide detailed descriptions of the equipment operation and procedures used that will be necessary to follow to duplicate this work.

The goal of this experiment was to collect quantitative measures of rate for the surface oxidation of UO_2 , from known values of partial pressure of oxygen, water vapor, and temperature, to time and, from the raw data, develop a mathematical oxidation rate model. To this end, two samples of UO_2 were weathered in strictly controlled environmental conditions. The samples were periodically analyzed using PL spectroscopy as the primary means of investigation. This analysis enabled us to track changes in the UO_2 particles' surface oxidation. From this we were able to monitor and track the time rate of change of the particle surface and the development of the uranyl ion as it formed on the sample.

Particulate samples of UO_2 and UO_3 were cold pressed into tungsten screens. Previous research by Major Richard Schueneman determined the optimal angle for the front face of the Hansen Cell and the sample chamber of the Jobin-Yvon Spex FL3-22 Spectrofluorometer (Fluorolog-3) to maximize the fluorescent intensity of the samples. This angle is inscribed on the Hansen Cell where the two halves are connected and was used for all measurements. PL measurements and analysis of UO_3 was conducted before

UO₂. The PL emission spectra collected from the pressed UO₃ powder was used as a benchmark for comparison of the oxidized UO₂ samples.

Standards and Samples

The Department of Energy's New Brunswick Laboratory in Argonne, Illinois, provided the UO₂ powder used in this research. It was produced by Mallinckrodt Chemical Works, St. Louis, Missouri. There are no known dates of manufacture records available. CeracTM Inc provided the UO₃ powder used in this research. The UO₃ powder came with a certificate of analysis listing the typical purity of the powder, spectrographic analysis for elemental impurities, and crystal structures based on x-ray diffraction measurements (see Table 2 below). The UO₃ powder from Cerac was enclosed in a zip-lock bag that was contained in a metal can. The metal can was double wrapped in plastic, zip-lock bags. The UO₂ powder from the Department of Energy (DOE) was contained within a glass jar inside a zip-lock bag. This was all placed within a cardboard can. Likewise, it was double wrapped in zip-lock bags after opening. Uranium oxide powder was only removed from its respective storage containers within a glove box under a nitrogen environment.

Table 2. Uranium oxide certificate information.

Oxide	Lot Number	Crystal Structure	Mesh Size	Purity	Impurities
UO ₂	V-4152SM65	Face-Centered Cubic	Unk	~ 88.1 %	Unk
UO ₃	X22886	Orthorhombic (γ)	Unk	99.8 %	9 elements

The UO_3 powder from Cerac was last used in 2001. All handling of the UO_3 powder was done in a glove box that had been under an extended nitrogen purge [Schueneman, 2001]. After the derivative samples were extracted, the UO_3 powder was sealed as described above. As we will see later in Chapter IV, these handling procedures resulted in a lower partial pressure of oxygen for the UO_3 powder for a period in excess of three years and resulted in a reduction of the UO_3 towards U_3O_8 .

The UO_2 powder from DOE had no certified analysis available. It was never issued a New Brunswick Laboratories Certification for Research Material. Additionally, no certified uranium assay was determined for this sample. A typical expected uranium assay and isotopic values for a UO_2 sample would consist of approximately 88.1% by weight ^{238}U and a content of 0.71% by weight content of ^{235}U , with a relative atomic mass of approximately 283.03.

Two sets of benchmark UO_3 samples were prepared and two UO_2 samples were prepared (see Table 3 below) from the uranium oxide powders provided. All samples were carefully prepared and stored in a glove box that had been nitrogen purged for a period in excess of two weeks. This allowed for a layer of nitrogen to form on the prepared samples and reduce the oxidation of our samples.

Before any measurements were taken of these samples, the weathering system was baked at 150 °C for 48 hours under reduced pressure of approximately 10^{-4} torr to reduce the presence of oxygen, water vapor, and/or other complexes. The prepared uranium oxide samples were then placed inside the Hansen Cell and placed in the weathering system. The samples were introduced to this clean, low-pressure

environment and allowed to stabilize before any measurements were taken. This allowed for the removal of the nitrogen environment the samples were prepared in.

Table 3. List of prepared uranium oxide samples.

Standard	Derivative Sample ID	Oxide Amount	Molar Amount
UO ₃ (Cerac TM)	T101K	0.08 g [UO ₃]	2.80×10 ⁻⁴ [mols UO ₃]
UO ₃ (Cerac TM)	T101L	0.05 g [UO ₃]	1.75×10 ⁻⁴ [mols UO ₃]
UO ₂ (DOE)	T200A	0.06 g [UO ₂]	2.22×10 ⁻⁴ [mols UO ₂]
UO ₂ (DOE)	T200B	0.08 g [UO ₂]	2.96×10 ⁻⁴ [mols UO ₂]

Of particular interest is that when UO₂ is exposed to an oxygen rich environment, it rapidly oxidizes to an oxygen excess structure UO_{2+x}, where x is approximately 0.60 for dry oxygen and between 0.12 and 0.20 for moist oxygen [Colmenares, 1984]. This oxidation rate has been reported in the time frame of minutes to hours. During the preparation of the UO₂ powder, care was taken to maintain a strict non-oxidizing, nitrogen environment. In the course of the experimental analysis we exposed the UO₂ powder to both wet and dry environmental conditions and analyzed them over the period of days to weeks, therefore our UO₂ sample were actually UO_{2+x}. For convenience, we will refer to UO_{2+x} as simply UO₂ unless any confusion would result. If necessary for clarification, the more precise UO_{2+x} will be used.

Oxidation and Weathering Apparatus

A vacuum system, temperature controlled Hansen Cell, and a water vapor introduction system were used to oxide the pressed UO₂ and UO₃ powder samples in a controlled and monitored environment.

The vacuum system used in this research was designed and constructed by MAJ Richard Schueneman. It consisted of a series of two vacuum pumps connected to a manifold of stainless steel tubes and fittings and was capable of attaining and sustaining a pressure of 10^{-5} torr. The entire vacuum system was layered with heat strips capable of sustaining 200 °C and covered with heavy-duty aluminum foil for insulation. The heat strips were used in conjunction with the vacuum system to remove down to one or two monolayers of foreign molecules (ie. water, oxygen, carbon dioxide, etc.) from the surface of the sample and the Hansen Cell. The establishment of a clean, high vacuum environment provided a reference point for the introduction of Grade 5.0 oxygen, and later distilled water vapor and oxygen, onto the UO₂ sample surface. Appendix A contains a detailed description of the vacuum system, the Hansen Cell, and the equipment used for water vapor introduction. Appendix D provides the procedures used to operate the vacuum system.

The Hansen Cell provided the controlled environment necessary for the oxidation of the UO₂ samples after establishing a clean, high vacuum. The Hansen Cell was fitted with a 25-watt heater that was connected to a Lakeshore 330 Temperature Controller that allowed precise temperature control of the UO₂ sample up to 200°C. Appendix A contains a detailed description of the Hansen Cell and Appendix E describes the procedures for using the Lakeshore Temperature Controller.

This system allowed for the exposure of the pressed UO₂ powder samples to a wide range of temperature, partial pressure of oxygen, and partial pressure of water vapor conditions. The temperature, partial pressure of oxygen, and partial pressure of water

vapor were selected after a review of the previous oxidation experiments conducted at the Air Force Institute of Technology and a literature review of similar experimental setups. The oxidation environments and temperature settings used in this research did not cause the formation of uranyl on the surface of the prepared UO_2 samples.

Photoluminescence Spectroscopy

In-situ Photoluminescence (PL) Spectroscopy was the primary means of analysis of the pressed UO_2 powder samples.

Equipment

A Jobin-Yvon Spex Horiba Fluorolog-3 double excitation, double emission monochromator spectrofluorometer with pulsed 150-watt xenon lamp and optional phosphorimeter attachment was utilized in obtaining the PL measurements. Appendix A contains a detailed description of the Fluorolog-3 and Appendix G provides the equipment's operating instruction.

Data Collection

Of the three different PL Spectroscopy scan modes available with this piece of equipment (lifetime, excitation, and emission) only emission scans were used. The emission scans of the UO_3 samples involved exciting the samples at a fixed wavelength of 425 nm with the xenon lamp and monitoring the photoluminescent emission at varying wavelengths from 470 to 740 nm. After several scans of the UO_3 with no interesting

spectra peaks past 600 nm, the measurements were limited between 470 to 600 nm. The emission scans of the pressed UO_2 powder were similarly scanned and measured with the same parameters but were broken down into two separate measurements, one from 470 to 660 nm and the second from 660 to 740 nm.

For the first UO_3 sample, labeled T101K, a baseline emission spectrum was taken immediately after being placed in the Hansen Cell and vacuum system. The sample was then exposed to ambient atmospheric conditions where the temperature was steady at 25°C but the partial pressure of oxygen and relative humidity were unknown. Periodic PL measurements were taken at regular intervals for 155 hours under these oxidizing conditions. The sample showed the characteristic peaks of UO_3 immediately. The intensity of the peaks increased an order of magnitude over the first 26 hours of oxidation and then began to decrease. The decrease in intensity continued for the next 129 hours. After 155 hours, the characteristic UO_3 peaks were no longer evident in the spectra. The UO_3 sample was then vacuum reduced down to approximately 10^{-4} torr partial pressure of oxygen and its temperature elevated to 150°C . These conditions were kept steady for 15 hours. Three PL spectra were taken of the sample under these reducing conditions. The spectra showed no significant change. After the vacuum reduction and baking of the UO_3 sample, the sample was allowed to return to ambient temperature of 25°C before approximately 600 torr of pure, dry oxygen was introduced to the system and the Hansen Cell. After the oxygen was introduced, the sample temperature was elevated to 100°C . The UO_3 sample was then allowed to oxidize under these conditions for 25 hours. Three PL spectra were taken of the sample under these oxidizing conditions. The spectra

decreased in intensity from the previous measurements without any of the characteristic peaks associated with UO_3 . UO_3 sample T101K was oxidized and reduced for approximately 200 hours, or 8 days. Following this analysis, the sample was removed from the Hansen Cell, placed between two Mylar sheets, sealed in a glass jar labeled T101K, and placed in the glove box under a nitrogen environment for storage. The vacuum system was then evacuated down to 10^{-4} torr and heated to 150°C for a period of 48 hours.

A new UO_3 sample was prepared, labeled T101L, and placed in the Hansen Cell. This sample was immediately exposed to a reduced partial pressure of oxygen environment. After stabilizing the pressure at approximately 10^{-2} torr, where the temperature was steady at 24°C , periodic PL measurements were started. The sample showed prominent peaks characteristic of UO_3 . The sample was allowed to vacuum reduce in this environment for approximately 44 hours, during which time, 5 measurements were taken. As previously reported, the intensity of the spectra decreased over time in this reducing environment. Following the vacuum reduction, 54 torr of pure, dry oxygen was introduced into the weathering apparatus and the Hansen Cell. After two hours in this pure oxygen environment, PL measurements were started. The sample remained in this oxidizing environment for 60 hours, during which time, 5 measurements were taken. The intensity of the spectra increased, however only marginally at this low partial pressure of dry oxygen. Following this portion of the experiment, the oxidation was continued at this pressure of dry oxygen, but with an elevated temperature of 100°C . As soon as the increased temperature setting was reached in the Hansen Cell sample

holder, measurements were started. The sample remained in this oxidizing environment for 48 hours, during which time, 8 measurements were taken. The spectra initially decreased intensity over the first two hours and then began increasing with time over the next 46 hours. Following this analysis, the sample was treated as the previous sample and removed from the Hansen cell, placed between two Mylar sheets and then sealed in a glass jar labeled T101L. It was also placed in the glove box under a nitrogen environment for storage. Following the UO_3 reduction and oxidation experimentation, the vacuum system was then evacuated down to 10^{-4} torr and heated to 150°C for a period of 48 hours, before beginning analysis of UO_2 . The UO_3 sample, T101L, was reduced and re-oxidized for approximately 150 hours, or 6 days.

Based on the observance and measurement of the characteristic UO_3 peaks increase and decrease in intensity as a function of both oxygen introduction and vacuum reduction in both samples, we concluded the baseline study with UO_3 and commenced with the dry and wet oxidation of UO_2 .

The first UO_2 sample, labeled T200A, was prepared and placed in the Hansen cell. The weathering system had been evacuated and baked for over 48 hours. The Hansen cell and sample were placed in the system and exposed to the vacuum. The system was allowed to stabilize at low pressure and then filled with 760 torr of pure, dry oxygen. PL Measurements were started immediately after placing the Hansen Cell and sample into the weathering system. None of the characteristic peaks of UO_3 were present. After introducing the dry oxygen, the temperature was raised to 70°C . After 132 hours in this oxidizing environment, the temperature was increased to 100°C . After

174 hours, the temperature was increased to 150°C. After 240 hours, the temperature was increased again to 200°C. The UO₂ sample was allowed to remain in this oxidizing environment for 295 hours, or 12 days, during which time, no indication of UO₃ was observed. Due to time constraints and approaching deadlines, the dry oxidation of UO₂ experiment was discontinued with no UO₃ formation discernable by PL spectroscopy on the surface of the UO₂ sample at this temperature.

The second UO₂ sample, labeled T200B, was prepared, placed in the Hansen Cell, and placed in the weathering system. As in the previous experiment, the weathering system had been evacuated and baked for 48 hours. The Hansen cell and UO₂ sample were placed in the system and evacuated at 100°C. After baking and evacuating the entire system, the temperature was allowed to return to ambient. When the system stabilized at this reduced pressure, a flask of distilled water, that had the surface of the liquid evacuated until it reached the boiling point, was connected to the weathering system and 60 torr of distilled water vapor was introduced into the system. Following the water vapor introduction, 700 torr of pure, dry oxygen was introduced into the weathering system. PL measurements were started immediately after the system was stabilized. Initially, the spectra showed no indication of UO₃ or its characteristic spectrum. After 48 hours of ambient temperature, the temperature was increased to 110°C. This temperature was maintained for the next 865 hours. The water vapor was replaced in the weathering system at 570 hours and the valve connecting the two systems was left open with the water temperature maintained at 70° C for the duration of this experiment. This was done to ensure that water vapor was circulating throughout the

weathering system at all times and not allow the water to condense and pool at the bottom of the weathering system. After 865 hours at 110° C, the temperature control was turned off and the sample temperature was allowed to return to an ambient temperature of approximately 28° C. The UO₂ sample remained in these conditions for the next 264 hours. The wet oxygen oxidation of UO₂ experiment was concluded after 1031 hours with no UO₃ formation discernable by PL spectroscopy on the surface of this UO₂ sample at this temperature.

Surface Analysis

The uranium oxide particles were measured for their surface area. Analysis was conducted to gather quantitative data on the specific surface area per unit mass.

Equipment

A NOVA-1000 (NO Void Analysis), Gas Sorption Analyzer was utilized for the surface analysis of the UO₂ powder. The system had not been used since 1997; therefore a complete calibration of all stations was completed prior to data acquisition. Appendix A contains a complete description of the NOVA-1000 and Appendix I contains the procedures and setting used to measure the particle's size.

Data Collection

The NOVA-1000 High Speed Gas Sorption Analyzer was moved from the laboratory in Building 644, Environmental Sciences, and set up for operation in Building

470. A vacuum pump was connected and a feed line of Ultra-High Purity Nitrogen was connected. A diagnostic test of the system was conducted. A 12 mm sample holder was selected as a best fit for the particle surface measurement analysis. The sample holder was cleaned with methanol and allowed to dry. The sample holder and UO_2 powder were introduced into the glove box in accordance with the procedures of Appendix B. A small portion was poured into the sample holder and measured at 1.81 g. The sample was sealed with a film of X-Ray Mylar, removed from the glove box, and moved to the NOVA-1000.

Prior to the surface measurements, the system and sample cell were calibrated in accordance with the procedures outlined in the NOVA-1000 Operations Manual. Following the system calibration, the UO_2 sample was placed in the Vacuum Degassing station and heated to 300°C for 5 minutes. The out-gassing was accomplished to remove any organics, water vapor, or other gas molecules clinging to the UO_2 sample. The sample was moved to Analysis Station 1 for analysis. First, the current atmospheric pressure was calculated by the NOVA-1000. The equipment then measured the volume of the sample in the calibrated 12 mm sample cell and with the inputted mass, calculated the density of the UO_2 sample. An analysis setup was input into the Nova and a 25-point BET surface analysis of the sample was conducted. The results obtained are summarized in Chapter IV. Five repeat 25-point analyses were conducted to obtain a good statistical data spread. The analyses were conducted over a period of five days. Each surface analysis was preceded with vacuum degassing at 300°C and current atmospheric pressure

measurement. The sample density was calculated and recorded at the beginning of each analysis.

A copy of the Nova Data Reduction Software™ was obtained from the manufacturer and installed on a computer for analysis of the raw data taken from the NOVA-1000.

IV. Analysis and Results

Chapter Overview

This chapter contains the results and analysis for the UO_3 reduction and oxidation experiments and the UO_2 dry and wet oxygen oxidation experiments. The results and analysis of the data collected during this research is presented in the following sequence:

1. Ambient environmental oxidation of UO_3
2. Vacuum reduction and re-oxidation of UO_3
3. Dry oxidation of UO_2
4. Wet oxidation of UO_2
5. Surface analysis and particle measurements

Photoluminescence Measurements

This section contains the spectra of the UO_3 benchmark samples both oxidized under ambient environmental conditions and vacuum reduced and re-oxidized in pure, dry oxygen at temperatures ranging from ambient at 30° C to 100° C. The results of the dry and wet oxidation of UO_2 in a pure oxygen environment at temperatures of 200° C and below are also presented. The parameters used to obtain the PL spectra of all pressed uranium oxide powder samples were developed by previous researchers and are listed in Table 4 below.

Table 4. Parameters for uranium oxide PL measurements.

Parameter	Setting
Emission Monochromator	470 to 740 nm
Emission Monochromator Increment	1 nm
Excitation Monochromator	425 nm
Excitation Monochromator Increment	N/A
Sample Window	3 msec
Delay Time	0.10 msec
Delay Time Increment	N/A
Time per Flash	40 msec
Number of Flashes per Data Point	500
Signal	Sc
Excitation Slit Width	14.7 mm
Emission Slit Width	14.7 mm
PMT Cooling Temperature	10° C
Number of Flashes per Scan	135,000
Estimated Time per Scan	30 min

Photoluminescence spectra of uranium oxides samples

The PL spectra presented in this section were obtained from the pressed uranium oxide powder samples prepared in accordance with Appendix C. Table 4 above is a complete list of the Fluorolog-3 parameters and settings used to collect the emission spectra for all uranium oxide samples. Deviations from these parameters will be discussed when applicable. Figure 9 below provides the characteristic PL spectra found for all UO_3 samples with peaks identified at 489 nm, 509 nm, 531 nm, and 553 nm with a shoulder identified at 581 nm. The emission peaks for the UO_3 samples measured are consistent with the peaks reported in previous research conducted at AFIT by Schueneman [Schueneman, 2001] and the peaks reported in earlier literature by Hanchar [Hanchar, 1999]. The UO_3 and UO_2 spectra were collected with the following settings: excitation monochromator set at 425 nm, delay time of 0.15 msec, excitation and emission band-pass of 14.7 nm, and 500 xenon flashes per data point (except as noted).

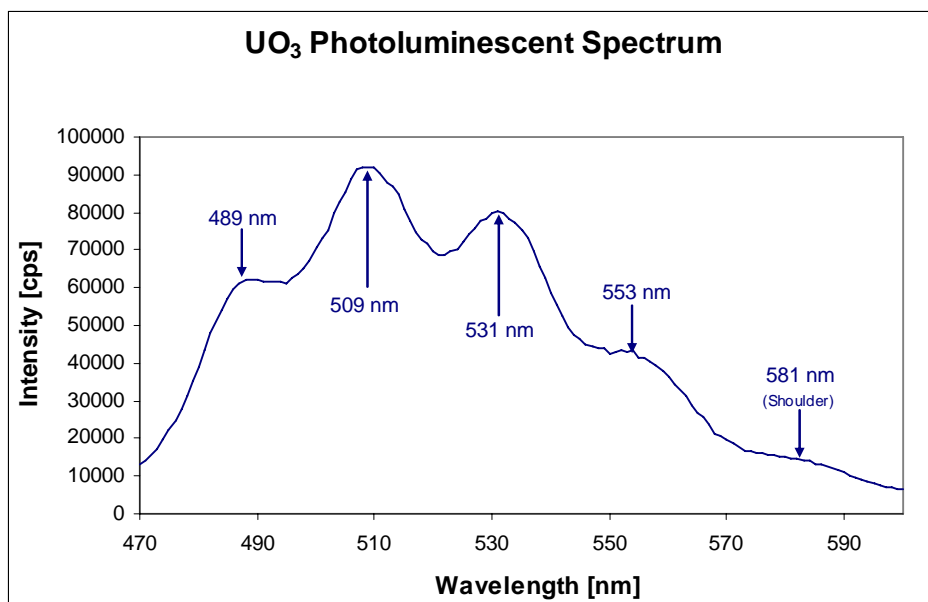


Figure 9. Lamp-corrected, front-face PL emission scan of UO₃ sample T101L. The peaks identified in the figure above are in excellent agreement with previous research conducted here at AFIT [Schueneman, 2001] and elsewhere [Hanchar, 1999].

Figures 10 and 11 below show the initial PL emission scans of UO₃ samples T101K and T101L. Note the difference in intensity between the two samples. T101K was the first uranium oxide powder sample prepared and as such, it was pressed slightly off-center, resulting in less interaction with the xenon lamp light. The UO₃ sample T101L was prepared more carefully, resulting in a more centered geometry of the uranium oxide powder and better interaction with the incident light.

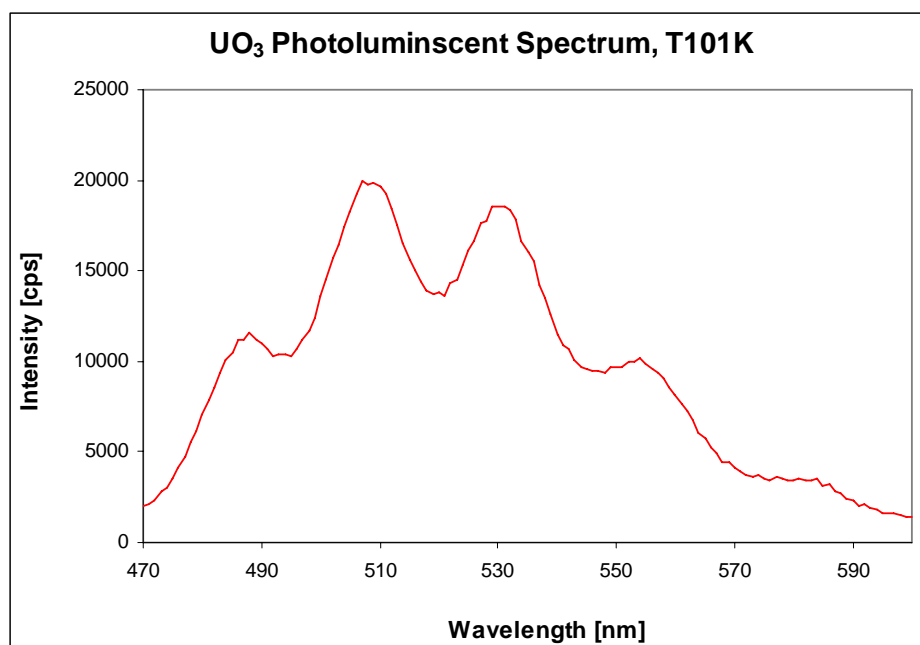


Figure 10. Lamp-corrected, front-face PL emission scan of UO₃ sample T101K. This UO₃ spectrum was collected with the following settings: excitation monochromator set at 425 nm, delay time of 0.15 msec, excitation and emission band-pass of 14.7 nm, and 500 xenon flashes per data point.

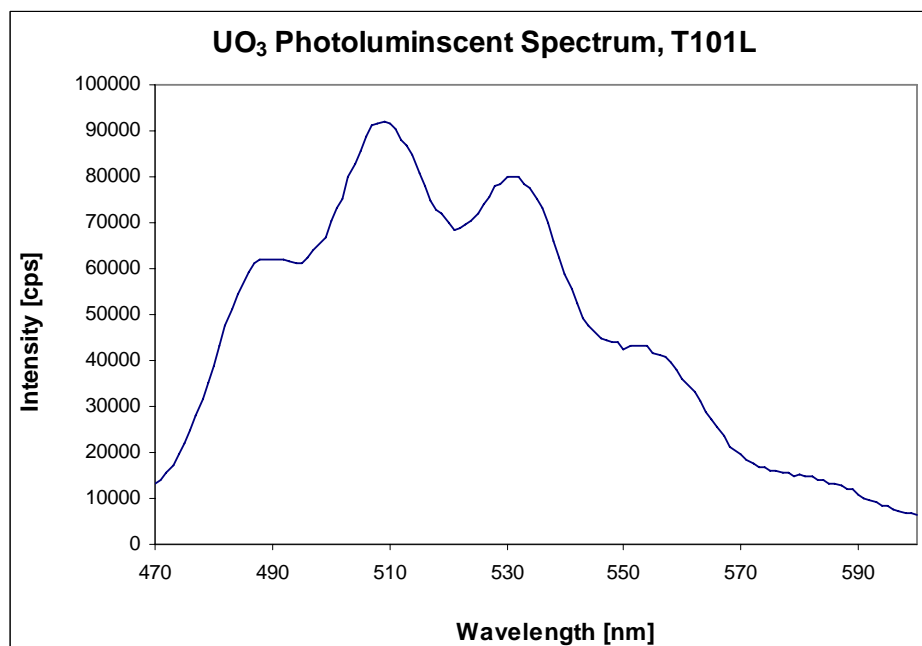


Figure 11. Lamp-corrected, front-face PL emission scan of UO₃ sample T101L. This UO₃ spectrum was also collected with the following settings: excitation monochromator set at 425 nm, delay time of 0.15 msec, excitation and emission band-pass of 14.7 nm, and 500 xenon flashes per data point.

In Figure 12 below, the two most intense PL emission scan spectra of UO_3 samples T101K and T101L are compared. Here we clearly see the difference in intensity between the two uranium oxide samples. The peaks of both samples are consistent, only less intense for sample T101K.

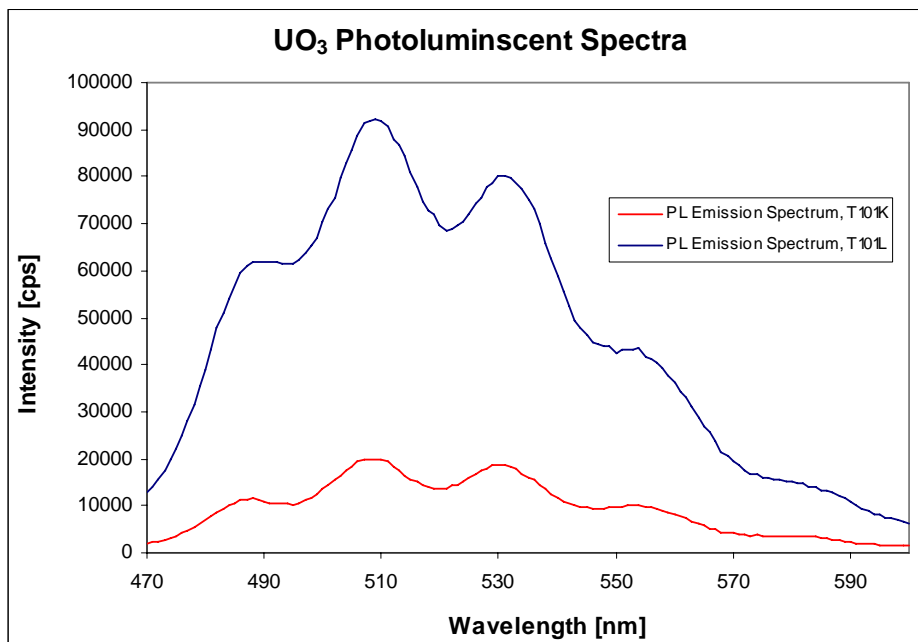


Figure 12. Lamp-corrected, front-face PL emission scan comparison of UO_3 samples T101K and T101L. The intensity of T101L was much higher due to the preparation of the samples and the placement of the UO_3 powder on the tungsten screen, T101L was more evenly centered.

The results of the oxidation of the UO_3 samples under various atmospheric conditions and temperatures are presented later in this chapter.

Figures 13 and 15 below show the initial UO_2 spectra taken from 660 nm to 740 nm and from 470 to 660 nm in Figures 14 and 16 prior to oxidation. Emission scan parameters were identical to those used for obtaining the UO_3 spectra above except for the data used to generate Figures 14 and 16, which only used 200 flashes per interval.

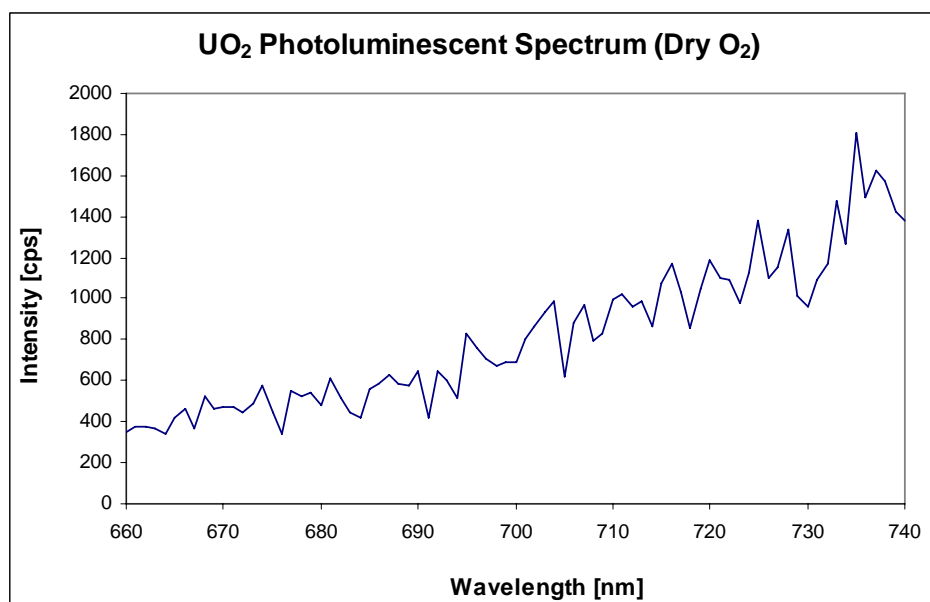


Figure 13. Initial lamp-corrected, front-face PL emission scan of UO₂ sample T200A scanned from 660 to 740 nm using 500 flashes per data point prior to exposure to dry oxygen and increased temperature.

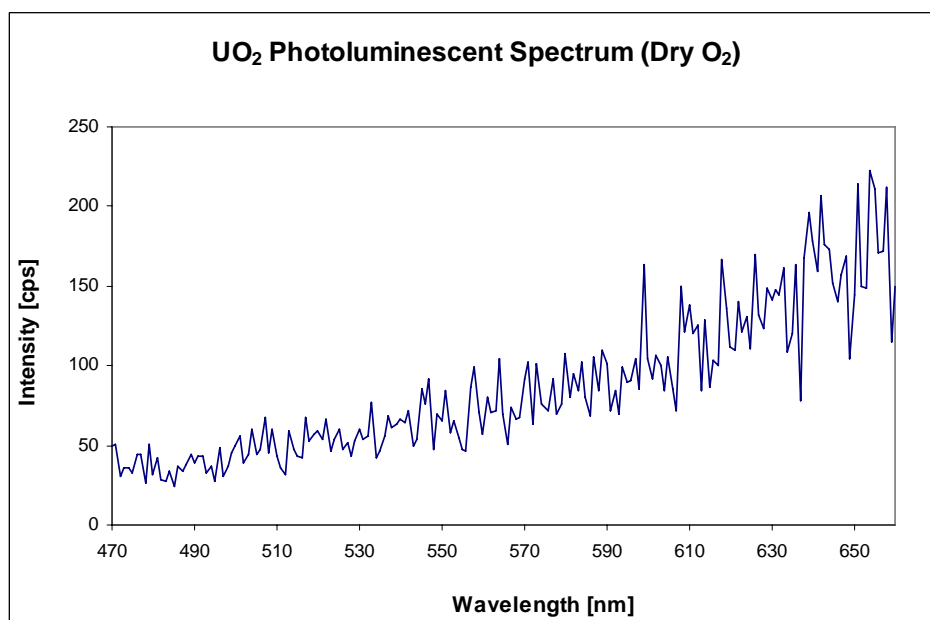


Figure 14. Initial lamp-corrected, front-face PL emission scan of UO₂ sample T200A scanned from 470 to 660 nm using only 200 flashes per data point prior to exposure to dry oxygen and increased temperature. None of the characteristic UO₃ peaks were evident in this sample at this time.

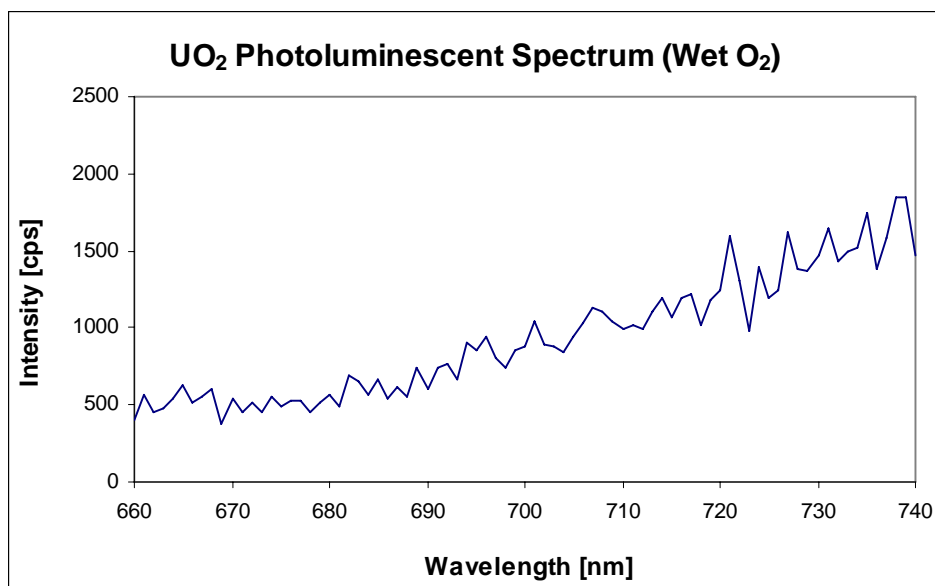


Figure 15. Initial lamp-corrected, front-face PL emission scan of UO_2 sample T200B scanned from 660 to 740 nm using 500 flashes per data point prior to exposure to wet oxygen and increased temperature.

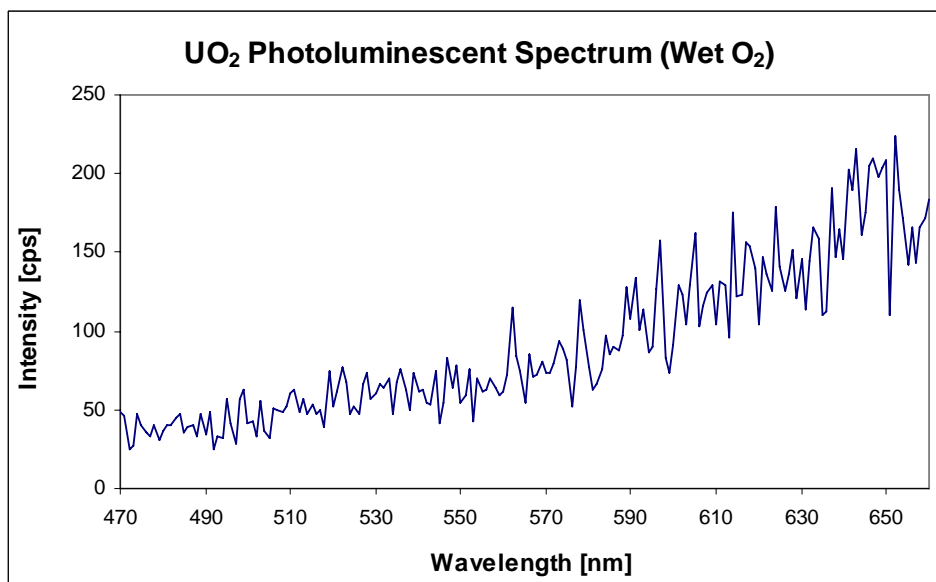


Figure 16. Initial lamp-corrected, front-face PL emission scan of UO_2 sample T200B scanned from 470 to 660 nm using only 200 flashes per data point prior to exposure to wet oxygen and increased temperature. Again, none of the characteristic UO_3 peaks were evident in this sample.

The reduction from 500 to 200 flashes per data point resulted in a reduction of the overall intensity of the spectrum generated but did not affect the shape of the spectrum. As expected, there were none of the characteristic peaks associated with UO_3 found in either spectra.

The characteristic PL emission spectrum of UO_3 shown in Figure 9 above occurs between 470 and 660 nm. In this research, all UO_2 PL emission spectra were taken in two steps, one from 660 to 740 nm, using more flashes per data point, and the second from 470 to 660 nm, using less flashes per data point. Our PL emission scans of UO_2 under both dry and wet oxygen oxidation environments were primarily taken between 660 and 740 nm in an attempt to locate and model the emergence of a peak at 695 ± 2 nm published in previous research [Schueneman et al., 2001], shown in Figure 17 below. The PL emission scans taken between 470 and 660 nm were taken to monitor the emergence of the characteristic UO_3 peaks in the event the peak at 695 ± 2 nm did not emerge.

The spectra shown below in Figure 17 is a collection of unsmoothed, red PL emission spectra that was presented in 2001 by Schueneman et al., for octahedral U(IV) on UO_2 that was oxidized in 760 torr of oxygen at 70°C . The same parameters were used in his PL spectra collection as this research. This spectrum was reported to be stable in milli-torr vacuum for more than one week at 70°C . At elevated temperature, 150°C , the emission signature decreases in intensity with time [Schueneman et al., 2001]. Formation and modeling of this peak was the focus of this research.

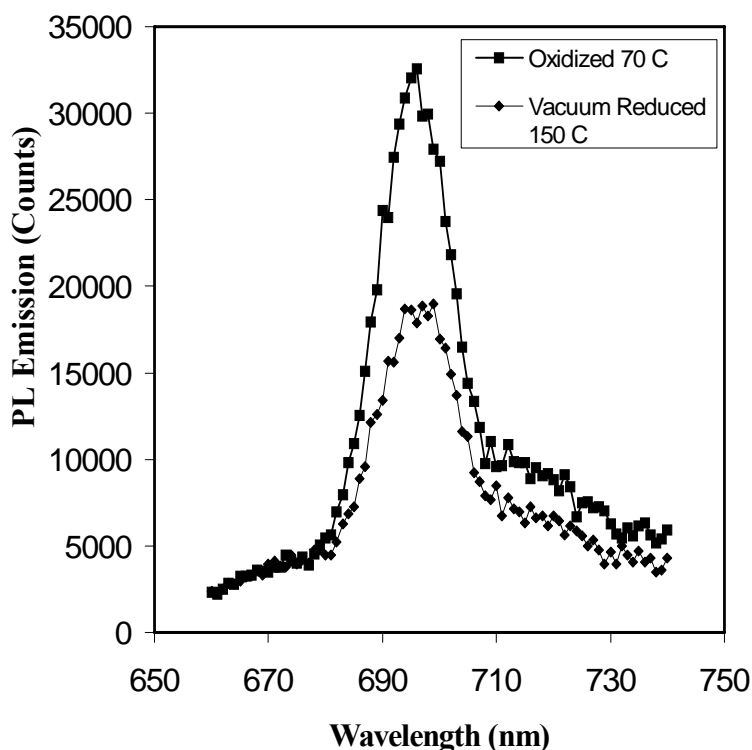


Figure 17. Unsmoothed, red PL emission spectra presented in 2001 by Schueneman et al., for octahedral U(IV) on UO_2 that was oxidized in 760 torr of oxygen at 70°C . PL spectra excitation at 425 nm with 14.7 nm band-pass. The U(IV) signature is stable in milli-torr vacuum for more than one week at 70°C . At elevated temperature, 150°C , the emission signature decreases in intensity with time [Schueneman et al., 2001].

In Figure 18 below, a comparison is made between the spectra of UO_3 and UO_2 . The PL emission spectrum of UO_3 is two orders of magnitude more intense than that of UO_2 . From this, we can see that any formation of UO_3 on the surface of the uranium oxide particles should result in an increase in intensity of the UO_2 PL emission signature.

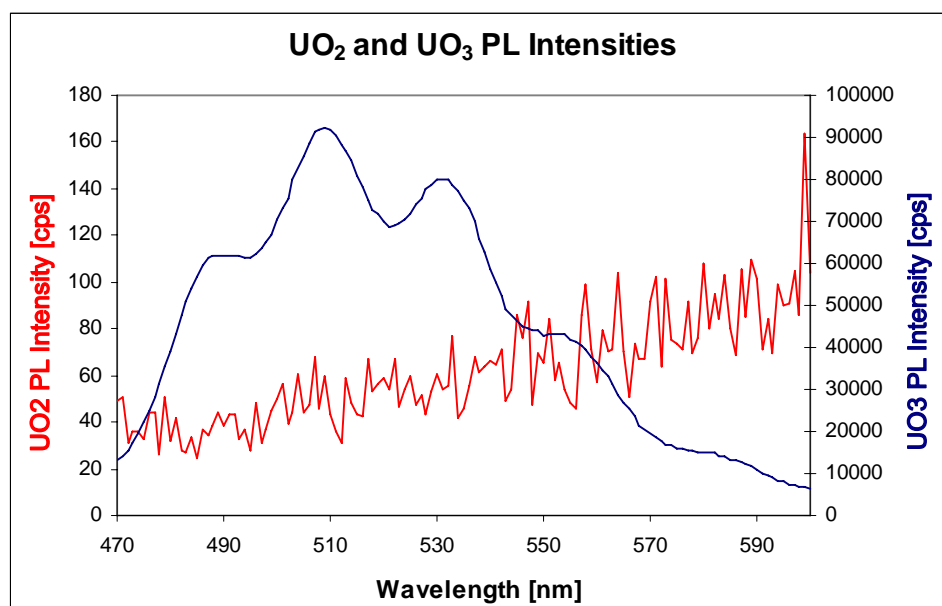


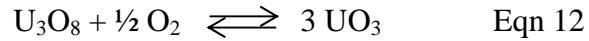
Figure 18. Initial lamp-corrected, front-face PL emission scan comparison of UO_2 to UO_3 . Both were scanned from 470 to 600 nm prior to exposure to oxygen and increased temperature. None of the characteristic UO_3 peaks were evident in the UO_2 sample. Note the extreme variation in scales from UO_3 to UO_2 , a difference of two orders of magnitude.

UO_3 Oxidation and Reduction

Ambient Environmental Oxidation of UO_3

The first pressed UO_3 powder sample, T101K, was analyzed as the sample was allowed to oxidize under ambient environmental conditions of temperature, moisture, and partial pressure of oxygen. The sample was placed in the system and allowed to oxidize for 155 hours at 28° C. During the first 26 hours of exposure to ambient atmospheric conditions, the intensity increased dramatically. This result is attributed to the handling and storage of the UO_3 sample powder. The UO_3 powder was handled and the samples prepared as well as stored in a pure nitrogen environment. The transition of UO_3 , which

has a significant and prominent PL emission spectrum, towards U_3O_8 in the presence of reduced partial pressures of oxygen is given in the equation below.



This denotes that U_3O_8 reacts with oxygen to form UO_3 , at high partial pressures of oxygen. This reaction can occur in both directions. As UO_3 is exposed to a reduced partial pressure of oxygen, in this case exposed to pure nitrogen, it oxidizes toward U_3O_8 . The UO_3 sample powder was kept in a nitrogen environment for approximately three years, during which time, the content of the sample consisted of a great deal of U_3O_8 . U_3O_8 does not have a PL emission spectrum. After preparing the sample in nitrogen, it was exposed to ambient air which contains approximately 20% oxygen. This exposure quickly oxidized the sample towards UO_3 and the increase of intensity of the PL emission spectrum.

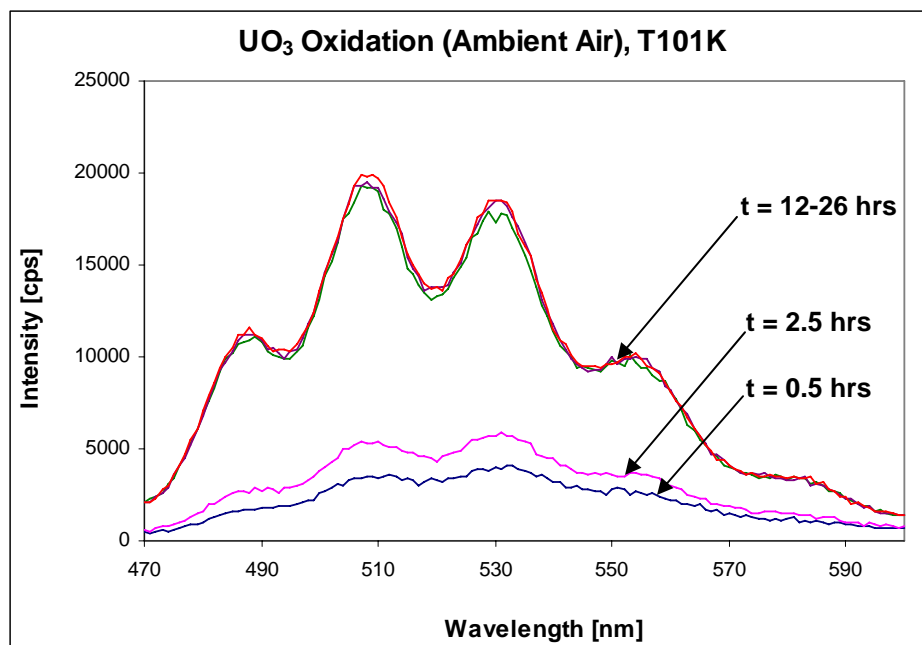


Figure 19. Lamp-corrected, front-face PL emission scan of UO_3 sample T101K. This figure shows the first five spectra taken of this sample after exposure to ambient air for 26 hours at 28°C . The intensity increased significantly. The intensity increase is accredited to the addition of oxygen to the sample after three years in storage in a pure nitrogen environment.

Figure 19 above shows the results of the periodic PL measurements taken of the spectra as the UO_3 reacted with the oxygen and moisture of the air in the laboratory. Integration of the area under the curve of the spectrum generated by the Fluorolog-3 gave us a quantitative analysis tool as the sample was oxidized. The area under each PL emission spectrum was integrated using both Gram32 Software and Excel in order to quantify the change in intensity of the PL emission spectra as the uranium oxide samples react with the oxygen and moisture, and other compounds and complexes. The left limit was set at 470 nm and the right at 600 nm for all UO_3 emission spectra integrated. A zero-order reaction kinetic curve was fitted to the change in integrated area with respect to time in order to determine the rate of oxidation of PL emission intensity.

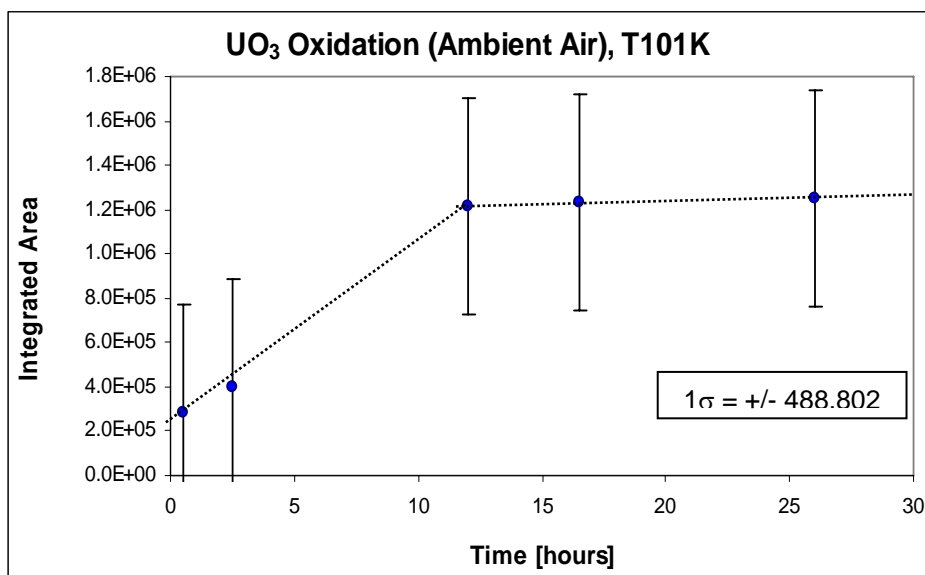


Figure 20. Results of the integration of the base line between 470 and 600 nm for UO_3 sample T101K after oxidation in ambient air for 26 hours at 28° C. The intensity increased linearly for the first 12 hours, signifying a zeroth order oxidation process, after which, the rate of oxidation slowed significantly. The intensity increase is accredited to the addition of oxygen to the sample after three years in storage in a pure nitrogen environment.

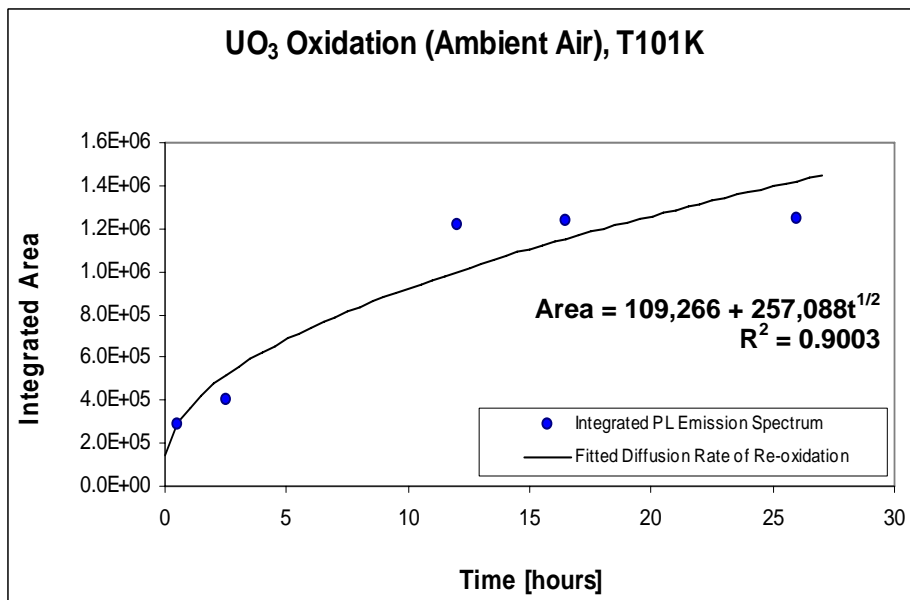


Figure 21. Results of the integration of the base line between 470 and 600 nm for UO_3 sample T101K after oxidation in ambient air for 26 hours at 28° C. This figure has been fitted with an exponential, diffusion driven curve.

The results of the base-line integration are plotted in Figures 20 and 21 above. The empirically fitted diffusion equation is presented in equation 13 below. The correlation coefficient is 0.9003. Based on the graphic data results, the behavior of the re-oxidation appeared to follow a rate of increase in the intensity limited by a zero-order reaction kinetics.

$$Area = 109,266 + 257,088 \cdot t^{1/2} \quad \text{Eqn 13}$$

This demonstrates that the initial oxidation of the ‘reduced in nitrogen’ UO_3 sample in ambient air is more closely modeled by a zeroth order oxidation process.

After the initial increase, the UO_3 sample T101K was continuously exposed in ambient air for an additional 129 hours. During this time, the intensity of the PL emission spectra decreased significantly, as seen in Figure 22 below. Similar to the oxidation phase, the PL emission reduction was integrated using both Gram32 Software and Excel in order to quantify the change in intensity of the PL emission spectra as the uranium oxide samples continued to react with the oxygen and moisture, as seen in Figure 22. Both software systems were in excellent agreement for integration value of each spectrum. The parameters were left the same for all UO_3 emission spectra integrated. A curve was fitted to the change in integrated area with respect to time in order to determine the rate of oxidation of PL emission intensity.

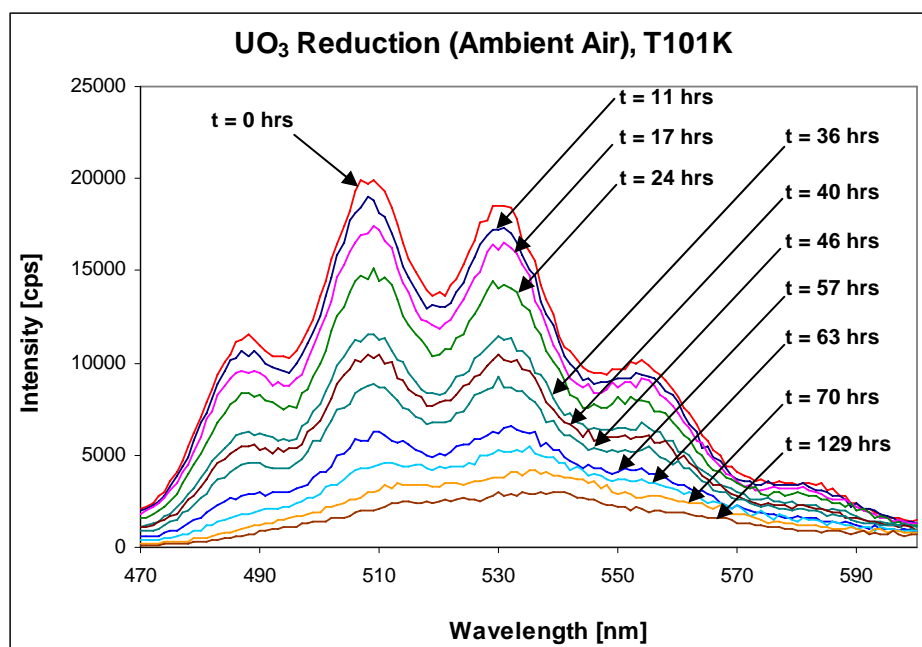


Figure 22. Lamp-corrected, front-face PL emission scan of UO_3 sample T101K. This figure shows intensity reduction of the sample in ambient air. This reduction followed the initial oxidation and subsequent intensity increase. This reduction occurred after exposure to ambient air for 129 hours at 28°C . The intensity decreased significantly during this time, almost completely eroding the characteristic UO_3 emission spectrum.

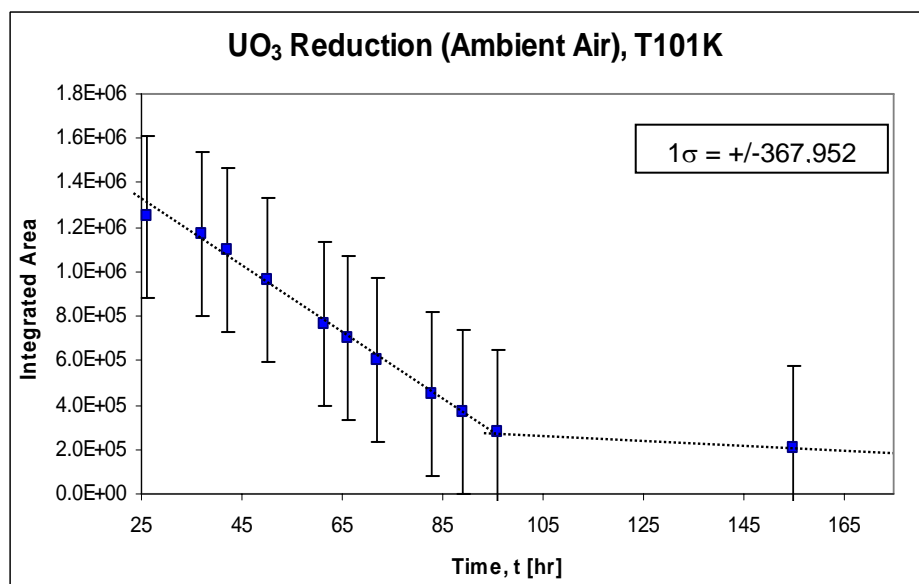


Figure 23. Results of the integration of the base line between 470 and 600 nm for UO_3 sample T101K after reduction in ambient air for 129 hours at 28°C . The intensity decreased linearly for the first 70 hours, also signifying a zeroth order reduction process similar to the oxidation intensity increase we saw after placing the UO_3 sample in ambient air. After 70 hours, the rate of oxidation slowed significantly.

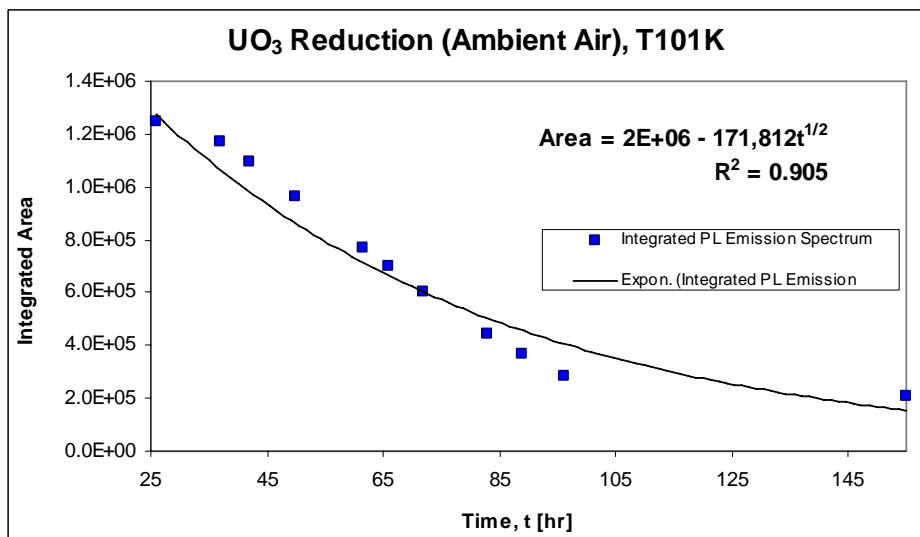


Figure 24. Results of the integration of the base line between 470 and 600 nm for UO₃ sample T101K after oxidation in ambient air for 129 hours at 28° C. This figure has been fitted with an exponential, diffusion driven curve.

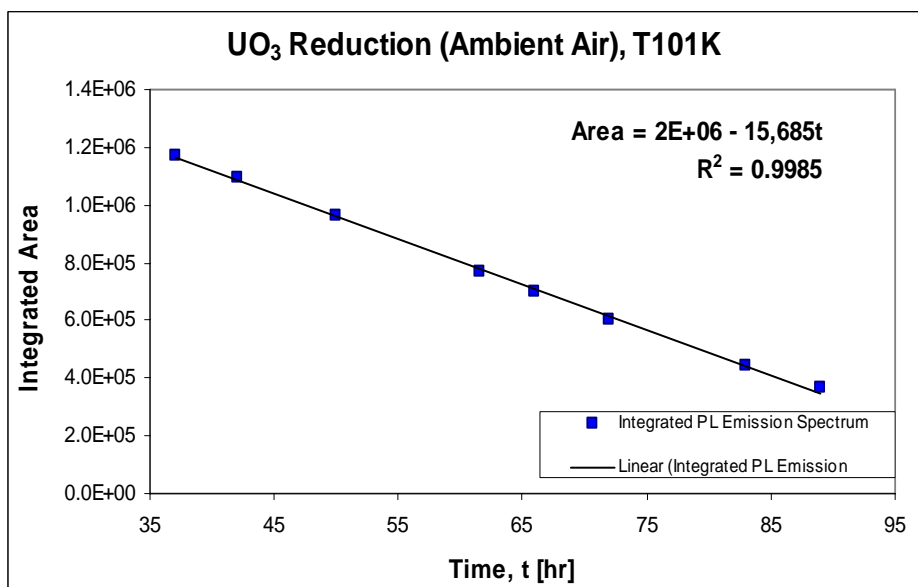


Figure 25. Results of the integration of the base line between 470 and 600 nm for UO₃ sample T101K after oxidation in ambient air for 129 hours at 28° C. This figure is a plot of integrated intensity versus the time. Note the high Correlation Coefficient developed from this data.

The results of the base-line integration are plotted in Figures 23 and 24 above. The empirically fitted diffusion equation is presented in equation 14 below. The correlation coefficient is 0.905. The behavior of the reduction appeared to follow a rate of increase in the intensity limited by a zero-order reaction kinetics model.

$$Area = 2E + 06 - 171,812 \cdot t^{1/2} \quad \text{Eqn 14}$$

The ‘knee’ seen in Figure 23 above is attributed to the saturation of the UO_3 sample in water vapor. The chemical reaction of UO_3 with H_2O was not investigated, see Chapter V, Recommendations.

The UO_3 sample T101K was then exposed to a vacuum that had a partial pressure of 8×10^{-5} torr oxygen for 12 hours. In these 12 hours, the intensity of the spectrum decreased significantly. Additionally, the characteristic UO_3 peak signature was completely eroded. The amorphous peak seen in Figure 26 below also demonstrates a slight red shift. This reduction followed the reduction in ambient air at 28°C . Following the vacuum reduction, the UO_3 sample was then exposed to 654 torr pure, dry O_2 for 46 hours. After only 5 hours, the intensity quickly increased back to its previous intensity prior to exposure to the reduced O_2 pressure. However, note the red shift of the peak of the spectrum following the re-introduction of oxygen. This red shift was not characterized.

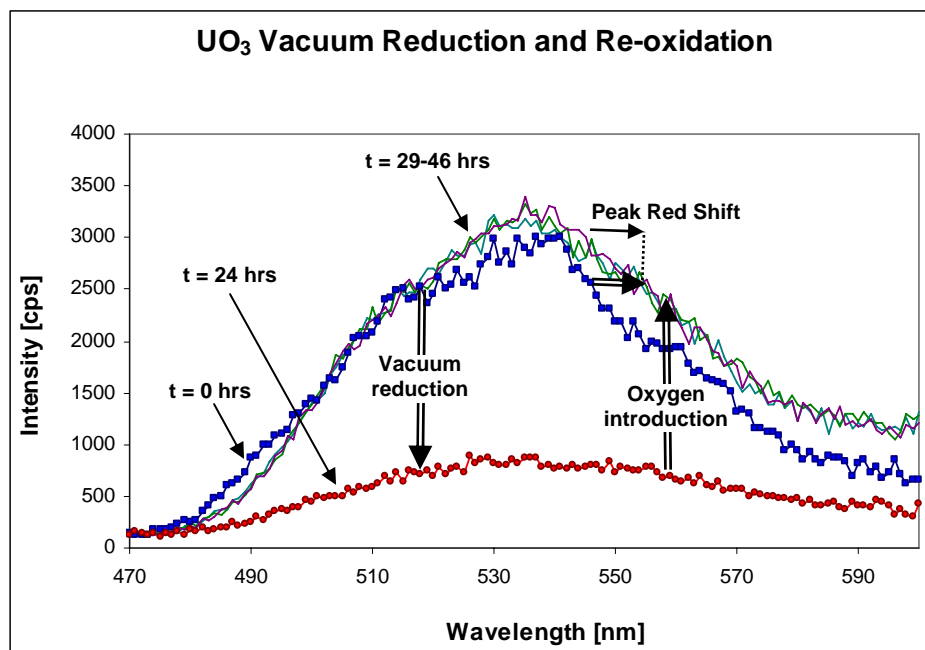


Figure 26. Lamp-corrected, front-face PL emission scan of UO_3 sample T101K. This figure shows a significant intensity reduction of the sample after exposure to a partial O_2 pressure of 8×10^{-5} torr for 24 hours. This reduction followed the reduction in ambient air at 28°C . Following the vacuum reduction, the UO_3 sample was exposed to 654 torr pure, dry O_2 for 46 hours. After only 5 hours, the intensity quickly increased back to its previous intensity prior to exposure to the reduced O_2 pressure. However, note the red shift of the peak of these spectra.

After 22 hours in 654 torr pure, dry oxygen at 28° C, the temperature was increased to 100° C and allowed to reduce in these conditions for an additional 25 hours, as shown in Figure 27 below. The ambient environmental oxidation, reduction, and follow-on re-oxidation experiment was terminated.

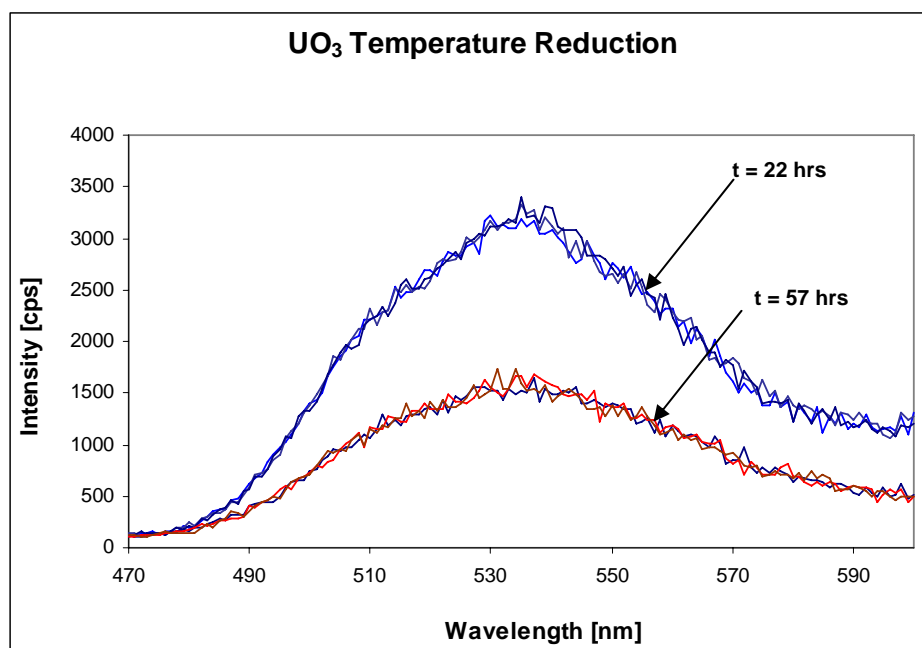


Figure 27. Lamp-corrected, front-face PL emission scan of UO₃ sample T101K. This figure shows a significant intensity reduction of the sample after exposure to a temperature of 100°C for 25 hours. This reduction followed the re-oxidation of the UO₃ sample at 28°C and exposure to 654 torr pure, dry O₂ for 46 hours. After only 4 hours, the intensity quickly decreased and stabilized at this pressure and temperature for the following 21 hours.

Insufficient data obtained from the oxygen introduction and temperature reduction of this UO₃ sample as seen in Figures 26 and 27 above, therefore the re-oxidation and temperature rate changes were not modeled for this sample. Additional data under similar atmospheric conditions is modeled with UO₃ sample T101L below.

A summary of the conditions and integration results of the ambient environmental oxidation of the UO₃ sample, T101K, are listed in Table 5 below.

Table 5. UO₃ sample T101K upon exposure to ambient atmospheric conditions

Trial	Temp [°C]	P[O ₂]	Time [hours]	Integrated Area
		Pressure [torr]		
T101K_3	28	Ambient	0.5	284,855
T101K_4	28	Ambient	2.5	400,484
T101K_5	28	Ambient	12	1,212,534
T101K_6	28	Ambient	16.5	1,235,545
T101K_7	28	Ambient	26	1,246,963
T101K_8	28	Ambient	37	1,172,595
T101K_9	28	Ambient	42	1,095,681
T101K_10	28	Ambient	50	962,379
T101K_11	28	Ambient	61.5	765,911
T101K_12	28	Ambient	66	699,879
T101K_13	28	Ambient	72	605,287
T101K_14	28	Ambient	83	446,553
T101K_15	28	Ambient	89	366,654
T101K_16	28	Ambient	96	281,329
T101K_17	28	Ambient	155	206,001
T101K_1A	28	8×10 ⁻⁵	12	70,118
T101K_2A	28	654	5	230,756
T101K_2B	28	654	15	233,339
T101K_2C	28	654	22	232,522
T101K_3A	100	654	4	118,003
T101K_3B	100	654	15	118,550
T101K_3C	100	654	25	117,469

UO₃ Vacuum and Temperature Reduction, and Re-oxidation in dry Oxygen

Following sample preparation, being extremely careful to center the UO₃ powder on the tungsten screen, the second UO₃ sample, T101L, was immediately analyzed during vacuum reduction at approximately 1×10^{-2} torr total pressure, or approximately 2×10^{-3} torr partial pressure of oxygen, and an ambient temperature of 28° C for 44 hours. The PL measurement parameters used were identical to the previous UO₃ ambient environmental oxidation and reduction experiment and are outlined in Table 4. The emission wavelength scan was from 470 nm to 600 nm. The reduced partial oxygen pressure conditions resulted in the reduction of the intensity of the photoluminescent spectra taken, as shown in Figure 28 below.

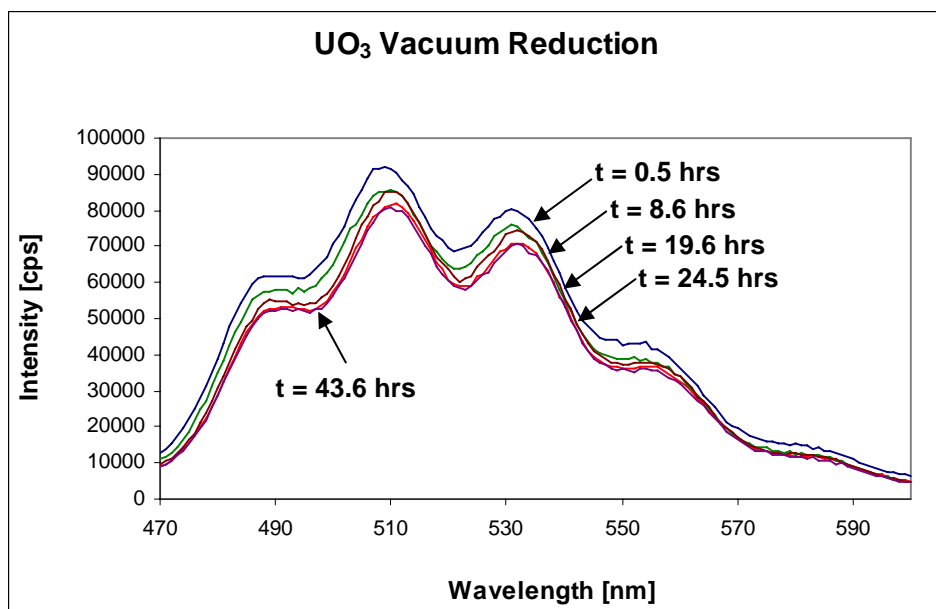


Figure 28. Lamp-corrected, front-face PL emission scan of UO_3 sample T101L. This figure shows an intensity reduction of the sample after exposure to a partial O_2 pressure of 2×10^{-3} torr for 44 hours.

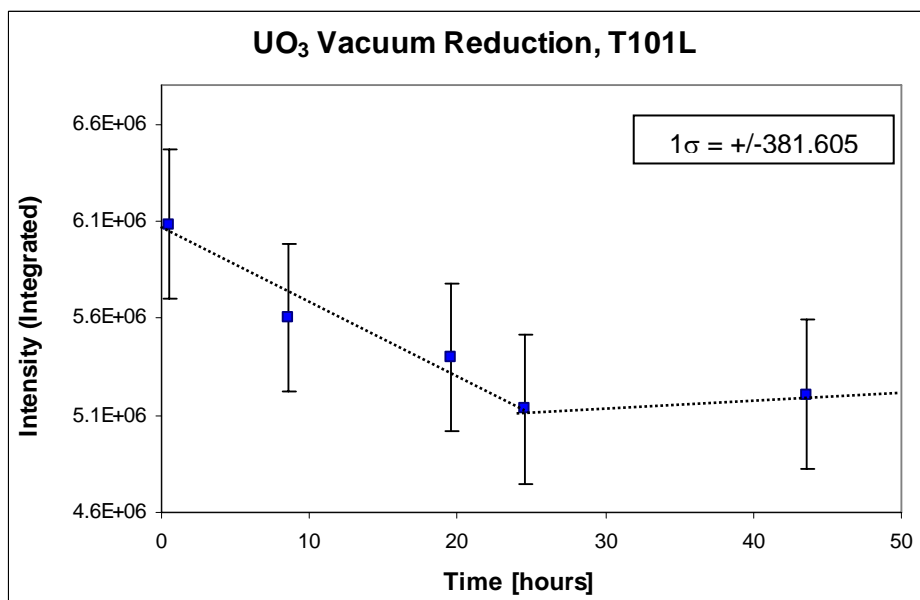


Figure 29. Results of the integration of the base line between 470 and 600 nm for UO_3 sample T101L after reduction in a partial pressure of O_2 of 2×10^{-3} torr for 44 hours. The intensity decreased linearly for the first 24 hours, also signifying a zeroth order reduction process similar to the oxidation intensity increase we saw after placing the UO_3 sample in ambient air. After 24 hours, the rate of oxidation slowed significantly and appeared to increase.

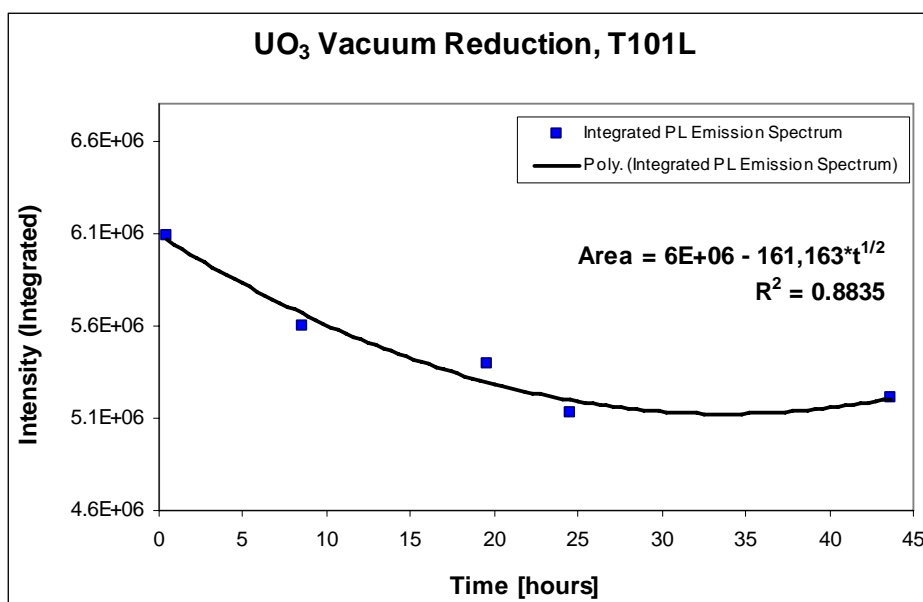


Figure 30. Results of the integration of the base line between 470 and 600 nm for UO_3 sample T101L after vacuum reduction 43.6 hours at 28° C. This figure has been fitted with an exponential, diffusion drive curve.

The UO_3 sample T101L was continuously exposed to a reduced partial pressure of oxygen for 43.6 hours. During this time, the intensity of the PL emission spectra decreased significantly, as seen in Figure 30 above. Similar to the previous experiment, the PL emission reduction was integrated using both Gram32 Software and Excel in order to quantify the change in intensity of the PL emission spectra as the uranium oxide sample reacted at this pressure, as seen in Figures 29 and 30 above. The parameters were left the same for all UO_3 emission spectra integrated. A curve was fitted to the change in integrated area with respect to time in order to determine the rate of oxidation of PL emission intensity.

The results of the base-line integration are plotted in Figure 30 above. The exponential diffusion drive diffusion equation is presented in equation 12 below. The

correlation coefficient is 0.8835. The behavior of the reduction appeared to follow a rate of increase in the intensity limited by a zero-order reaction kinetics model.

$$Area = 6E + 06 - 161,163 \cdot t^{1/2} \quad \text{Eqn 15}$$

The ‘knee’ seen in Figure 29 above is attributed to the limitation of the weathering system and the partial pressure of oxygen it was able to maintain.

After the vacuum reduction, 54 torr of pure, dry O₂ was introduced into the weathering system and allowed to oxidize for 60 hours at 28° C. This low pressure of oxygen did not return the sample back to its original intensity, see Figure 31 below, but it did increase slightly and stabilize at this increased partial oxygen pressure.

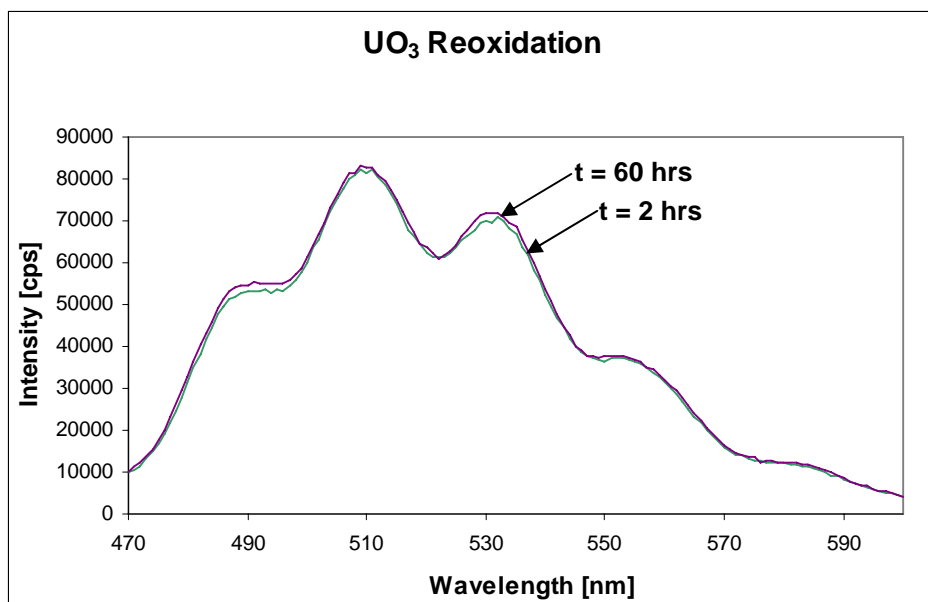


Figure 31. Lamp-corrected, front-face PL emission scan of UO₃ sample T101L. This figure shows only a slight intensity increase of the sample after exposure to a partial O₂ pressure of 54 torr for 60 hours at 28° C.

Insufficient data was obtained from the oxygen introduction of this UO₃ sample as seen in Figure 31 above, therefore the re-oxidation rate changes were not modeled for this sample.

After the sample stabilized in these conditions, the temperature was increased. Under these conditions, there was an initial large increase in intensity and was followed by a subsequent stabilization at this increased temperature, see Figure 32 below.

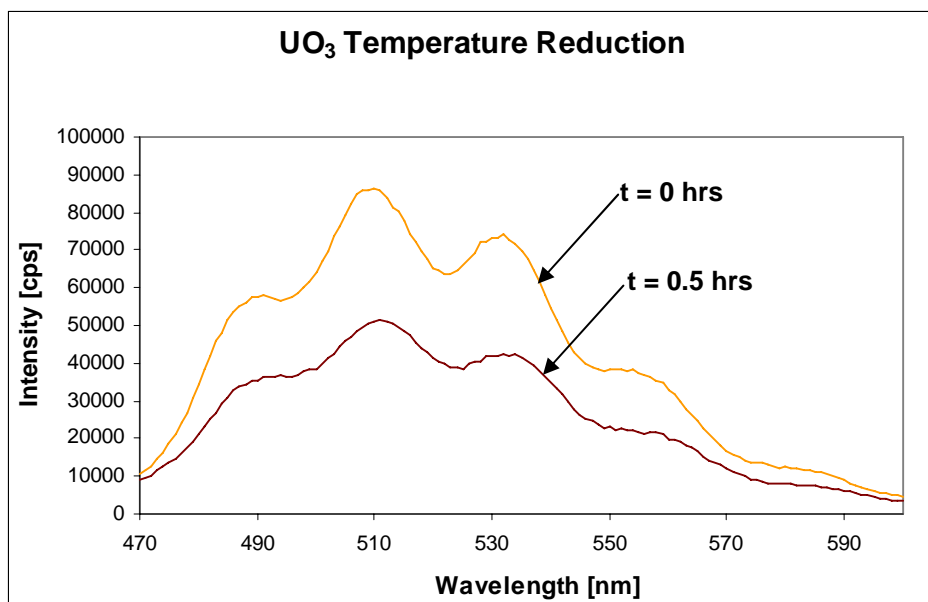


Figure 32. Lamp-corrected, front-face PL emission scan of UO₃ sample T101L. This figure shows only a significant decrease in intensity of the sample after exposure to a temperature of 100° C for only 0.5 hours. Partial O₂ pressure of 54 torr was maintained, minus the slight expansion of the gas in the system after the increase in temperature.

Analysis of this data is compiled in the next paragraph to demonstrate the very large effect temperature has on the PL emission spectra collected in the following section, dry and wet oxygen oxidation of UO₂.

Following the temperature increase and the rapid decrease in PL emission intensity of the UO₃ sample, it remained in these conditions for the next 151 hours. During which time the PL emission spectrum increased, although not to the level as before the temperature increase, see Figure 33 below. This temperature reduction and re-oxidation was modeled in Figure 34 below.

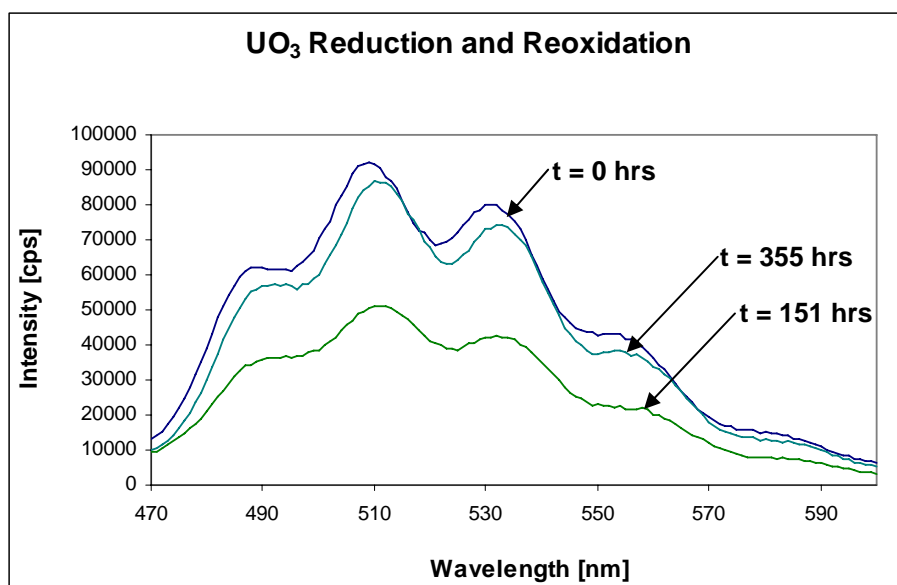


Figure 33. Lamp-corrected, front-face PL emission scan of UO_3 sample T101L. This figure shows a significant decrease in intensity of the sample after exposure to a temperature of 100°C for only 0.5 hours. Partial O_2 pressure of 54 torr was maintained, minus the slight expansion of the gas in the system after the increase in temperature.

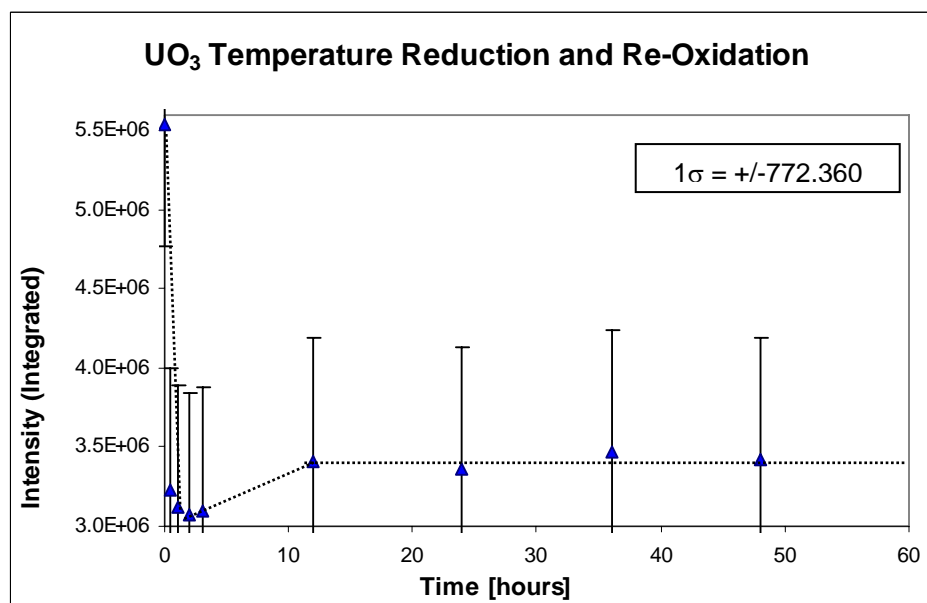


Figure 34. Results of the integration of the base line between 470 and 600 nm for UO_3 sample T101L after reduction at a temperature of 100°C and a partial pressure of O_2 of 54 torr for 335 hours. The intensity decreased linearly for the first 0.5 hours, also signifying a zeroth order reduction process similar to the oxidation intensity increase we saw after placing the UO_3 sample in ambient air. After 12 hours, the rate of oxidation slowed significantly and appeared to stabilize.

In Figure 32 above, the UO_3 sample experienced a significant reduction in its PL emission intensity when exposed to an increased temperature. Originally, I expected the intensity to increase with increasing temperature due to the general rate increase of chemical reactions at higher temperatures. The sample was still being exposed to 54 torr dry oxygen; therefore I expected the sample to convert chemically into pure UO_3 , which would increase the intensity of the PL emission spectrum. After seeing the massive decrease in intensity and the failure of the sample to return to its original intensity at elevated temperature, I propose that additional reactions are taking place at these higher temperatures of which I am unaware. This data is important in that the following oxidation experiments with dry and wet oxygen oxidation were all conducted at elevated temperatures ranging from ambient to 200°C .

In Figures 35 and 36 below, the rate of oxidation at 100°C and 54 torr pure, dry oxygen is plotted as the integration of the curve versus time following the initial temperature reduction.

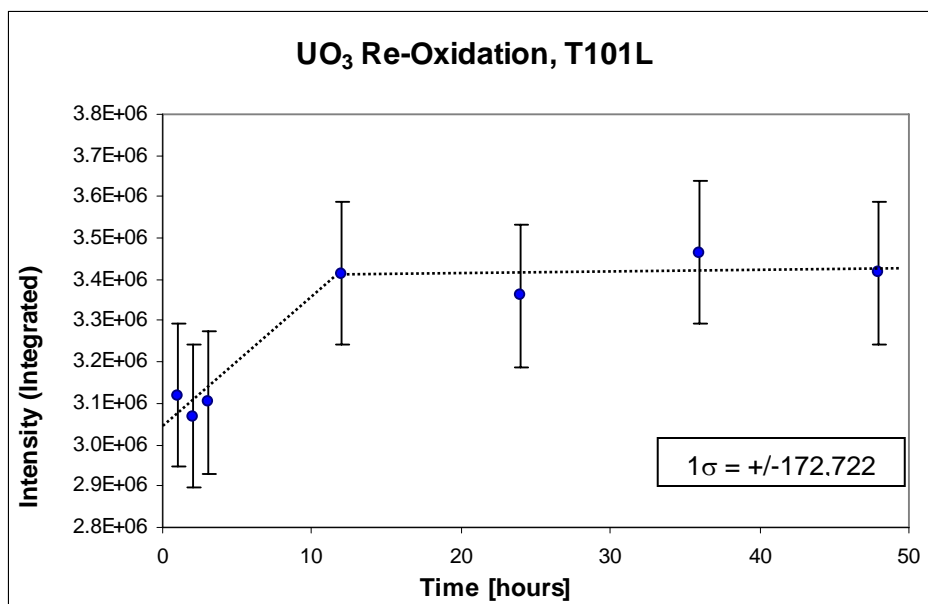


Figure 35. Results of the integration of the base line between 470 and 600 nm for UO₃ sample T101L after oxidation in 54 torr O₂ for 48 hours at 100° C. This figure is a result of the UO₃ PL emission intensity following the temperature reduction.

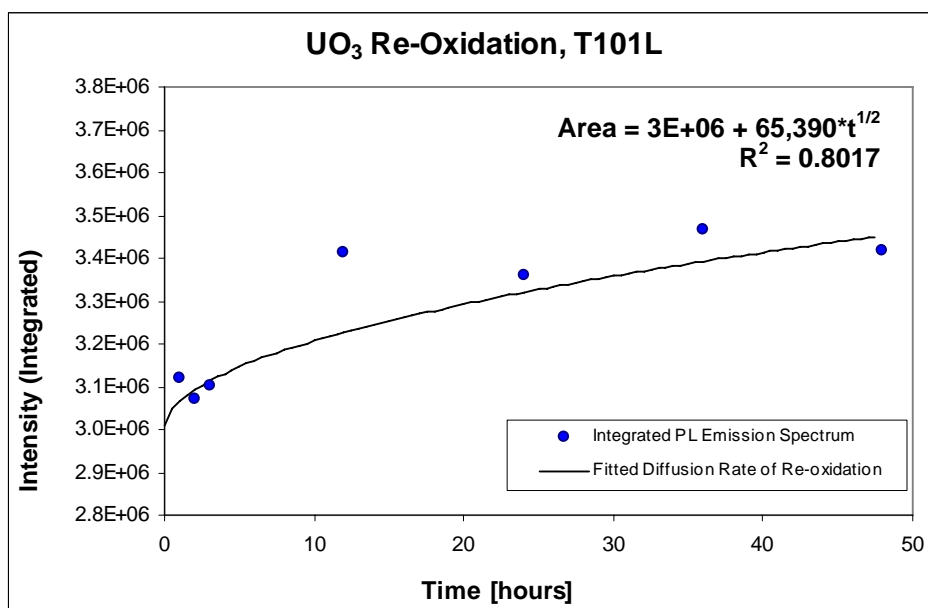


Figure 36. Results of the integration of the base line between 470 and 600 nm for UO₃ sample T101K after oxidation in 54 torr O₂ for 48 hours at 100° C. This figure has been fitted with an exponential curve. The exponential curve demonstrates that the re-oxidation is occurring through a diffusion controlled process.

The area under each PL emission spectrum was integrated using Gram32 Software in order to quantify the change in intensity of the PL emission spectra as the uranium oxide samples react at this increased temperature and reduced partial pressure of oxygen. A curve was fitted to the change in integrated area with respect to time in order to determine the rate of oxidation of PL emission intensity.

The results of the base-line integration are plotted in Figure 36 above. The empirically fitted diffusion equation is presented in equation 16 below. The correlation coefficient is 0.8017. The behavior of the re-oxidation appeared to follow a rate of increase in the intensity limited by diffusion.

$$Area = 3E + 06 + 65,390 \cdot t^{1/2} \quad \text{Eqn 16}$$

Measurements were ceased and the temperature was allowed to return to ambient of 28° C. Following an extended weekend, another PL measurement was taken at 335 hours. The intensity had increased to close to pre-reduction integral quantities, see Figure 33 above. The UO₃ reduction and oxidation experiments were then terminated and the UO₂ dry oxidation experiment was commenced.

A summary of the conditions and integration results of the reduction and re-oxidation of the UO₃ sample, T101L, is listed in Table 6 below.

Table 6. UO₃ Reduction and Oxidation Data Table of Sample T101L

Trial	Temp [°C]	P[O ₂]	Time [hours]	Integrated Area
		Pressure [torr]		
T101L_1	28	2×10^{-2}	0.5	6,074,524
T101L_2	28	2×10^{-2}	8.6	5,592,855
T101L_3	28	2×10^{-2}	19.6	5,388,334
T101L_4	28	2×10^{-2}	24.5	5,124,377
T101L_5	28	2×10^{-2}	43.6	5,200,783
T101L_6	28	54	2	5,249,485
T101L_7	28	54	12	5,440,437
T101L_8	28	54	24	5,385,058
T101L_9	28	54	36	5,411,182
T101L_10	28	54	60	5,362,378
T101L_A1	28	54	0	5,537,439
T101L_A2	100	56	0	3,225,873
T101L_A3	100	56	1	3,114,387
T101L_A4	100	56	2	3,063,550
T101L_A5	100	56	3	3,096,390
T101L_A6	100	56	12	3,407,559
T101L_A7	100	57	24	3,354,598
T101L_A8	100	57	36	3,458,089
T101L_A9	100	57	48	3,410,215
T101L_B1	28	57	335	5,534,557

UO₂ Dry Oxidation

Following the reduction and re-oxidation of the two UO₃ samples under various atmospheric conditions, the dry oxidation in pure oxygen of the initial UO₂ sample, labeled T-200A, was started. Before commencing the UO₂ oxidation experiment of this research, the weathering system was temperature and vacuum purged. Prior to pressing the UO₂ sample, most of the water vapor and organics were removed by evacuating and baking the weathering system for 48 hours. The vacuum system was evacuated down to 4×10^{-5} torr for 48 hours and heated to 150 °C for the last 24 hours of the vacuum purge. The UO₂ sample was created in accordance with Appendix C. Sample T-200A had a mass of 0.06-g, which corresponds to 2.22×10^{-4} moles (UO₂).

UO₃ sample T-200A was placed in the Hansen Cell and weathering system and the Hansen Cell sample holder temperature was adjusted to 70° C. An initial PL spectrum from 660 nm to 740 nm and from 470 nm to 660 nm was taken to verify that there were no indications of the uranyl ion present, see Figures 37 and 38 below. Only four PL emission scan were taken from 470 nm to 660 nm. You can see from the spectrum below that no indication of the characteristic uranyl peaks located at 489 nm, 509 nm, 531 nm, 553 nm, or the 581 nm shoulder peak as shown in Figure 6 above were present in our sample. Additionally, the peak identified in earlier research by Schueneman [Schueneman, et al., 2001] at 695 ± 2 nm was not evident in the PL emission spectrum, see Figure 17 above.

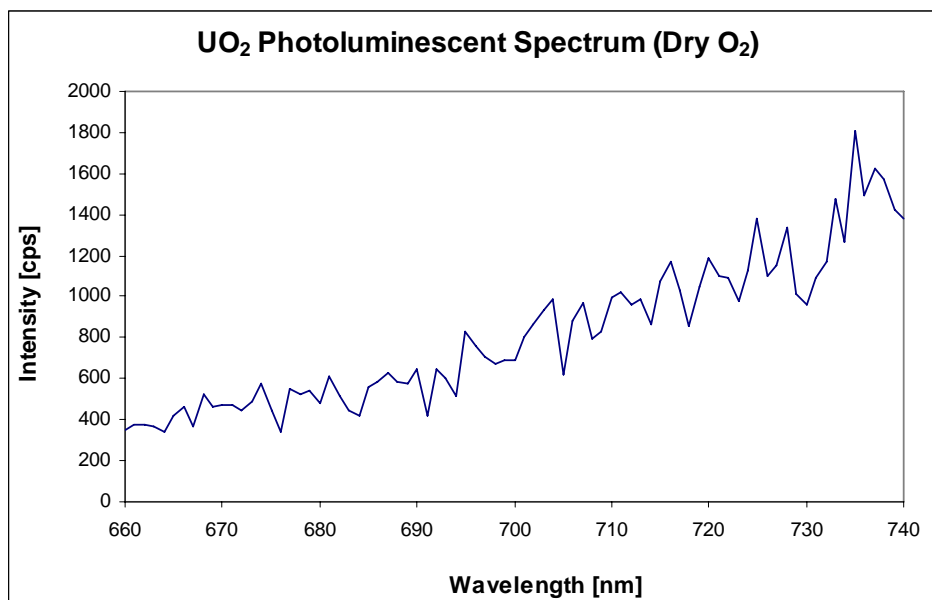


Figure 37. Initial lamp-corrected, front-face PL emission scan of UO_2 sample T200A scanned from 660 to 740 nm using 500 flashes per data point prior to exposure to oxygen and increased temperature.

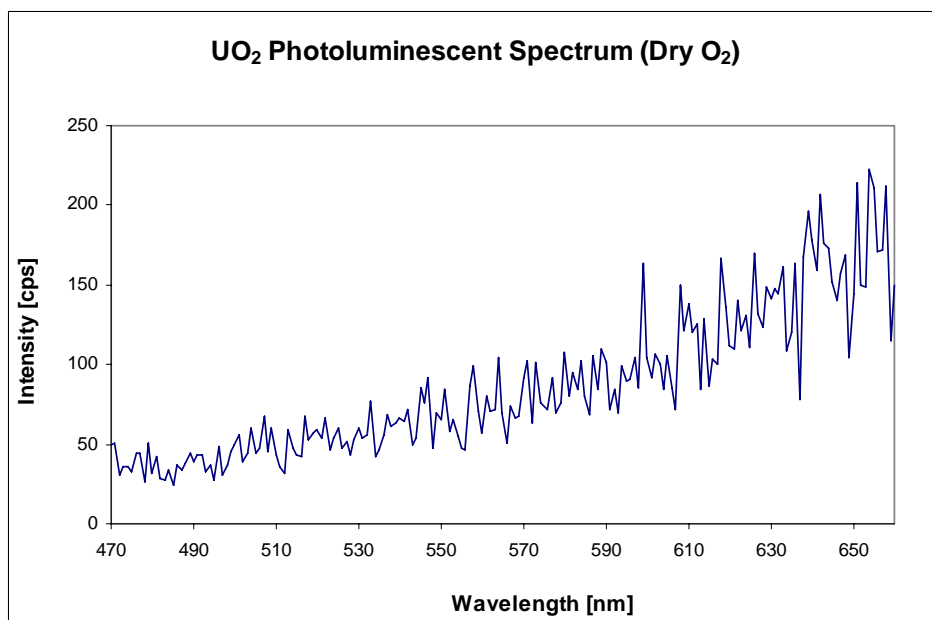


Figure 38. Initial lamp-corrected, front-face PL emission scan of UO_2 sample T200A scanned from 470 to 660 nm using only 200 flashes per data point prior to exposure to oxygen and increased temperature. None of the characteristic UO_3 peaks were evident in this sample at this time.

In Figure 37 above, the initial PL emission scan of the UO_2 sample, T200A, measured from 470 nm to 740 nm at 70° C and a partial O_2 pressure of approximately 8×10^{-5} torr of oxygen is shown. Following this PL emission scan of the UO_2 sample, a second PL measurement was taken after introducing 100 torr of dry oxygen into the weathering system. After two hours under these conditions, a spectrum from 660 nm to 740 nm was taken to establish a baseline photoluminescence signature of this sample, as shown in Figure 38 above. Again, the spectrum has no indication of the characteristic peaks of UO_3 or a peak at 695 nm.

Following the second PL emission scan of the UO_2 sample, 760 torr of dry Grade 5.0 oxygen was introduced into the weathering system and periodic measurements were started. After 122 hours at 70° C, the temperature was increased to 100° C in an attempt to accelerate the oxidation process. After 169 hours at 100° C, the temperature was again increased to 150° C. After 240 hours, the temperature was increased to 200° C. The temperature was kept at 200° C for the remainder of the dry oxidation experiment.

The environmental conditions were kept constant except for the temperature for 295 hours and periodic PL measurements were taken at approximately 12-hour intervals. The intensity remained generally constant throughout the measurements and no indication of the characteristic uranyl peaks located at 489, 509, 531, 553, or the 581 nm shoulder peak were present in our sample. Additionally, the peak at 695 nm did not emerge in any of the PL emission spectra taken during this experiment.

Due to time constraints and approaching deadlines, the dry oxidation of UO_2 experiment was discontinued and the wet oxidation begun. Figure 39 below shows a comparison of the initial and final PL emission spectrum of UO_2 sample T200A after 295 hours in these conditions from 660 nm to 740 nm. Figure 40 below shows a comparison of the initial and final PL emission spectrum of UO_2 sample T200A after 295 hours in these conditions from 470 nm to 660 nm.

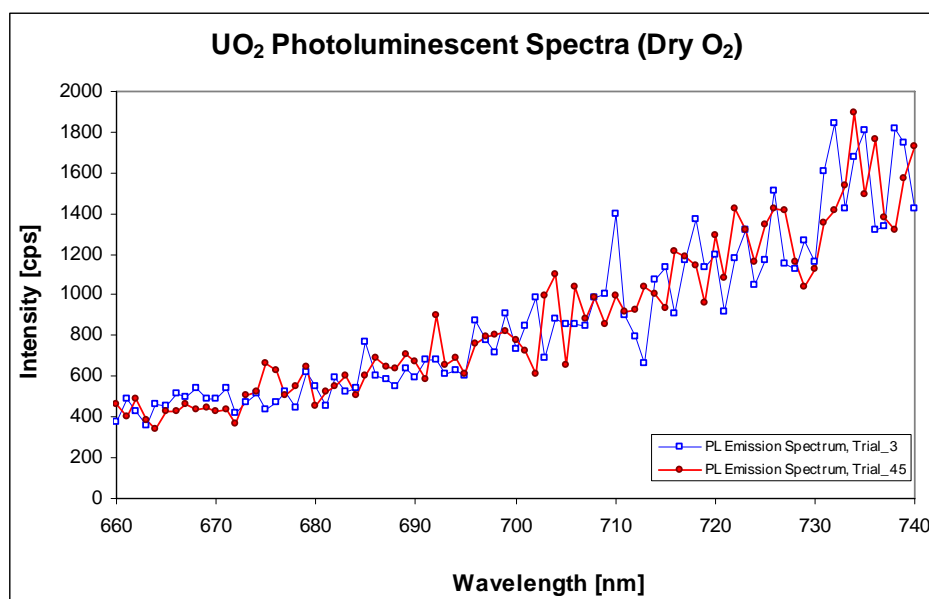


Figure 39. Initial and final lamp-corrected, front-face PL emission scans of UO_2 sample T200A scanned from 660 nm to 740 nm in 760 torr pure, dry O_2 at temperatures ranging from ambient to 200° C. The UO_3 peak at 695 nm did not emerge in this sample at the conclusion of this experiment.

The final temperature setting at 200° C damaged the Hansen Cell sample holder ring. This delayed the follow-on wet oxidation experiment by three days until the machine shop was able to repair the device.

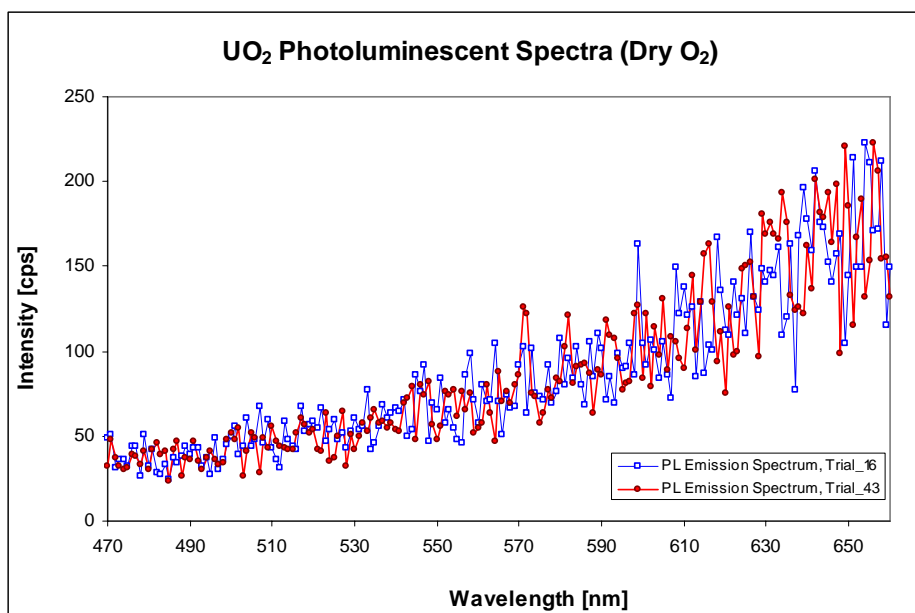


Figure 40. Initial and final lamp-corrected, front-face PL emission scans of UO_2 sample T200A scanned from 470 nm to 660 nm in 760 torr pure, dry O_2 at temperatures ranging from ambient to 200°C . None of the characteristic UO_3 peaks were evident in this sample at the conclusion of this experiment.

The area under each PL emission spectrum, the base-lines from 660 nm to 740 nm and the base-line from 470 nm to 660 nm, was integrated using Gram32 Software in order to quantify the change in intensity of the PL emission spectra as the uranium oxide samples react at this increased temperature and high partial pressure of pure, dry oxygen. From Figure 17 above, we know that the peak we are looking for is located at 695 ± 2 nm, or primarily under the curve limits from 680 nm to 710 nm. From this, I also integrated the PL emission spectra from 680 nm to 710 nm to get a more accurate assessment of the development of this peak. From this integration of the spectra collected, Figures 41 and 42 below demonstrate that UO_3 did not form on the UO_2 sample in sufficient quantities to increase the PL emission spectra.

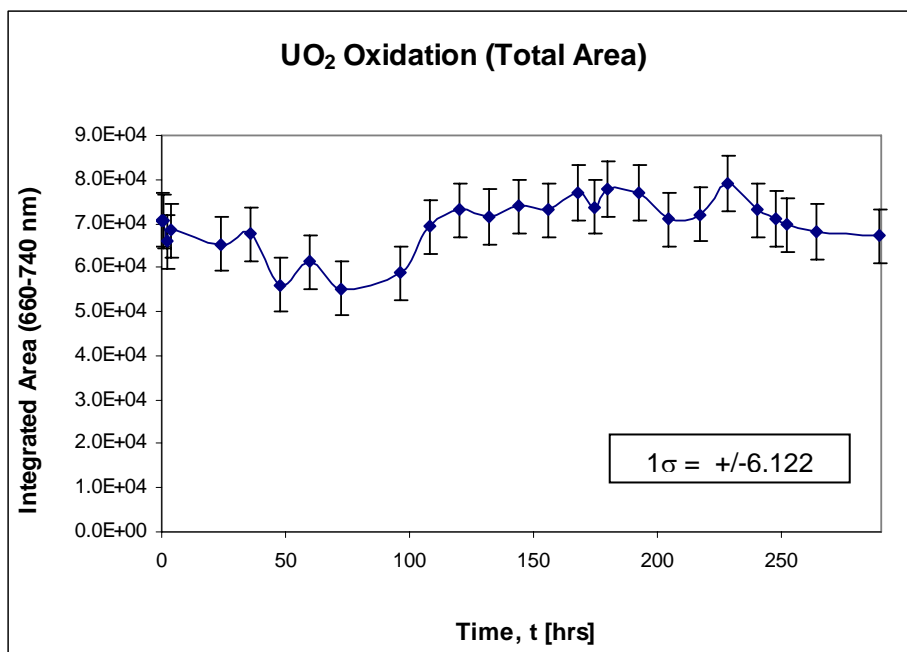


Figure 41. Results of the integration of the base line between 660 nm and 740 nm for UO₂ sample T200A after oxidation at temperatures ranging from ambient at 28° C to 200° C and a partial pressure of O₂ of 760 torr for 295 hours. The integration of the intensity over time demonstrates minor fluctuations, but no trends.

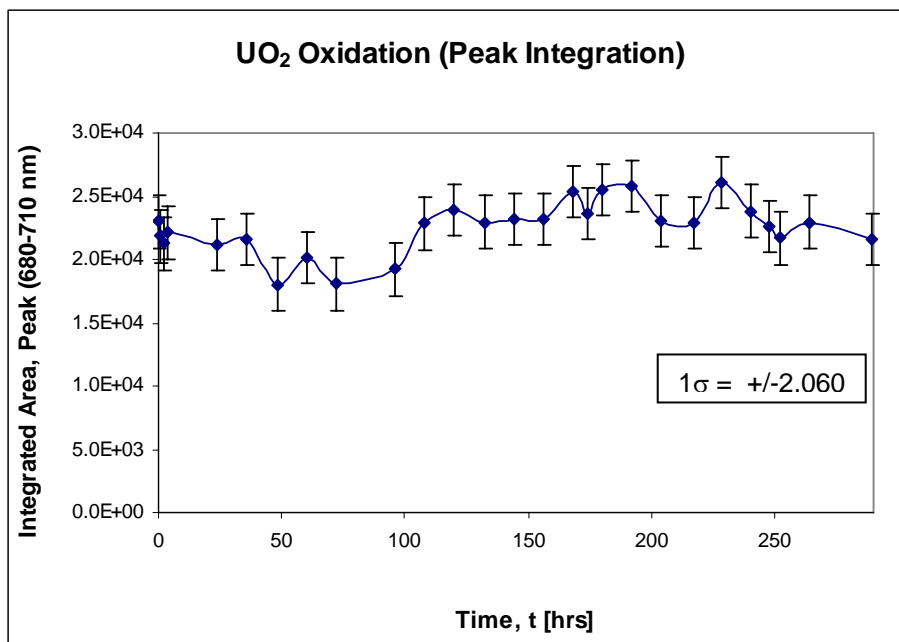


Figure 42. Results of the integration of the base line between 680 and 710 nm for UO₂ sample T200A after oxidation at temperatures ranging from ambient at 28° C to 200° C and a partial pressure of O₂ of 760 torr for 295 hours. Likewise for this figure, the integration of the intensity over time demonstrates minor fluctuations, but no trends.

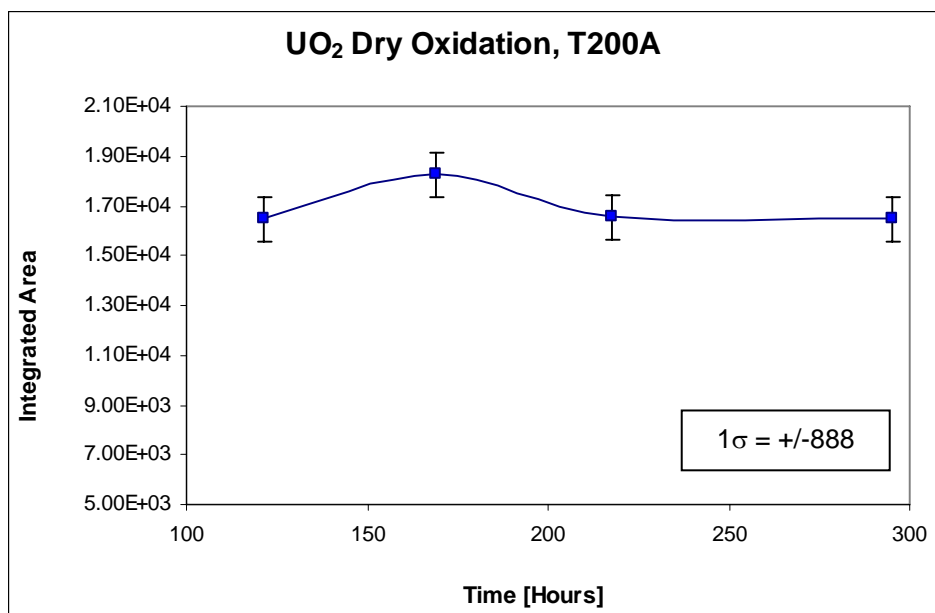


Figure 43. Results of the integration of the base line between 470 and 660 nm for UO₂ sample T200A after oxidation at temperatures ranging from ambient at 28° C to 200° C and a partial pressure of O₂ of 760 torr for 295 hours. Only four PL emission spectra were collected with these parameters. Additionally, the integration of the intensity over time demonstrates also minor fluctuations, but no trends.

A summary of the conditions and integration results of the dry oxidation of the UO₂ sample, T200A, is listed in Table 7 below.

Table 7. UO₂ Dry Oxidation Data Table

Trial	Temp [°C]	Pressure [torr]	Time [hours]	Integrated Area
T200A_1	30	4×10 ⁻⁴	0	N/A
T200A_2	70	100	2	N/A
T200A_3	70	760	0	70,731.43
T200A_4	70	760	1	70,515.19
T200A_5	70	760	2	65,898.13
T200A_6	70	760	4	68,377.34
T200A_7	70	760	24	65,300.89
T200A_8	70	760	36	67,630.17
T200A_9	70	760	48	55,976.19
T200A_10	70	760	60	61,365.54
T200A_11	70	760	72	55,246.99
* T200A_12	70	760	72.75	*
T200A_13	70	760	96	58,813.12
T200A_14	70	760	108	69,302.03
T200A_15	70	760	120	73,086.59
* T200A_16	70	760	121.5	*
T200A_17	100	770	132	71,510.00
T200A_18	100	770	144	73,948.79
T200A_19	100	770	156	70,065.62
T200A_20	100	770	168	76,965.67
* T200A_21	100	770	168.75	*
T200A_22	150	780	174.25	73,719.96
T200A_23	150	780	180	77,794.70
T200A_24	150	780	192	76,977.08
T200A_25	150	780	204	71,013.63
T200A_26	150	780	217	72,014.30
* T200A_27	150	780	217.5	*
T200A_28	150	780	228	79,064.22
T200A_29	150	780	240	73,104.72
T200A_30	200	790	247.25	71,075.31
T200A_31	200	790	252	69,652.71
T200A_32	200	790	264	68,143.96
T200A_33		Equipment malfunction – No data taken		
T200A_34	200	790	289	67,250.66
T200A_35	200	780	289.5	66,670.62
T200A_36	200	780	290	67,569.64
T200A_37	200	780	290.5	66,714.00
T200A_38	200	770	291.5	67,722.49
T200A_39	200	770	292	67,317.92
T200A_40	200	770	292.5	66,281.40
T200A_41	200	760	293	67,982.96

Table 7 (continued). UO₂ Dry Oxidation Data Table

Trial	Temp [°C]	Pressure [torr]	Time [hours]	Integrated Area
T200A_42	200	760	293.5	68,289.17
* T200A_43	200	760	295	*
T200A_44	200	760	300	69,510.66
T200A_45	200	760	312	70,930.42

* Denotes spectra taken from 470 nm to 660 nm.

UO₂ Wet Oxidation

Following the oxidation of UO₂ sample T200A, the weathering system was again evacuated and baked for 48 hours to minimize the presence in the system of any moisture content, complexes or compounds. Another UO₂ sample, T200B, was created in accordance with Appendix C and placed in the Hansen Cell. Sample T-200B had a mass of 0.08-g, or 2.96×10^{-4} moles (UO₂).

The UO₂ sample in the Hansen Cell was placed in the weathering system and exposed to vacuum. Our wet oxidizing environment was created by first clearing a flask of distilled water (purity of 18.2 MΩ·cm) of all gases present. The flask was heated to approximately 70° C and exposed to a vacuum, which caused the water to boil. The vacuum removed the gas over the water. This process was repeated three times to remove all gas and leave only water vapor in the flask. The flask was sealed with an internal petcock. The flask of water and water vapor was connected to the weathering system. The flask petcock was opened and 60 torr of water vapor was introduced into the weathering system, see Appendix H. After stabilizing the system, 700 torr of dry, Grade 5.0 oxygen was introduced into the weathering system.

The UO₂ sample, T200B, was allowed to stabilize in this environment for two hours, after which a PL measurement was taken. As expected, there was no indication of the characteristic uranyl peaks located at 489 nm, 509 nm, 531 nm, 553 nm, or the 581 nm shoulder peaks were present in our sample. Additionally, the peak identified in earlier research by Schueneman [Schueneman, et al., 2001] at 695 ± 2 nm, as shown in

Figure 17 above, was not evident in the PL emission spectrum, see Figures 44 and 45 below.

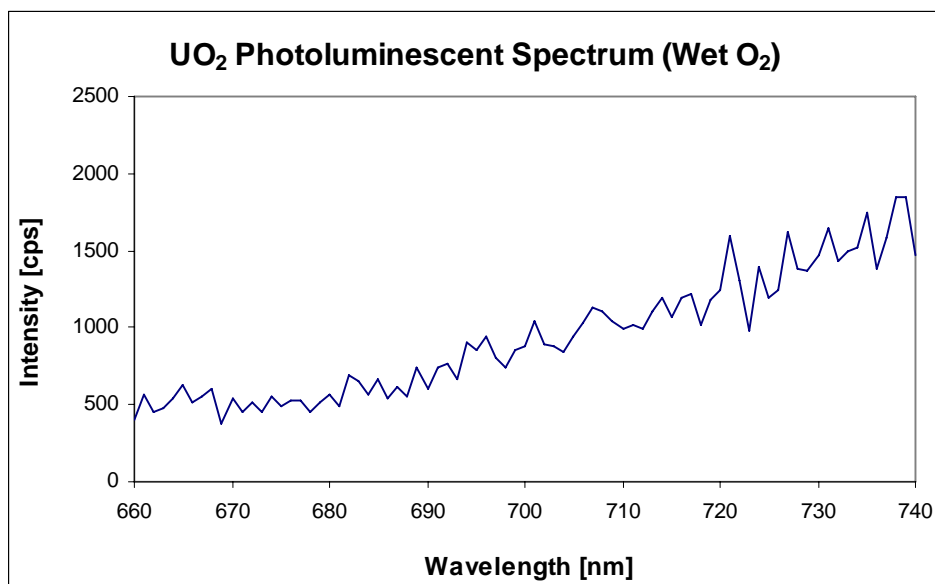


Figure 44. Initial lamp-corrected, front-face PL emission scan of UO₂ sample T200B scanned from 660 to 740 nm prior to exposure to wet oxygen and increased temperature.

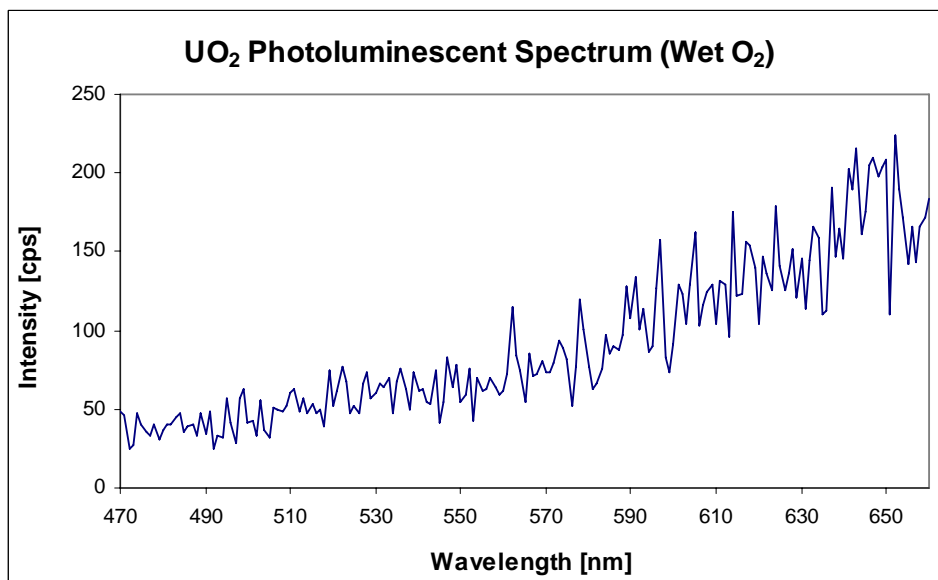


Figure 45. Initial lamp-corrected, front-face PL emission scan of UO₂ sample T200B scanned from 470 to 660 nm prior to exposure to wet oxygen and increased temperature.

After 20 hours in these conditions, the temperature was increased to 110° C in an attempt to accelerate the chemical reaction of UO_2 with oxygen and water vapor. Periodic PL emission measurements were taken at approximately 12-hour intervals, later at 24-hour intervals, see Table 8 below.

During the time interval of the measurements between approximately 330 hours to 390 hours, there was a significant increase in the intensity of the spectra recorded without the development of a recognizable peak. This was originally taken as an indication of oxidation occurring on the UO_2 sample. Around hour 389, the cover for the photomultiplier tube was discovered to be missing. It had slipped and was lying on the floor. The cover was replaced, at which time, the intensity returned to a value commiserate with those taken at hour 318 (see Conclusions and Recommendations for a full treatment of this event and lessons learned).

PL emission scans were continued in these conditions at regular intervals for 809 hours, after which the temperature controller was turned off and the UO_2 sample allowed to return to an ambient temperature of 28° C.

There was no indication of the characteristic UO_3 peaks located at 489 nm, 509 nm, 531 nm, and 553 nm present in our wet oxygen oxidized UO_2 sample. Additionally, the peak identified in earlier research at 695 nm was not present.

Figure 46 below shows a comparison of the initial and final PL emission spectrum of UO_2 sample T200B after 1030 hours in these conditions from 660 nm to 740 nm.

Figure 47 below shows a comparison of the initial and final PL emission spectrum of UO_2 sample T200A after 1031 hours in these conditions from 470 nm to 660 nm.

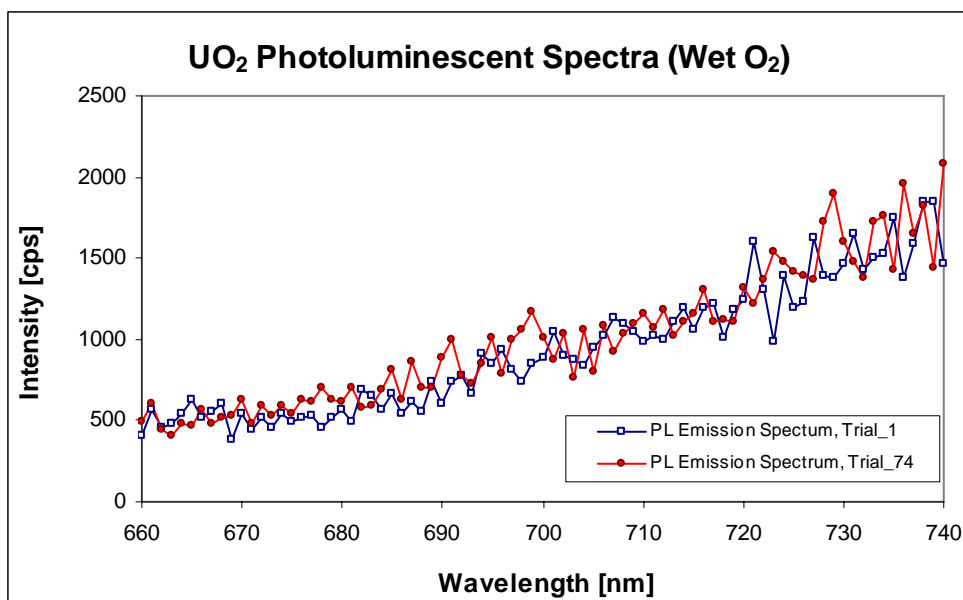


Figure 46. Initial and final lamp-corrected, front-face PL emission scans of UO_2 sample T200B scanned from 660 nm to 740 nm in 60 torr distilled water vapor and 700 torr pure O_2 at temperatures ranging from 110°C and below. The UO_3 peak at 695 nm did not emerge in this sample at the conclusion of this experiment.

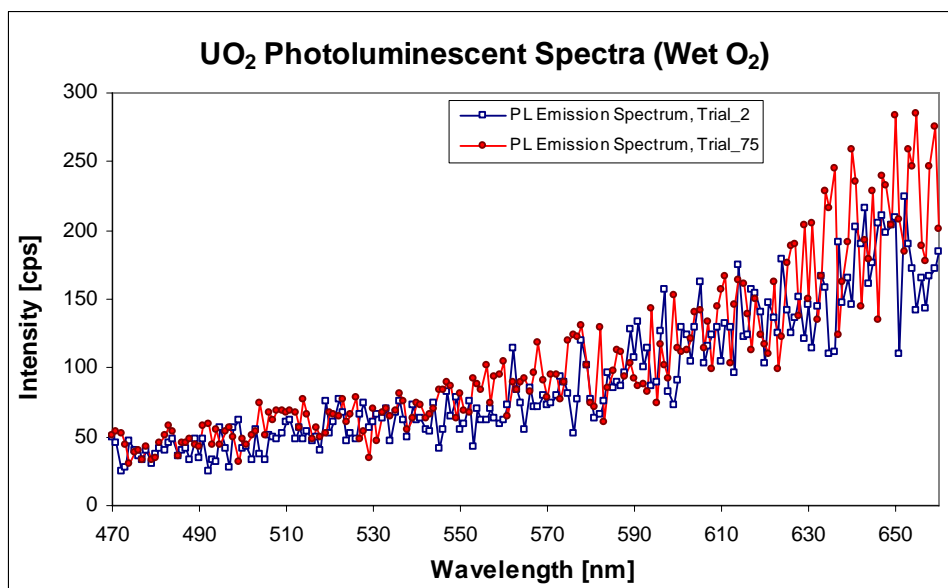


Figure 47. Initial and final lamp-corrected, front-face PL emission scans of UO_2 sample T200B scanned from 470 nm to 660 nm in 60 torr distilled water vapor and 700 torr pure O_2 at temperatures ranging from 110°C and below. None of the characteristic UO_3 peaks were evident in this sample at the conclusion of this experiment.

Using identical parameters as the dry oxygen oxidation experiment, the area under each PL emission spectrum, the base-lines from 660 nm to 740 nm and the base-line from 470 nm to 660 nm, was integrated using both Gram32 Software and Microsoft Excel™ in order to quantify the change in intensity of the PL emission spectra as the uranium oxide samples react at this increased temperature and high water vapor pressure and partial pressure of pure oxygen. From Figure 17 above, we know that the peak we are looking for is located at 695 ± 2 nm, or primarily under the curve limits from 680 nm to 710 nm. From this, I also integrated the PL emission spectra from 680 nm to 710 nm to get a more accurate assessment of the development of this peak. From this integration of the spectra collected, Figures 48 and 49 below demonstrate that a fluorescing phase of UO_3 did not form on the UO_2 sample in sufficient quantities to increase the PL emission spectra. Additionally, the UO_3 characteristic signature shown in Figure 9 above demonstrates that the most prominent peak in the 470 nm to 660 nm range occurs at 509 nm. This peak was also integrated from 496 nm to 524 nm to obtain a more accurate assessment of the development of the peak as it emerged.

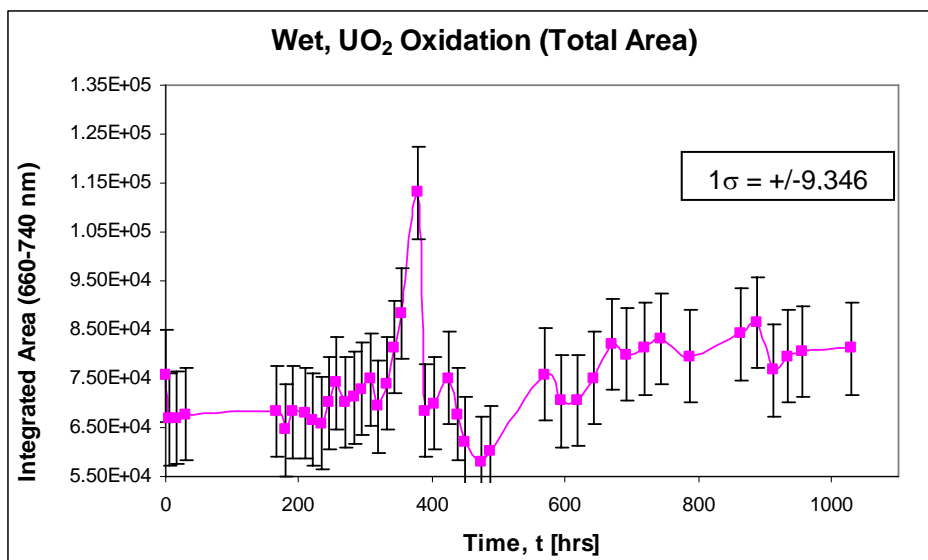


Figure 48. Results of the integration of the base line between 660 nm and 740 nm for UO₂ sample T200B after oxidation at 110° C in 60 torr distilled water vapor and a pressure of 700 torr of pure O₂ for 1030 hours. The integration of the intensity over time demonstrates only a slight increase over time (excluding the peak located at 350 hours).

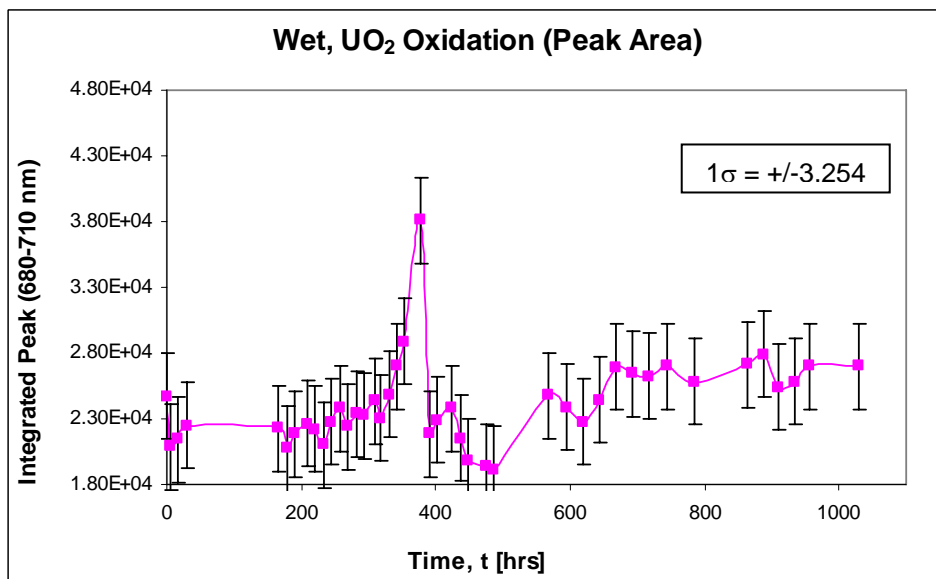


Figure 49. Results of the integration of the peak area between 680 nm and 710 nm for UO₂ sample T200B after oxidation at 110° C in 60 torr distilled water vapor and a pressure of 700 torr of pure O₂ for 1030 hours. The integration of the intensity over time demonstrates only a slight increase over time (again, excluding the peak located at 350 hours).

Figure 48 above demonstrates the results of the base-line integration of the UO_2 sample T200B after exposure to 60 torr of distilled water vapor and 700 torr of pure oxygen at 110° C for 1030 hours. The limits for the integration were set from 660 nm to 740 nm, the entire PL emission scan. While the intensity of the area under the spectrum curve did increase over time, the peak expected at 695 nm did not emerge. The peak located at approximately hour 350 was discussed earlier.

Figure 49 above demonstrates the results of the peak area integration of the UO_2 sample after exposure to 60 torr of distilled water vapor and 700 torr of pure oxygen at 110° C for 1030 hours. The limits for the integration were set from 680 nm to 710 nm. Again, while the intensity of the area under the expected peak area did increase over time, the peak did not emerge.

Figure 50 below demonstrates the results of the base-line integration of the UO_2 sample after exposure to 60 torr of distilled water vapor and 700 torr of pure oxygen at 110° C for 1031 hours. The limits for the integration were set from 470 nm to 660 nm, the entire PL emission scan. While the intensity of the area under the spectrum curve did increase over time, the characteristic UO_3 peaks shown in Figure 9 above did not emerge.

Figure 51 below demonstrates the results of the peak area integration of the UO_2 sample after exposure to 60 torr of distilled water vapor and 700 torr of pure oxygen at 110° C for 1031 hours. The limits for the integration were set from 496 nm to 524 nm. Again, while the intensity of the area under the expected peak area did increase over time, the peak did not emerge.

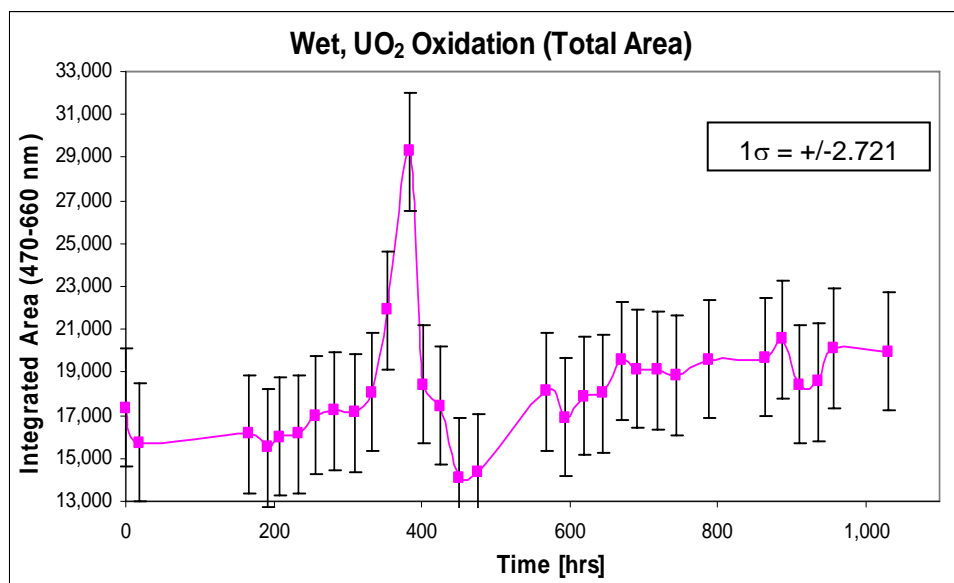


Figure 50. Results of the integration of the base line between 470 nm and 660 nm for UO₂ sample T200B after oxidation at 110° C in 60 torr distilled water vapor and a pressure of 700 torr of pure O₂ for 1031 hours. The integration of the intensity over time demonstrates only a slight increase over time (excluding the peak located at 350 hours).

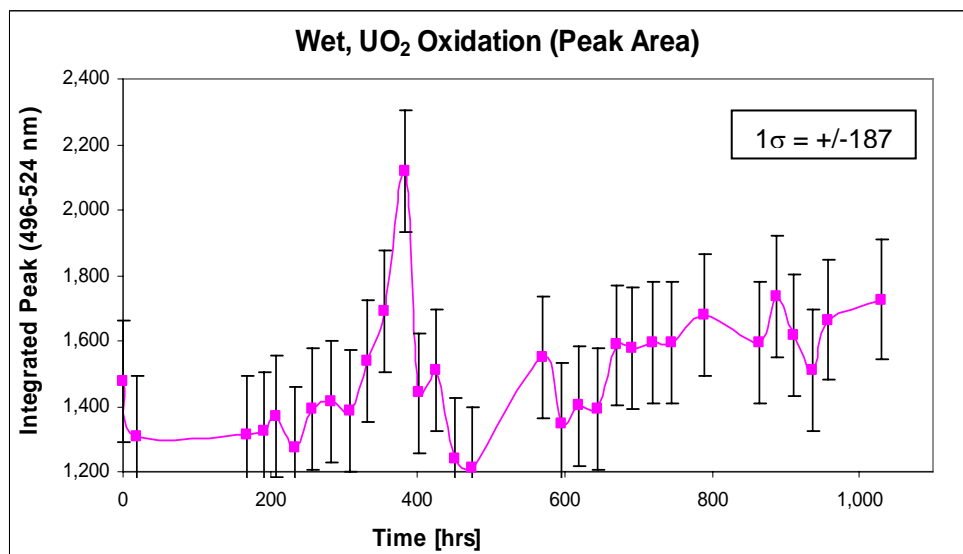


Figure 51. Results of the integration of the peak area between 496 nm and 524 nm for UO₂ sample T200B after oxidation at 110° C in 60 torr distilled water vapor and a pressure of 700 torr of pure O₂ for 1031 hours. The integration of the intensity over time demonstrates only a slight increase over time (again, excluding the peak located at 350 hours).

In Figure 52 below a comparison of the final scan of UO₂ sample T200A oxidized under dry oxygen conditions at temperatures ranging from ambient to 200° C for 895 hours is compared to the final scan of UO₂ sample T200B oxidized under wet oxygen conditions at 110° C for 1031 hours. The final PL emission spectrum of the UO₃ sample T200B was more intense than that generated by T200A, however the difference is negligible.

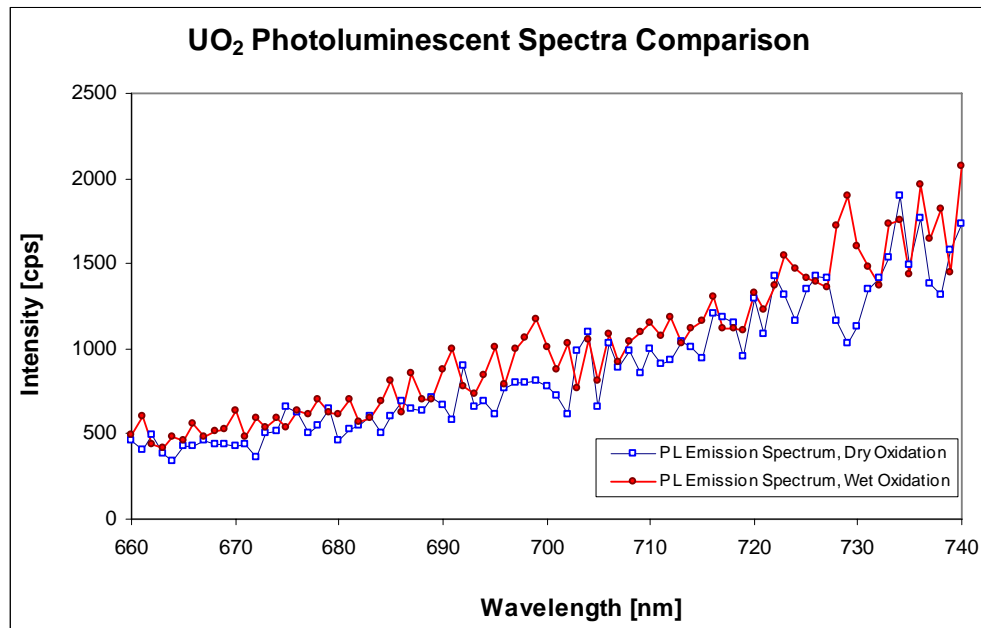


Figure 52. Final lamp-corrected, front-face PL emission scans of UO₂ samples T200A and T200B scanned from 660 nm to 740 nm. Although T200B was slightly more intense than T200A, the differences are negligible; no conclusions are developed from this data. The peak at 695 nm did not emerge in either sample at the conclusion of this research.

An analysis of the results from this experiment suggest that the oxidation of UO_2 under wet oxygen conditions at elevated temperatures does not lead to a phase of UO_3 that contained the uranyl ion, and hence fluoresces, in the time allotted for this research. Previous research [Schueneman, 2001] demonstrates that the oxidation of UO_2 under similar environmental conditions, but at lower temperatures, will lead to the chemical transition of UO_2 towards a fluorescent phase of UO_3 as measured by PL emission spectroscopy and the development of a recognizable peak at 695 nm. From the data gathered during the temperature reduction of UO_3 , the PL emission spectrum of UO_3 is significantly degraded with the introduction of elevated temperatures. After the UO_3 sample was degraded by high temperatures and subsequently re-oxidized under pure, dry oxygen, the PL emission spectrum intensity did not return to the levels prior to increasing the temperature. This suggests that other chemical reactions are taking place at these elevated temperatures that could suppress the PL emission spectrum by way of transitioning from a UO_3 phase that fluoresces to one that does not. Therefore, as UO_2 oxidizes with oxygen, or oxygen and water vapor, and transitions towards UO_3 , which has a prominent PL emission signature, the peak being developed could be eroding faster than it is being created.

A summary of the conditions and integration results of the wet oxidation of the UO_2 sample, T200B, is listed in Table 8 below.

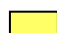
Table 8. UO₂ Wet Oxidation Data Table

Trial	Temp [°C]	Pressure [torr]	Time [hours]	Integrated Area
T200B_1	35	760	0	75,633.29
* T200B_2	31	753	0.75	* 17,367.86
T200B_3	30	760	6	66,796.31
T200B_4	30	752	16	67,026.27
* T200B_5	30	752	19	* 15,733.63
T200B_6	110	736	30	67,668.02
T200B_7	110	736	167	68,321.04
* T200B_8	110	736	167.5	* 16,149.40
T200B_9	110	736	179	64,576.05
T200B_10	110	736	191	68,152.17
* T200B_11	110	736	191.5	* 15,505.26
T200B_12	110	736	208.5	67,974.92
* T200B_13	110	736	209	* 15,985.64
T200B_14	110	736	220	66,575.36
T200B_15	110	736	233.5	65,880.08
* T200B_16	110	736	234	* 16,136.52
T200B_17	110	736	244	70,011.21
T200B_18	110	736	257	74,196.11
* T200B_19	110	736	257.5	* 16,994.92
T200B_20	110	736	270	70,211.79
T200B_21	110	736	282	71,233.45
* T200B_22	110	736	283	* 17,205.50
T200B_23	110	736	294	72,865.05
T200B_24	110	736	308.5	74,923.88
* T200B_25	110	736	309	* 17,125.77
T200B_26	110	736	318	69,336.98
T200B_27	110	736	331.5	74,063.34
* T200B_28	110	736	332	* 18,081.01
T200B_29	110	736	342	81,386.04
T200B_30	110	736	354	88,369.41
* T200B_31	110	736	354.5	* 21,898.10
T200B_32	Equipment malfunction – no data taken			
T200B_33	110	736	378.5	112,981.06
* T200B_34	110	736	382.5	* 29,294.58
T200B_35	110	736	390	68,417.27
T200B_36	110	736	402	69,938.05
* T200B_37	110	736	402.5	* 18,417.64
T200B_38	110	736	425	75,156.24
* T200B_39	110	736	426	* 17,457.74
T200B_40	110	736	438	67,710.10
T200B_41	110	736	449.5	61,9232.74

Table 8 (continued). UO₂ Wet Oxidation Data Table

Trial	Temp [°C]	Pressure [torr]	Time [hours]	Integrated Area
* T200B_42	110	736	450	* 14,119.91
T200B_43	110	736	474	57,910.54
* T200B_44	110	736	475	* 14,335.29
T200B_45	110	736	487	60,166.45
T200B_46	110	736	569	75,852.21
* T200B_47	110	736	569.5	18,108.40
T200B_48	110	790	594	70,500.75
* T200B_49	110	790	594.5	16,916.40
T200B_50	110	845	618	70,571.33
* T200B_51	110	845	618.5	17,904.84
T200B_52	110	826	643.5	75,092.13
* T200B_53	110	826	644.5	18,020.58
T200B_54	110	826	669	81,995.31
* T200B_55	110	826	670	19,557.28
T200B_56	110	823	691.5	79,946.73
* T200B_57	110	823	692	19,142.88
T200B_58	110	819	718.25	81,160.02
* T200B_59	110	819	718.75	19,099.57
T200B_60	110	818	743.5	83,194.69
* T200B_61	110	818	744.25	18,855.76
T200B_62	110	812	786.25	79,594.03
* T200B_63	110	818	789	19,579.03
T200B_64	110	802	863	84,134.33
* T200B_65	110	808	863.5	19,693.98
T200B_66	45	810	887	86,483.47
* T200B_67	45	810	887.5	20,557.26
T200B_68	30	800	911	76,674.36
* T200B_69	30	800	911.5	18,425.07
T200B_70	28	796	935	79,613.89
* T200B_71	28	796	935.5	18,556.85
T200B_72	28	799	957	80,575.72
* T200B_73	28	799	957.5	20,116.72
T200B_74	29	794	1030	81,147.37
* T200B_75	29	794	1031	19,956.08

* Denotes spectra taken from 470 – 660 nm.

 Denotes data taken with PM tube cover removed.

Surface analysis

During the wet oxidation experiment, the surface analysis and particle size measurements were taken of the UO_2 powder. The UO_2 powder used was from the same batch of material used for both the dry and wet oxidation experiments. The UO_2 powder was transferred and measured under a pure nitrogen environment in a glove box that had been nitrogen purged for the previous three weeks. A small portion of UO_2 was placed in a 12 mm sample container and weighed using an electronic scale accurate to three digits at 1.810 g. The sample was then transferred to the NOVA-1000 for analysis. The sample parameter are described Appendix I. The same sample was analyzed six times to develop a good standard deviation in the measurements. The results of the measurements are presented in Table 9 below. After applying the Q-Test to the measured data, the surface area values for Trial_n4c3001 and Trial_n510202 were discarded.

The NOVA-1000 also measured the volume and from the entered value for mass, developed a value for the density of the material. The results of these measurements are presented in Table 10 below.

Table 9. BET surface area results and comparison.

Trial	25-Point BET		Single-Point BET	
	Surface Area [m ²]	Spec Surface Area [m ² /g]	Surface Area [m ²]	Spec Surface Area [m ² /g]
n4c3001	1.167369	0.644955	2.389183	1.319991
n4c3101	1.245438	0.688087	2.179548	1.204170
n4c3102	1.390756	0.768374	2.780359	1.536110
n510101	1.338195	0.739334	2.866907	1.583926
n510201	1.433696	0.792097	2.972534	1.642284
n510202	1.183900	0.654100	2.508927	1.386148
* Average	1.352021	0.746973	2.699837	1.491623
* Standard Dev.	0.081081	0.044796	0.355650	0.196492

* Excludes values from the first and last trials.

The NOVA-1000 was calibrated and the sample cell was cleaned with methanol and calibrated before being utilized. The Nova Data Reduction™ software was requested and received from the Quantachrome Corporation and installed on the accompanying computer. This software processed all data included in this presentation.

The UO₂ sample was vacuum out-gassed under a reduced pressure of approximately 10⁻² torr and at a temperature of 300° C prior to each measurement to remove all moisture and other gases from the surface of the particles. A preset standard of 770 mm Hg for atmospheric pressure was used for all measurements. The first measurement had some fluctuations at the beginning of the scan but smoothed out (see Figure 53 below) as the measurement continued.

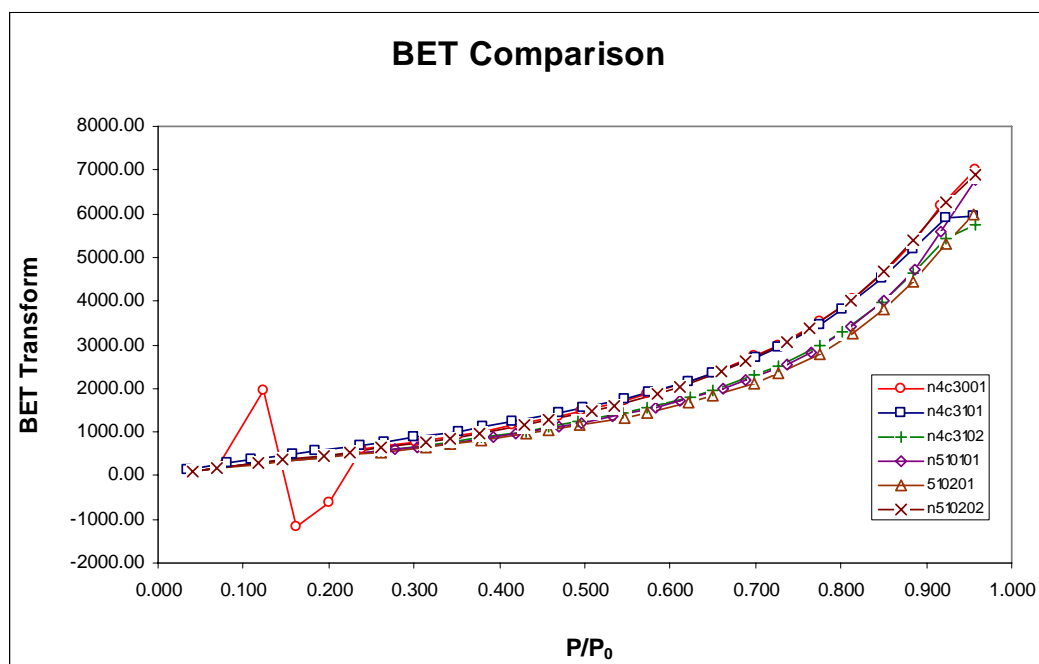


Figure 53. The 25-Point BET comparison of all measurements taken of the UO_2 powder sample. Note the separation between the first and last measurements compared to the other measurements.

Table 10. BET volume and density results and comparison.

Trial	Sample Volume [cm³]	Sample Density [g/cm³]
n4c3001	0.1313	13.7902
n4c3101	0.2157	8.3908
n4c3102	0.2200	8.2268
n510101	0.2104	8.6025
n510201	0.2249	8.0497
n510202	0.1120	16.1580
* Average	0.2178	8.3175
* Standard Dev.	0.006175	0.2356

* Excludes values from the first and last trials.

The value established for the density of UO₂ is 10.96 g/cm³ (Source: CRC, 61st Edition). The value established for the density of U₃O₈ is 8.30 g/cm³. Similar to the BET surface analysis and measurements, after applying the Q-Test to the measured data, the density values for Trial_n4c3001 and Trial_n510202 were discarded. This suggests that the UO₂ sample was in fact U₃O₈. Analysis by X-Ray Diffraction Spectroscopy can determine the exact surface composition of the particles, see Chapter V, Recommendations.

Note: the Q-Test is used to identify statistical outliers in data. Values for the Q-Test are given as a 90% confidence interval that the outlier should be included.

$$Q_n = \frac{|x_a - x_b|}{R} \quad \text{Eqn 17}$$

Where:

R is the range of all data points

x_a is the suspected outlier

x_b is the data point closest to x_a

V. Conclusions and Recommendations

Chapter Overview

The goal of this research was to use *in-situ* Photoluminescent (PL) Spectroscopy to measure the time rate change of oxidation of a UO_2 sample as it chemically reacts with dry oxygen and wet oxygen and transitions towards UO_3 under these set environmental conditions. The UO_2 samples were exposed to a range of temperatures below 200°C and monitored periodically to detect the growth of UO_3 on the sample's surface.

Conclusions of Research

The *in-situ* PL spectroscopy measurements did not detect the presence of a form of UO_3 with the uranyl ion present on the UO_2 samples, neither at the beginning, as expected, nor the end of the oxidation experiments. Quantitative data was gathered by integrating the area under the curve of the full spectrum generated by PL measurements. For both the dry and wet oxidation experiments, the integrated area had minor fluctuations in the intensity of the spectra, which could be explained by variations in the light and temperature conditions in the laboratory and the sensitivity of the photomultiplier tube. The characteristic spectrum of UO_3 with the uranyl ion present, shown in Figure 9, did not appear.

UO_3 is known to have one amorphous phase and six crystalline phases, of which four contain the uranyl ion and three, do not. During PL spectroscopy, the presence of

the uranyl ion is responsible for the observed photoluminescence. The oxidation of UO_2 to U_3O_8 is relatively quick when compared to the continued oxidation of U_3O_8 to UO_3 . The UO_2 samples were not oxidized long enough for the formation of a UO_3 phase with the uranyl ion on the surface of the UO_2 samples. Any UO_3 formed on the surface of the UO_2 particles was not one of the known phases that exhibit photoluminescence and therefore could not be characterized by *in-situ* PL spectroscopy.

The precursor to the UO_2 oxidation experiments, UO_3 oxidation and reduction, was consistent with previous research conducted and reported at AFIT.

Recommendations for Action

Future Research

Future experiments should be conducted at reduced temperatures, approximate ambient temperatures, to more accurately model the actual temperature range a loose UO_2 particle will experience prior to collection and analysis. Additionally, temperature reduction experiments of UO_3 demonstrated a significant reduction in the PL emission spectrum, possibly a phase transition of UO_3 towards a different phase of UO_3 which does not exhibit photoluminescence. Future experiment should be developed which evaluate the degradation of UO_3 and possible phase transitions of UO_3 at elevated temperatures to better develop and understand the end state of UO_2 oxidation. Additional spectroscopy techniques must be incorporated in future research to accurately determine the surface condition of the oxidized UO_2 particle as well as all phases of UO_3 which may

have formed. X-Ray Diffraction Spectroscopy and Neutron Diffraction Spectroscopy are two spectroscopy techniques that can be used to accurately determine the final crystal structure of the oxidized UO_2 particles. These spectroscopy techniques can also be used to determine the phase of UO_3 as it is formed on the particle's surface.

The Fluorolog-3 uses a photomultiplier to amplify the emission signal generated from the uranium oxide sample. The photomultiplier is extremely sensitive to light and was covered by a black cloth to prevent any ambient light from entering the photomultiplier tube. Even with this cover, differences in the intensity of the spectrum generated were influenced with the lights being turned on versus the lights being turned off. Additionally, the photomultiplier was affected with the ambient temperature of the laboratory. Initial measurements were conducted at 28 °C, but some subsequent measurements during the wet oxidation of UO_2 were conducted with an air conditioning unit turned on which lowered the ambient temperature to 24 °C. The lower temperature in the laboratory resulted in a slight decrease in the overall intensity of the spectra taken. A thermometer is located in the vicinity of the Fluorolog-3. Recommend that one, measurements be taken at night when the traffic through the laboratory has ceased and the researcher can conduct the experiment in completely dark conditions, and two that the ambient temperature be monitored and maintained at a constant temperature for all measurements. These two conditions would greatly aid in stabilizing the fluctuations in the integrated area of the spectra taken over time.

The density measurements conducted using the NOVA-1000 indicated that the UO_2 sample was in fact U_3O_8 . Since the experiment was a determination of the

formation of UO_3 ; the end state in the uranium dioxide oxidation process, the oxidation process monitored by *in-situ* PL was the same. However, to accurately report the oxidation of UO_2 towards UO_3 , higher quality material must be used. Additionally, X-Ray Diffraction Spectroscopy or Neutron Diffraction Spectroscopy could be used to accurately determine the composition of the particle's surface. This should be included in future research to determine if the particle's surface composition is such that it may not emit a PL emission spectrum.

The Hansen cell should be replaced with a device that can sustain a higher vacuum. The Hansen cell was the weak link in the vacuum system. When connected to the vacuum and weathering system, it maintains a seal with only one o-ring. This seal was insufficient to maintain the vacuum conditions generated in the vacuum system, although lubricating the seal with vacuum grease permitted a lower vacuum than without.

Finally, future research into the oxidation of UO_2 powder must be started as early as possible to maximize the time available for oxidation. Any delays at the beginning of the research window must be eliminated so the oxidation can commence.

Appendix A. Equipment

This appendix contains a comprehensive listing and description of all the equipment used in the uranium dioxide oxidation research. Appendices B through I contain the operating instructions and settings used throughout the experiment. Additional information and instructions can be found in the individual equipment operating manuals. Most of the equipment operates with high voltages, high temperatures, or high vacuum and may contain radioactive materials so use caution and follow all safety procedures. The “Uranium Oxidation Protocol” outlines the basic procedures to follow when working with the loose uranium oxide powders and the prepared uranium oxide samples.

A-1. Glove Box

A-2. Hydraulic Press and Dies

A-3. Vacuum System

A-4. Water Vapor Introduction

A-5. Hansen Cell

A-6. Photoluminescence Spectrometer

A-7. Particle Surface Analysis

A-1. Glove Box

A Plas-LabsTM Model 818-GB Glove Box was utilized to provide the controlled atmospheric environment that was required when working with loose uranium dioxide (UO_2) powder in preparing our samples for measurement. A photo is shown in Figure 54 below.



Figure 54. Plas-LabsTM 818-GB Glove Box

The Glove Box consists of a working volume and an airlock system. The side airlock system is used to introduce and remove items from the working volume of the Glove Box while providing a means of controlling the introduction of ambient air and the release of the controlled atmosphere of the working volume as well as any loose particulates of UO_2 . The airlock has two doors. The outer door opens to the laboratory

environment and the inner door opens to the working volume of the Glove Box. The airlock has a volume of 0.19-cubic meters and is equipped for the introduction of nitrogen and connection to a vacuum system. The Glove Box is also equipped with a pair of HypalonTM gloves that are used to manipulate items and equipment located in the working volume of the Glove Box. The Glove Box has a grounded electrical power strip in the working volume to provide 110-volt power to requisite electronic equipment. It also has one vacuum valve and three gas valves that allow for control of the atmospheric conditions within the airlock and working volume of the Glove Box. Additionally, a Caver® Hydraulic Press has been placed inside the working volume of the Glove Box for use in preparing our UO₂ samples. Appendix B contains the procedures that are to be followed to add and remove items from the Glove Box.

WARNING: Failure to operate the Glove Box in strict adherence with applicable safety precautions could result in contamination of the laboratory with loose UO₂ powder and the working volume of the Glove Box with ambient air.

A-2. Hydraulic Press and Dies

A manual Carver® hydraulic press with 24,000-pound capacity was used to press the UO₂ powder into the tungsten screen, see Figure 55 below. The press has a variable position head and a mechanical gauge that indicates the amount of force being applied. A

set of custom dies was created for the previous experiment [Schueneman] for preparing the UO_2 powder samples.



Figure 55. Carver® hydraulic press.

The preparation and pressing of the uranium oxide samples required the design and fabrication of dies that would not deform due to the hardness of the uranium oxide powders or the high pressures used in pressing the uranium oxide powders into the tungsten screen (see Figure 56). The surfaces of the dies that came in direct contact with the uranium oxide powders were hardened steel (Rockwell C greater than 50) and all other pieces were medium strength alloyed steel. After approximately twenty pressings, the plug and bottom plate had surface damage from the uranium oxide powders that was

visible with the naked eye. See Appendix F for the procedures used to prepare a sample with the press and dies.



Figure 56. Custom pressing dies for sample creation.

A-3. Vacuum System

A vacuum system was designed and built [Schueneman, et. al.] to remove all but a monolayer of molecules covering the surface of the uranium oxide samples and provide a means of introducing research grade gases at any pressure up to 760-torr into the Hansen cell. The vacuum system contains all 316-stainless steel tubing and 316-stainless steel Swagelock® fittings mated to a Varian Turbo Pump and an Alcatel Drytel Pump. The system has additional fittings to allow for more than one type of gas to be introduced into the system at any one time.

Figures 57 and 58 below contain drawings [Schueneman, 2001] and photographs of the complete upper and lower vacuum system with key components identified. Figure

59 below provides a picture of the Multi-Gauge controller. Table 11 below has a listing of all materials and equipment used to build the vacuum system.

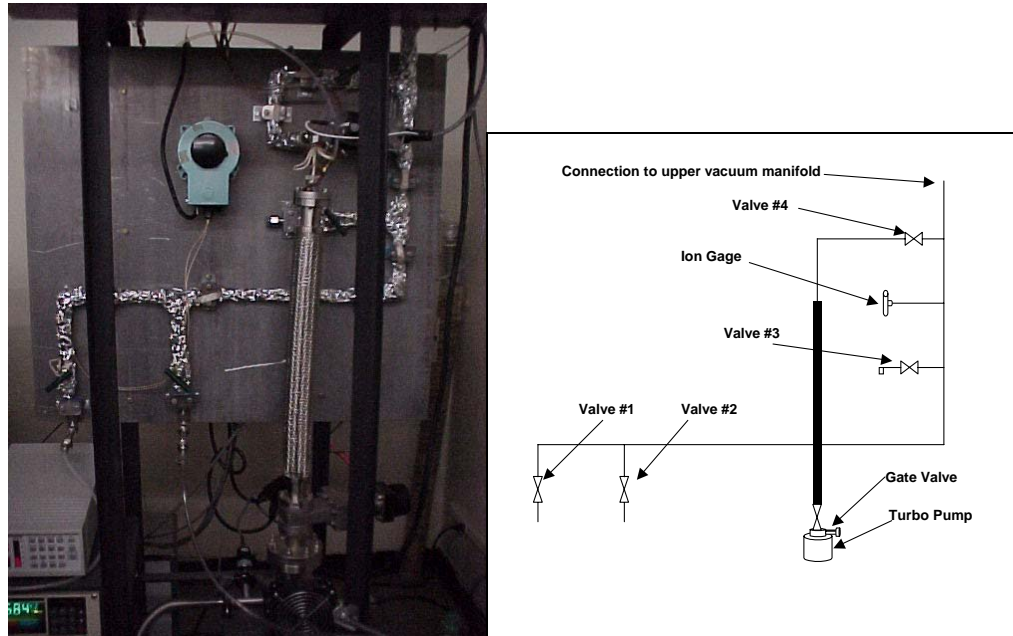


Figure 57. Photo and drawing of lower vacuum system.

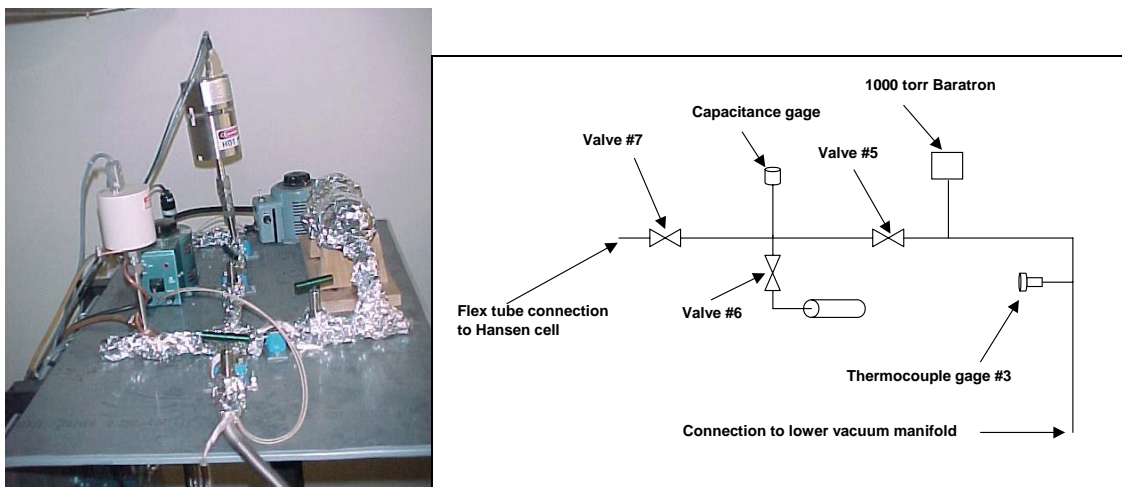


Figure 58. Photo and drawing of upper vacuum system.

All Varian vacuum gages were connected to the Multi-Gauge controller and the MKS Baratron was connected to the MKS supplied power supply and digital display.

The Multi-Gauge controller was damaged during shipment and did not operate properly during the first use. All the internal circuit boards were installed incorrectly and had to be re-installed before the ion gage and the capacitance gage functioned. The external case of the Mutli-Gauge controller was cracked near the attachment point to the pumping cart and a support was installed on the end of the controller to prevent further damage to the case and internal components. The capacitance gage was the primary gage used between 100 torr and 8.9×10^{-3} torr and the ion gage was used for vacuum measurements below 1.3×10^{-3} torr. All gages were zeroed after installation according to the manufacture's directions.

During the initial system bake out, the Drytel pump was used to replace the original Varian diaphragm pump in order to short the time to reach high vacuum. Due to the limitations of the diagram pump, the Drytel pump was used for the entire research period as a roughing pump for the turbo pump. After the system bake out, a vacuum of 1.2×10^{-5} torr was achieved. High vacuum pressures were not possible due to the incorporation of o-rings in the system and the use of Swagelock[®] fittings.



Figure 59. Photo of the Varian the Multi-Gauge controller.

Table 11. Vacuum System Materials Listing.

Equipment	Model	Serial Number	Manufacture
¼ inch OD copper tube	N/A	N/A	Assorted
¼ inch OD PVC tube	N/A	N/A	Assorted
¼ inch OD tube fittings	Assorted	N/A	Watts
½ inch SS flex hose	24 inch length, non-braided	N/A	Swagelock®
1 liter sample container	304L-HOF4-1000	N/A	Whitey
100 torr capacitance gage	VCMH12TAA	LIF80185	Varian®
2 ½ inch SS flex hose	FLB02503600	N/A	Varian®
316 SS tube, ½ inch OD	0.049 wall thickness	N/A	N/A
Aluminum foil	N/A	N/A	Assorted
Conflat flanges	Assorted types	N/A	Varian
Drytel pump	Drytel 31	D1703	Alcatel
Gate valve	L8500301	LVG80744	Varian®
Heat tapes	AWH-051-100DMSP	N/A	Amptek
Ion gage	0563-K2466-304	N/A	Varian®
Needle valves	SS-8BG	N/A	Swagelock®
Swagelock® fittings	Assorted 316 SS	N/A	Swagelock®
Thermocouple gages	Type 0531	N/A	Varian®
Turbo pump	V-70LP 969-9366	85802	Varian®
Turbo pump controller	Turbo V-70	81145	Varian®
Vacuum gage controller	Multi-Gauge	LIE80407	Varian®
Vacuum pump cart	Turbo cart pumping station	N/A	Varian®
Voltage regulators	3PN1010	N/A	Staco Energy
Voltage regulators	3PN117B	N/A	Power Stat
Water cooler	RTE-11	R94335109	Neslab
Baratron	631A13TBEH	000573907	MKS
Cable for baratron	CB631-3-M1	N/A	MKS
Digital display for baratron	PDR-C-1C	000606234	MKS
Power supply for baratron	260 PS-3B	000610525	MKS
Oxygen regulator	4122311-540	00-72029	Controls Corp of Amer
Compressed Oxygen Gas	331076	N/A	BOC Gases

A-4. Water Vapor System

Water vapor was used in conjunction with research grade oxygen in this experiment to simulate the natural atmosphere found in the environment, only for this research, under strict control and at known quantities. Distilled water measured at 18-M Ω -cm was used to minimize contamination to the uranium oxide samples and the weathering system.



Figure 60. System designed and used to introduce water vapor into the weathering system.

A-5. Hansen Cell

A PFD 12.5 System (Hansen cell) produced by R.G. Hansen and Associates was used to control the temperature and partial pressure of oxygen during the oxidation of the UO₂ samples. The Hansen cell assembly consists of a Model 3612 variable temperature pour-fill dewar, sample holder, 25-watt strap heater, platinum resistor (for temperature

control), a Model 2167-1 vacuum shroud, three quartz windows, a Lake Shore 330 temperature controller, and applicable electrical cables. The variable temperature pour-fill dewar has a vacuum port tube and a 26-pin instrumentation connector to permit connection to the vacuum system and Lake Shore temperature controller. A detailed equipment listing is included below in Table 12 below.

Table 12. Hansen Cell Assembly Equipment Listing

Equipment	Model	Serial Number	Manufacturer
Pourfill Dewar	3612	0088	R.G. Hansen
Vacuum Shroud	2167-1	2094	R.G. Hansen
Quartz Windows	3090	N/A	R.G. Hansen
26-Pin Electrical Cable	3062	N/A	R.G. Hansen
Seal-Off Valve	2945-1	N/A	R.G. Hansen
Platinum Resistor	PT 103	P2854	Lake Shore
Temperature Controller	330-11	35079	Lake Shore

The assembled Hansen cell is photo and schematic view of the pour-fill dewar with strap heater and sample holder attached is shown in Figure 61 below.

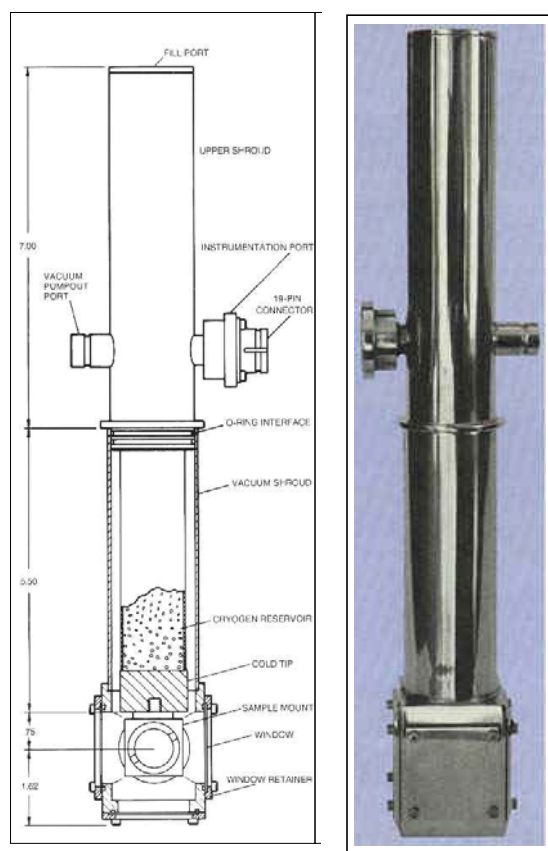


Figure 61. Hansen Cell schematic and Photo [Hansen website©, 2004].

The preparation and pressing of the uranium oxide samples required the design and fabrication of dies that would not deform due to the hardness of the uranium oxide powders or the high pressures used in pressing the uranium oxide powders into the tungsten screen. The surfaces of the dies that came in direct contact with the uranium oxide powders were hardened steel (Rockwell C greater than 50) and all other pieces were medium strength alloyed steel. After approximately twenty pressings, the plug and bottom plate had surface damage from the uranium oxide powders that was visible with the naked eye. See Appendix F for the procedures used to prepare a sample with the press and dies.

A-6. Photoluminescence Spectrometer

All phosphorescence measurements were performed on a model FL3-22 Jobin-Yvon Spex Fluorolog-3 Spectrofluorometer. The FL3-22 used double-grating spectrometers for excitation and emission of the samples to provide unsurpassed sensitivity, resolution, and stray light rejection. Steady state measurements and lifetime measurements were taken from the front face of the samples using a 9-Watt programmable flash lamp and a cooled photo multiplier tube (PMT). Figure 62 below provides a diagram of the FL3-22 setup and light path from the xenon lamp to the cooled PMT. Table 13 below contains a listing of all the components and software used by the FL3-22.

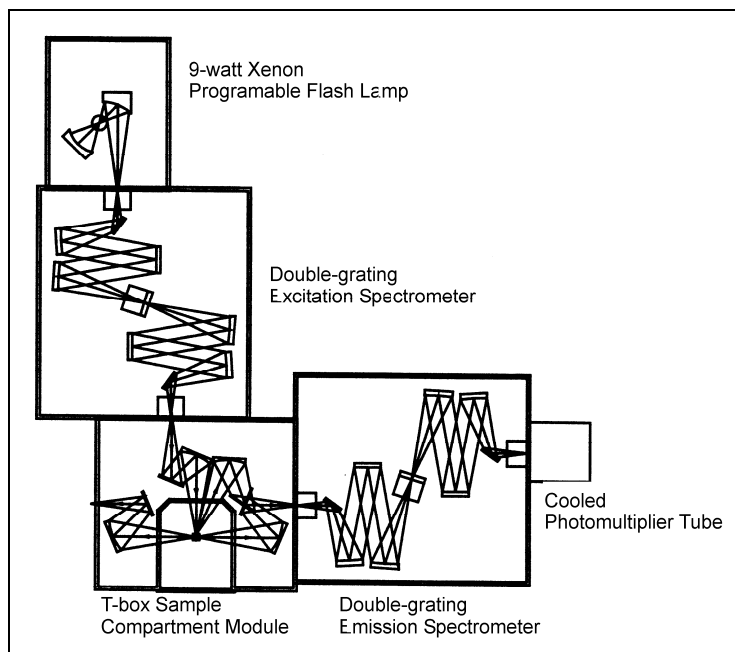


Figure 62. A diagram of the FL3-22 setup and light path from the xenon lamp to the cooled Photo-multiplier Tube (PMT).

Table 13. FL3-22 Component Listing

Equipment	Model	Serial Number	Manufacture
Cooled PMT w/pwr supply	PC 177CE005	N/A	Products for Research
Host computer	Dimension V400	511E1 / 84-465-37	Dell
Host Monitor	828F1	22794FB00889	Dell
Host printer	Desk Jet 670C	US86P1SOM5	HP
Phosphorimeter	193403	149 (Lamp) 150 (Controller)	SPEX
Photomultiplier tube	R928/0115/0381	21461-99-4	Products for Research
Spectrofluorometer	FL3-22	0293	Jobin Yvon
System computer	FL-1016	1494	Spectrac
System software	DataMax version 2.20	N/A	Jobin Yvon
System software	Grams/32 v. 4.11 level II	N/A	Galactic Industries
Water cooler	RTE-11	R96226022	Neslab

The standard holder for the FL3-22 sample chamber was replaced with a custom designed holder that permitted radial and vertical adjustments of the Hansen cell when installed. The radial and vertical positions for the holder used in this research were determined by maximizing the emission signal intensity of a UO_3 sample. Once the maximum signal was obtained, the positions were fixed and remained unchanged during the course of the research. Figure 63 below contains a photograph of the FL3-22 with the Hansen cell in the T-box Sample Compartment Module.

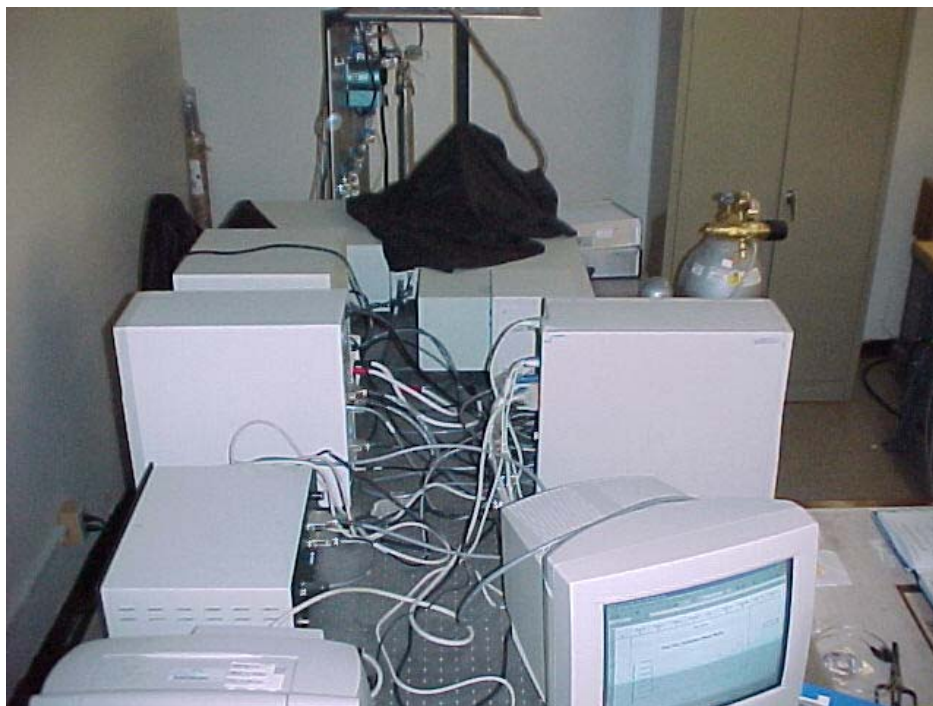


Figure 63. FL3-22 with Hansen Cell in T-Box Sample Compartment Module.

The FL3-22 was calibrated at the start of the research and this calibration was used for all measurements. During actual phosphorescence measurements, the Hansen cell was covered with three black cloths to prevent the room light from entering the optical path of the FL3-22. See Appendix G for the experimental parameters and procedures used for all phosphorescence measurements in this research.

A-7. Surface Analysis

The surface analysis measurements were obtained using a NOVA-1000 (No Void Analysis) Gas Sorption Analyzer from Quantachrome, Version 3.10. The raw data obtained was evaluated using Quantachrome's NOVA Enhanced Data Reduction

Program, Version 2.10, using the 25-Point BET Multi-Point method described in Chapter II.



Figure 64. NOVA-1000 High Speed Gas Sorption Analyzer.

Appendix B. Glove Box Operation

The following section outlines the procedures used to operate the glove box. Adherence to the steps and procedures in this section is essential to prevent contamination of the laboratory with loose uranium oxide powders.

The interior of the Glove Box was purged for two weeks prior to use with pure nitrogen and maintained throughout the duration of this research in order to minimize any uncontrolled oxidation of the bulk UO_2 powder and prepared samples prior to measurement. The flow of nitrogen into the Glove Box was controlled with a pressure regulator and needle valve assembly and the flow out was controlled with a flow meter. The outlet flow of nitrogen from the Glove Box was passed through a HEPA filter prior to exhausting into the laboratory area.

The glove box is composed of a working volume and an airlock system that facilitates moving items in and out of the working volume while providing a means of controlling the introduction of ambient air into the glove box and radiological contaminants out of the glove box. The airlock has an outer door, which opens to the laboratory environment, and an inner door, which opens into the glove box environment. The air lock has a working volume of 0.19 cubic meters and is equipped for the introduction of N_2 and connection to a vacuum system. The glove box was equipped with HypalonTM gloves (referred to as gloves from this point forward) so that sample preparation could occur in an N_2 environment.

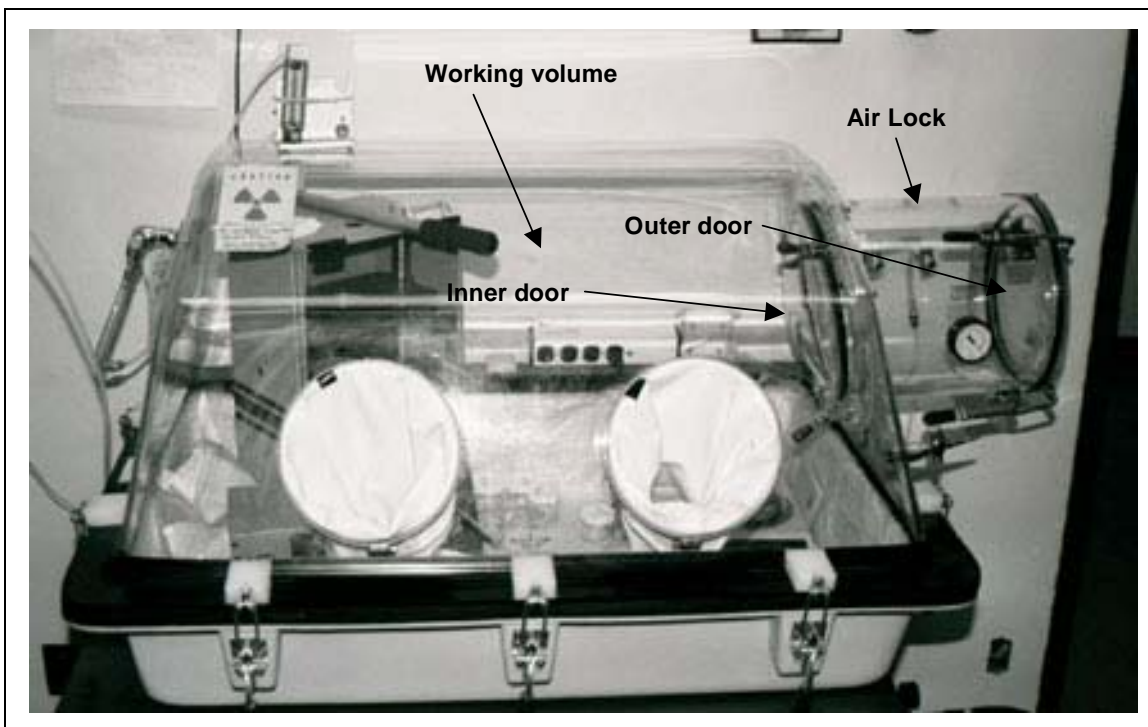


Figure 65. Glove box.

Prior to working with the uranium oxide powders, the glove box was cleaned to remove all materials from the previous oxidation experiments. The top of the glove box was removed and the Caver[®] hydraulic press was placed inside the glove box. All other equipment and materials used in this experiment were passed through the air lock. Table 14 below contains a listing of the materials necessary to operate the glove box.

Table 14. Equipment and materials used in operation of glove box.

Equipment	Purpose
α/β Counter	Used to detect contamination on items removed from glove box.
0 to 1.5 SCFM flow meter	Used to control flow rate of N ₂ through glove box.
0 to 50 psi regulator	Used to control pressure and flow rate of N ₂ into glove box.
Disposable gloves	Worn to keep hands from sticking to Hypalon TM gloves.
Filter paper	Used to conduct swipes on all items leaving the glove box.
Glove box	Maintains the N ₂ environment and contains radioactive powders
HEPA face mask	Used to prevent inhalation of uranium oxide powders.
HEPA filter	Used to filter N ₂ flowing out of the glove box.
Liquid N ₂ Dewar	Source of N ₂ gas inside glove box.
Methanol	Used to wash surface of items before removal from glove box.
Parafilm [®]	Used to cover waste uranium oxide powder containers.
Portable gamma rate meter	Used to check for uranium contamination on hands.
Tweezers	Used to place filter papers on planchets.
Utility wipes	Used to wipe contamination from items removed from glove box.
Vacuum pump	Used to purge air lock after opening to atmosphere.
White cotton lab coat	Used to prevent contamination of clothing with loose uranium oxide.
Zip lock bags	Used to dispose of contaminated materials inside glove box.

The following steps were developed for operating the Glove Box with minimal sample contamination and safety of the operator foremost in mind.

Step 1: Verify that nitrogen is flowing through the Glove Box by examining the flow meter installed on the working volume exhaust valve. During normal operations, the flow rate should be approximately 0.2 SCFM.

Step 2: Put on disposable latex gloves. This will make getting your hands in and out of the HypalonTM Gloves much easier and will prevent direct skin contact with any UO₂ particles.

Step 3: Put on a lab coat, TLD, and HEPA Facemask. Close the laboratory door and restrict access to only those personnel involved in preparing the UO₂ samples. Ensure that the radiation warning sign on the door indicates that radioactive materials are present in the room and a TLD is required for entry.

- Step 4: Close the inner door on the airlock. Open the outer door and place any materials and equipment in the airlock that are needed in the working volume of the Glove Box. Limit the amount of time the outer door is open by organizing the items ahead of time. Close the outer door when finished.
- Step 5: The airlock must now be purged of all ambient air before the inner door can be opened. Close the nitrogen valve and open the vacuum valve on the airlock. Turn on the vacuum pump and draw a minimum of 20-psi vacuum in the airlock (refer to the pressure gauge on the airlock itself). Turn off the vacuum pump, close the vacuum valve, open the nitrogen valve on the airlock, and fully open the needle valve on the nitrogen regulator. Allow the pressure to return to atmospheric normal in the airlock (vacuum gauge will read 0-psi). Repeat this process two more times. Return the needle valve to the initial position, slightly open, after the airlock is purged.
- Step 6: Open the inner airlock door and bring materials into the Glove Boxes working area. Leave the inner airlock door open about one-quarter of an inch except when working with loose UO_2 powder to permit a continuous flow of nitrogen through the Glove Box. When working with loose UO_2 powder, close the inner door to prevent the possible distribution of loose powder into the airlock and lab.
- Step 7: When ready to remove items from the Glove Box, close all loose powder containers (to include the waste container). Wash the surface of each item to be removed with methanol soaked wipes to remove any powder contamination. Place the used wipes in a Ziploc waste bag. Place the items in the airlock and close the inner door.

- Step 8: Open the outer airlock door and prepare swipes on all items in the airlock, the disposable gloves, and the inside of the airlock. If an item has more than 10-square centimeters of surface area, use multiple filter papers for the swipe. Place the swipes and items to be removed in the airlock and close the inner door. Using tweezers, place the swipes in empty planchets in the Canberra 2404 Alpha/Beta Counter and conduct a radiological survey of all swipes.
- Step 9: Confirm the absence of radiological contamination on your hands with a handheld gamma rate meter.
- Step 10: If the items in the airlock do not exceed the maximum allowable contamination levels (set at 20 dpm), remove the items from the airlock and close the outer door.
- Step 11: Purge the airlock as described in Step 5 above. Leave the inner door open approximately one-quarter of an inch to permit continuous nitrogen gas flow through the Glove Box.

Appendix C. Sample Preparation

This appendix was developed for the safe handling and sample preparation of the uranium oxide powders that were used in this research. In order to prevent cross contamination of the samples when changing the type of uranium oxide powder used, it is essential to properly clean and inspect the pressing dies, Hypalon gloves, and all instruments (tweezers, spoons, etc.) that have contact with the powder. This appendix consists of three sections: preparing the tungsten screen, cleaning the pressing dies, and pressing the UO₂ powder into samples. Table 15 below contains a listing of the materials used to cut and prepare a screen for pressing the uranium oxide powders.

Table 15. Equipment and materials used for tungsten screen preparation.

Equipment	Purpose
Disposable gloves	Worn at all times to: 1. Prevent depositing skin oils on screen surface. 2. Protection fingers from the rough edges of the screen. 3. Keep methanol off hands.
Glass petri dish	Used to soak tungsten screen pieces in methanol.
Heavy-duty scissors	Used to cut the tungsten screen.
Lucite patterns	Templates for cutting screen to required size.
Magnifying fluorescent lamp	Used to view the screen while cutting with scissors.
Mechanical pencil	To trace the templates on the screen surface.
Methanol	Used to remove surface oils and contaminants from screen.
Techwipes by Skilcraft®	Placed on lab table to provide clean working surface. Also used to air-dry tungsten screen pieces after soaking in methanol.
Tungsten screen	Used to hold the uranium oxide powders
Tweezers	Used to insert and remove tungsten screen from beaker.

C-1. Preparing the tungsten screen

This experiment used a two-mil thick pure tungsten screen sheets with 200×200 micrometer (μm) photochemical etched squares to hold the UO_2 powder in the Hansen Cell.

- Step 1: Place a clean Techwipe on the top surface of the lab table.
- Step 2: Put on disposable latex gloves and remove a sheet of tungsten screen from its protective packaging.
- Step 3: Trace the outline of the one-inch square Lucite pattern on tungsten screen with the mechanical pencil. Cut the screen on the pencil marks using the heavy-duty scissors and magnifying lamp. Return the remaining screen to its packaging.
- Step 4: Trace the outline of the one-inch circular Lucite pattern on the one-inch square piece of tungsten screen using the mechanical pencil. Cut the screen on the pencil marks using the heavy-duty scissors and magnifying lamp.
- Step 5: Place the circular piece of tungsten screen in the petri dish and cover to a sufficient depth to completely cover the screen with methanol. Soak the screen for a minimum of two hours.
- Step 6: Remove tungsten screen from the petri dish with tweezers and place on a clean laboratory wipe. Allow to air dry.
- Step 7: Transfer the prepared screen to the working volume of the Glove Box by following the instructions in Appendix B, Glove Box Operation. You may find it easier to move the tungsten screen into the Glove Box by placing it on a piece of clean filter paper.

C-2. Cleaning the Pressing Dies

This section explains how to clean the pressing dies and assumes that you have just finished pressing a sample. For the initial cleaning, ignore any steps pertaining to removing a sample from the dies. Cleaning of the dies between samples increases the quality of the sample. Figure 56 above shows a picture of the unassembled pressing dies and identification of the specific parts of the die assembly and Table 16 below gives a listing of the materials needed to clean the pressing dies.

Table 16. Equipment and materials used to clean the pressing dies.

Equipment	Purpose
250 ml glass beaker	Used to hold methanol.
Hex wrench	Used to disassemble and assemble the dies.
Metal spoon	Used to remove powder residue from surfaces of pressing dies.
Methanol	Used to wash uranium oxide powder residue from surfaces of pressing dies.
Tweezers	Used to insert and remove hex-head bolts from dies.
Utility wipes	Used to wash pressing dies.

Step 1: Place clean utility wipes on the bottom of the Glove Box. They will help contain any loose UO_2 powder that falls off the die.

Step 2: Disassemble the pressing dies by removing the four hex head bolts.

Step 3: Remove the plug and place it on the utility wipes. Separate the top plate from the intermediate and bottom plates.

Step 4: Hold the top plate over the appropriate waste powder beaker and remove any excess powder with a metal spoon. Place the top plate on the utility wipes.

Step 5: Remove the prepared sample, and after weighing, place it in either the Hansen Cell or the sample container. The following section contains instructions for

mounting a sample in the Hansen cell and Appendix D for instructions on placing a sample into a storage container.

C-3. Pressing Uranium Oxide Powders into Samples

This section provides the procedures used to press the uranium oxide into samples using the Carver® hydraulic press and pressing dies.

Table 17 below contains a listing of the materials and equipment necessary to prepare a uranium oxide sample.

Table 17. Materials and equipment used to prepare uranium oxide samples.

Equipment	Purpose
250 ml glass beaker	Used to hold methanol.
60 ml glass jars	Used to store prepared samples
Balance	Used to weigh empty screens and prepared samples.
Black marking pen	Used to mark 60 ml glass jar and XRF holder with sample number.
Disposable gloves	Worn to keep hands from sticking to Hypalon™ gloves on glove box.
HEPA face mask	Used to prevent inhalation of uranium oxide powders.
Hex wrench	Used to disassemble and assemble the dies.
Hydraulic press	Used to force uranium oxide powders into the tungsten screen.
Metal spoon	Used to transfer loose powder from the plastic bags to the pressing dies.
Methanol	Used to clean up loose uranium oxide powder.
Mylar XRF film	Used to hold prepared samples.
Pressing dies	Used to form the sample.
Tungsten screen	Used to hold the uranium oxide powders.
Tweezers	Used to insert and remove hex-head bolts from dies.
Utility wipes	Used to clean up loose uranium oxide powder and for a clean working surface inside the glove box.
White cotton laboratory coat	Used to prevent contamination of clothing with loose uranium oxide powders.
XRF holders	Used to support prepared sample between Mylar films.

Step 1: Put on lab coat, disposable latex gloves, TLD, and HEPA mask. Close the door to the room to limit the spread of any potential spills.

- Step 2: Visually inspect the bottom of the Glove Box for loose UO_2 powder and clean up with utility wipes and methanol if necessary. Place clean utility wipes on the bottom of the Glove Box.
- Step 3: Place the required number of 60-ml glass jars (go ahead and open the lids), tungsten screens, and any other equipment needed in the airlock of the Glove Box. Bring items into the working area of the Glove Box by following the procedures outlined in Appendix B.
- Step 4: Weigh an empty tungsten screen on the balance (also located in the working volume of the Glove Box) and record the empty weight in the uranium oxide logbook.
- Step 5: Place the intermediate plate on the bottom plate of the pressing dies and place the tungsten screen on the assembled pieces. Place the top plate on the intermediate and bottom plates to hold the screen in place and secure with the four hex-head bolts and hex wrench.
- Step 6: Place the assembled dies on the clean utility wipes on the bottom of the Glove Box.
- Step 7: Open the metal can containing the UO_2 powder with the square blade of the spoon. Remove the plastic bag containing the powder from the can.
- Step 8: Open the plastic bag and using the round blade of the metal spoon, transfer the UO_2 powder from the plastic bag to the hole in the pressing die. Place enough powder in the die to completely cover the tungsten screen.
- Step 9: Insert the plug into the hole of the pressing die until it makes contact with the powder. Rotate the plug to distribute the powder on the screen. Remove the

plug and visually inspect the tungsten screen to verify that it is completely covered with the UO_2 powder. Add more loose UO_2 if necessary.

Step 10: Install the plug in the die and place the whole assembly into the hydraulic press.

Visually center the die in the jaws of the press. Close the relief valve and raise the bottom jaw with the pump handle until the die makes contact with the top jaw of the hydraulic press.

Step 11: Place the handle extension on the press and apply 24,000-pounds of force to the die as measured with the mechanical force gauge on the press. Let the die remain in the press under this force for 20-minutes.

Step 12: After 20-minutes, open the relief valve and remove the handle extension from the press. Remove the die from the press.

Step 13: Remove the plug from the die and remove the four hex-head bolts from the die using the hex wrench.

Step 14: Remove the top plate from the die while holding the die over the petri dish marked for the particular UO_2 used in the current sample. Set the top plate of the pressing die on the beaker marked for the particular UO_2 powder used in the current sample.

Step 15: Using the fine pointed tweezers, remove the prepared sample from the bottom and intermediate plates. Scrape any excess powder from the screen surface into the petri dish with a razor blade. Place the prepared sample on the balance and record the sample weight in the uranium oxide logbook. Compute and record the actual oxide sample weight.

Step 16: If the sample is going into the Hansen cell, then follow the procedures in the next section and ignore the rest of this section.

Step 17: Remove the ring from the XRF holder and place a piece of Mylar XRF film over the XRF holder. Place the prepared sample on the Mylar XRF film and place a second piece of Mylar XRF film over the prepared sample. Secure the prepared sample and Mylar XRF films to the XRF holder with the ring. Write the sample ID on the base of the XRF holder with a black marker.

Step 18: Place the XRF holder containing the prepared sample in a 60-ml glass jar and screw down the lid. In order to lower the beta and gamma radiation emission from the sample jar, insert the XRF holder in the jar with the end containing the UO_2 sample first. Mark the sample ID on the lid of the jar with a black marker.

Step 19: Clean the pressing dies using the procedure outlined earlier.

Appendix D. Vacuum System Operation

The following two sections describe the steps necessary to pump down the vacuum system and introduce oxygen into the Hansen cell through the vacuum system.

D-1. Pumping Down the Vacuum System.

The steps in this section apply to a system pump down when the Hansen cell is attached to the stainless steel flex tube and a uranium oxide sample is installed in the sample holder. Refer to Figures 66 and 67 for valve designations. If the Hansen cell is not installed and the system must be pumped down, ignore all steps that relate to the Hansen cell and close valve #7.

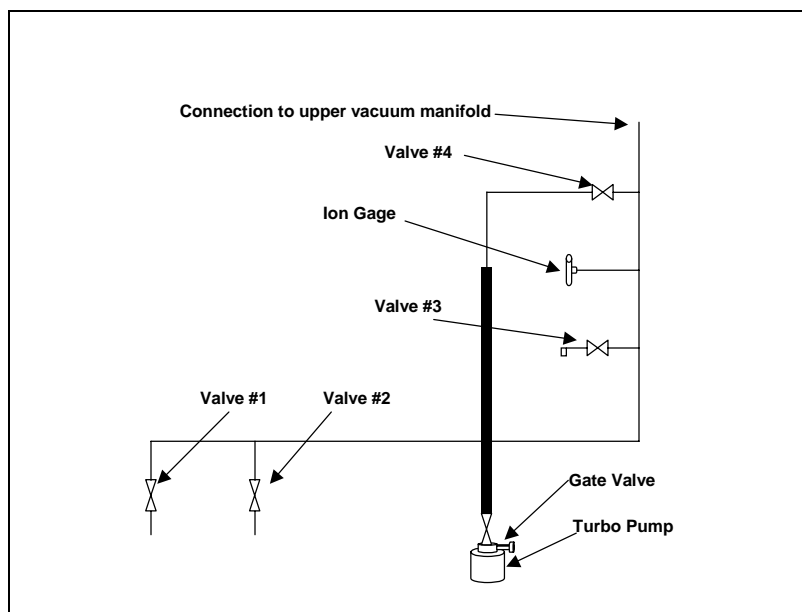


Figure 66. Drawing of lower vacuum system.

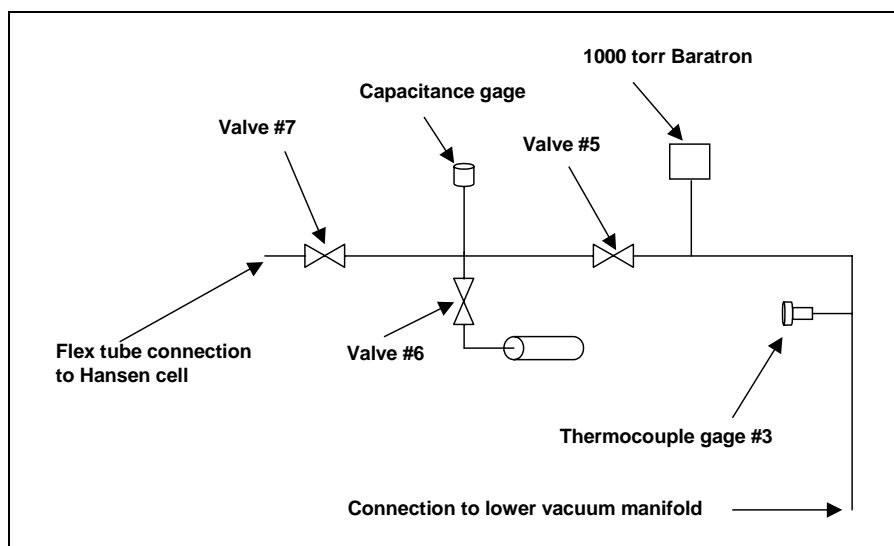


Figure 67. Drawing of upper vacuum system.

Step 1 Turn on the water cooler and set the temperature for 22°C (you will only have to set the temperature for the first time). The water cooler cycles room temperature water around the components (o-ring fittings and electronics) of the system that will not tolerate the bake out temperatures. Turn on the three voltage regulators that control the heat tape temperatures. Each heat tape should achieve a temperature of 150°C. Use a thermometer to verify the temperatures. Once you reach the desired temperature, mark the regulators and the shut them off only with the on/off switch and you will not have to adjust them again.

- Step 2 Close system valves #1, #2, and #3 and open all other valves. This will isolate the system from the atmosphere and allow establishment of vacuum in the system.
- Step 3 Turn on the Drytel pump with the power switch on the front of the pump and watch the pump speed indicator lights. The green light should turn one within 5 minutes to indicate that the pump has reached an operating speed of 27,000 RPM. If the light does not come on, verify that all valves are in the proper position (open or closed) and check for system leaks. If this does not correct the problem then the pump must be serviced.
- Step 4 Turn on the turbo pump using the V-70 Turbo Pump Controller by pressing the start/stop button. The turbo pump should reach an operating speed of 75,000 RPM in about a minute. If the turbo pump fails to reach this operating speed then verify that the Drytel pump is turned on and has reached its operating speed. The turbo pump will not reach operating speeds if its exit pressure is more than a few torr in pressure. Operating the turbo pump at high exit pressures will shorten the life of the pump, cause excessive pump heating, and fail to achieve high vacuum in the system.
- Step 5 Set the Hansen cell temperature to 120°C using the Lake Shore 330 controller using the procedures in Appendix C.
- Step 6 For the initial system pump down leave the heat tapes and water cooler turned on for 24 hours and for each subsequent pump down leave them on for 12 hours. Once the applicable time interval is reached, turn off the

voltage regulators using the on/off switches and wait 5 minutes before turning off the water cooler. Allow the vacuum pumps to run for an additional 12 hours.

Step 7 Check the system vacuum using the Multi-Gage Controller and the capacitance gage. Use the channel button on the controller to select the desired gage. See Figure 57 for a view of the Multi-Gauge Controller. If the capacitance gage display shows three zeros (system vacuum below 8.9×10^{-3} torr) then switch to the ion gage. Turn on the ion gage using the EMIS button on the Multi-Gauge controller. The system should have established a high vacuum (below 8×10^{-5} torr with the Hansen cell attached and below 3×10^{-5} torr without the Hansen cell) at this time. If the system still has poor vacuum, check for leaks using acetone on all fitting connections. The system vacuum when measured with one of the two thermocouple gages will drop if acetone is sprayed into a leak. Repair all leaks and repeat all steps starting with step #1. The system is now ready for introduction of oxygen or any other gas required for the experiment.

D-2. Oxygen Introduction into the Hansen Cell

This section describes the procedures used to introduce Grade 5.0 oxygen into the vacuum system and the attached Hansen cell after high vacuum is established. The vacuum system must be at room temperature (remember the ideal gas law) before attempting any of the steps below.

- Step 1 Close the gate valve and valve #4. If you are not going to use the sample container, close valve #6.
- Step 2 Turn off the turbo pump and Drytel pump. Verify that the ion gage is turned off. Set the Multi-Gauge controller to read the capacitance gage or thermocouple #3 depending upon the final oxygen pressure you want to introduce into the Hansen cell.
- Step 3 Verify that the Baratron has been turned of for a minimum of two hours and is set to read in units of mm Hg.
- Step 4 Purge the oxygen supply line into the vacuum system. Set the regulator on the oxygen cylinder to 5 psi. Loosen the fitting holding the plastic line on the vacuum system and allow oxygen to flow through the line and out through the loose fitting. Tighten the fitting while oxygen is flowing.
- Step 5 While watching the digital display for the Baratron, slowly open valve #1 and allow oxygen to pass into the vacuum system and enter the Hansen cell. Once the desired partial pressure of oxygen is established, close valve #1 and turn off the valve on the oxygen cylinder. Do not exceed 800 torr or the o-ring fitting may separate causing damage to the vacuum system. Some initial pressure adjustments will be necessary as the oxygen temperature and the vacuum system temperature stabilize. Expect pressure variation of up to five torr with daily fluctuations in the room temperature.

Appendix E. Temperature Controller Operation

This section describes the procedures used to operate the Lake Shore 330 temperature controller (referred to here after as the temperature controller) used in conjunction with the Hansen cell in this research. The temperature controller is a programmable unit that can be configured by the user to accept the temperature readings from silicon diodes, platinum resistors, and many different typed of thermocouples. Additionally, the temperature controller can provide power to either a 25-watt or 50-watt heating element. The temperature controller was shipped from the manufacture with channels A and B configured for use with silicon diodes and a 25-watt heater. In order to use the platinum resistor, the top cover of the temperature controller was removed and the pin switches for channel B were adjusted according to the supplied operators manual.

All normal operation adjustments were done with the front face controls on the temperature controller. The front face contained two LCD panels for sample and control displays, a segmented LCD display for heater intensity, and a 19-button keypad. During operation, the LCD displays will only provide information for one of the two channels at a time even if both channels are used. Figure 68 below contains a picture of the temperature controller and should be used as a reference for the rest of this appendix.



Figure 68. Lake Shore temperature controller.

E-1. Initial Set-up of the Temperature Controller.

- Step 1** Verify that the temperature controller is connected to the Hansen cell with the 26-pin cable and turn on the temperature controller with the switch located on the back panel.
- Step 2** The LCD sample and control displays will scroll through the default settings and should display the current sample and set point information when complete. If an error message is displayed, check the operators' manual for an explanation of the error codes. The sample and control units can be displayed as degrees Celsius, degrees Kelvin, or Ohms. To change the sample units, hold down the Units button and then press the up

arrow button until the desired units are shown in the display. Use the down arrow key to change the control units.

- Step 3 To set the control temperature (the temperature you want the sample heated to), press and release the Set Point button. The control display should flash the last digit. Enter in the desired control temperature and press the enter button when finished. If you make a mistake, press the escape button and repeat this step.
- Step 4 To set the rate of temperature change in degrees per minute, press and hold the Set Point button until the sample display contains the word rate and the control display indicates to current rate with the last digit flashing. Enter in the desired temperature rate and press the enter key when finished. Use the escape key to correct errors.
- Step 5 To enable the auto tuning mode, press and hold the Auto Tune button and cycle through the options with the up and down arrow buttons. Set the temperature controller to use the full auto-tuning mode by selecting the PFD option. This will minimize the temperature overshoot provide the highest amount of accuracy in control of the temperature during an experiment.

E-2. Operation of the Temperature Controller.

By default, the temperature controller is set up to return to the last state following a loss of power. This permits un-supervised recovery following a power loss in the laboratory. To disable this feature please refer to the operators' manual.

- Step 1 Verify the set point, rate, and auto tuning options described in section A above.
- Step 2 The heating element in the Hansen cell is controlled through the Heater button on the front face of the temperature controller. Press and release the heater button three times in succession to turn the heater on the high setting. This will provide up to 25-watts of power to the Hansen cell permitting temperatures as high as 200°C.
- Step 3 To turn off the heater, press and release the Heater button repeatedly until the word off is displayed in the control display.

Appendix F. Sample Mounting

This appendix provides the procedures used to install and remove a uranium oxide sample in the Hansen cell. The procedures apply to both the original aluminum sample holder and the copper sample holder used at the end of the research. See Figure 69 below for a photograph of the copper sample holder and identification of the locking ring.

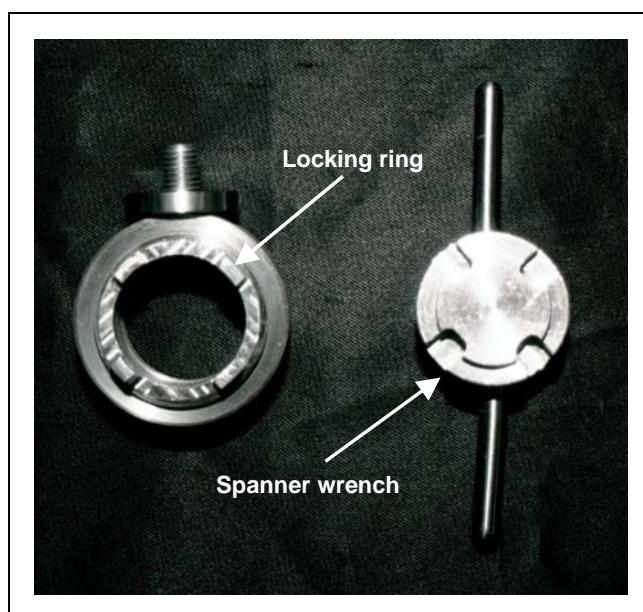


Figure 69. Sample holder and spanner wrench.

The Hansen cell had witness marks inscribed on the vacuum shroud and pour-fill dewar during the initial adjustment of the FL3-22 (see Section A-5, Appendix A). Figure 70 below is a photograph of the Hansen cell with the vacuum shroud and pour-fill dewar

assembled. The white line represents the inscribed witness marks. The alignment of the witness marks after every sample change and re-attachment to the vacuum system ensured repeatability of the phosphorescence measurements (see Appendix I).

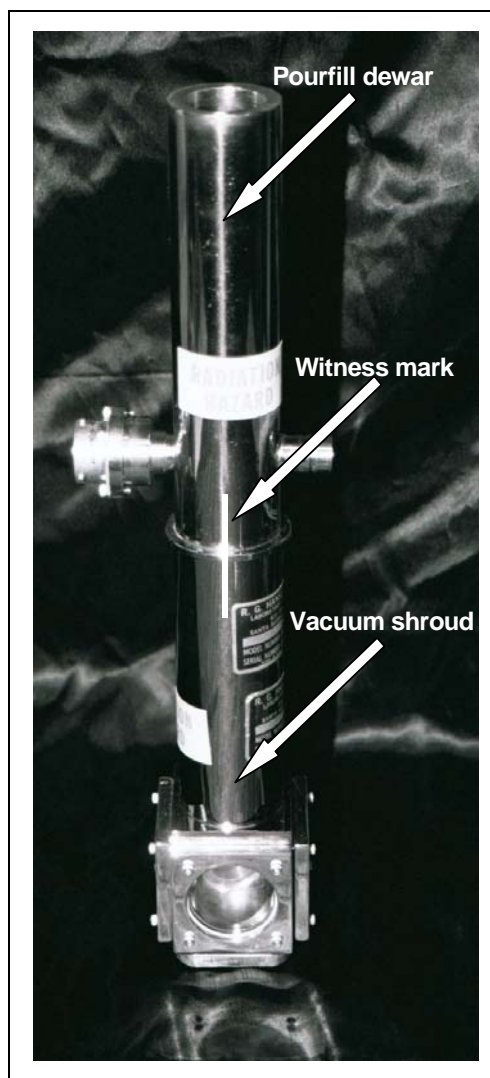


Figure 70. Hansen cell.

The steps listed below assume that the Hansen cell has already been disconnected from the vacuum system and the Lake Shore temperature controller. If the Hansen cell contains a uranium oxide sample, place two clean sheets of Mylar XRF film in the airlock with the Hansen cell. The new Mylar XRF sheets will be required to place the current sample into the sample storage container.

- Step 1 Put on lab coat, disposable gloves, TLD, finger ring, and HEPA mask.
- Step 2 Place the Hansen cell in the air lock of the glove box and transfer it to the working volume (see Appendix E).
- Step 3 Pull the vacuum shroud off the pour-fill dewar and set aside on a clean utility wipe.
- Step 4 Using the spanner wrench, remove the locking ring from the sample holder. The locking ring should only be finger tight.
- Step 5 Using metal tweezers, remove the uranium oxide sample from the sample holder and set the pour-fill dewar on top of the hydraulic press (this will help keep it clean and get it out of your way).
- Step 6 Put the uranium oxide sample in a storage container by following the steps in Appendix D.
- Step 7 Prepare a new uranium oxide sample by following the procedures in Appendix D or take an un-oxidized sample from a storage jar. Annotate in the uranium oxide logbook which sample you returned to the glove box and which sample you are installing in the Hansen cell.

- Step 8 Place the new sample in the sample holder with the front face (the side the powder was pressed from) of the sample towards the locking ring. Install the locking ring and tighten finger tight with the spanner wrench. Replace the vacuum shroud on the pour-fill dewar.
- Step 9 Remove the Hansen cell from the glove box following the steps in Appendix E.
- Step 10 After connecting the Hansen cell to the vacuum system and Lake Shore temperature controller, line up the witness marks. Check the alignment after establishing vacuum in the system.

Appendix G. Procedures for Photoluminescence Measurements

This appendix contains the procedures used to collect the photoluminescence measurements used in the research.

This section provides the procedures and setting used to collect phosphorescence (emission, excitation, and/or lifetime) spectra using the Jobin Yvon FL3-22 spectrometer. Appendix C provides the procedure to prepare a sample and Appendix F provides the procedure to mount the sample in the Hansen cell.

G-1. Initial calibration

The excitation and emission monochromator were calibrated using the xenon lamp and water Raman spectra. This required the use of the 450-watt Xenon continuous light source. For more detailed information, refer to the FL3-22 Operation and Maintenance Manual (Jobin Yvon-SPEX, 1996).

- | | |
|--------|--|
| Step 1 | Turn on the 450-watt xenon lamp, lamp controller, Spectrac computer, and Host computer. The equipment must be turned on in the order presented or damage to the Spectrac will occur. |
| Step 2 | Turn on the Neslab water cooler connected to the cooled PMT housing. When the temperature reaches 10 °C, turn on the power supply for the PMT cooler. Allow the system to cool down for a minimum of two hours before continuing with the calibration. |

- Step 3 Select the Experiment/Post Processing application in the DataMax selection screen.
- Step 4 Verify that the sample chamber is empty and covered with the lid.
- Step 5 From the pull down menus, select Collect/Experiment.
- Step 6 Click on the Exp Type button and select the Excitation Acquisition experiment type. An Excitation Acquisition dialog box (see Figure 71 below) should open on the screen.

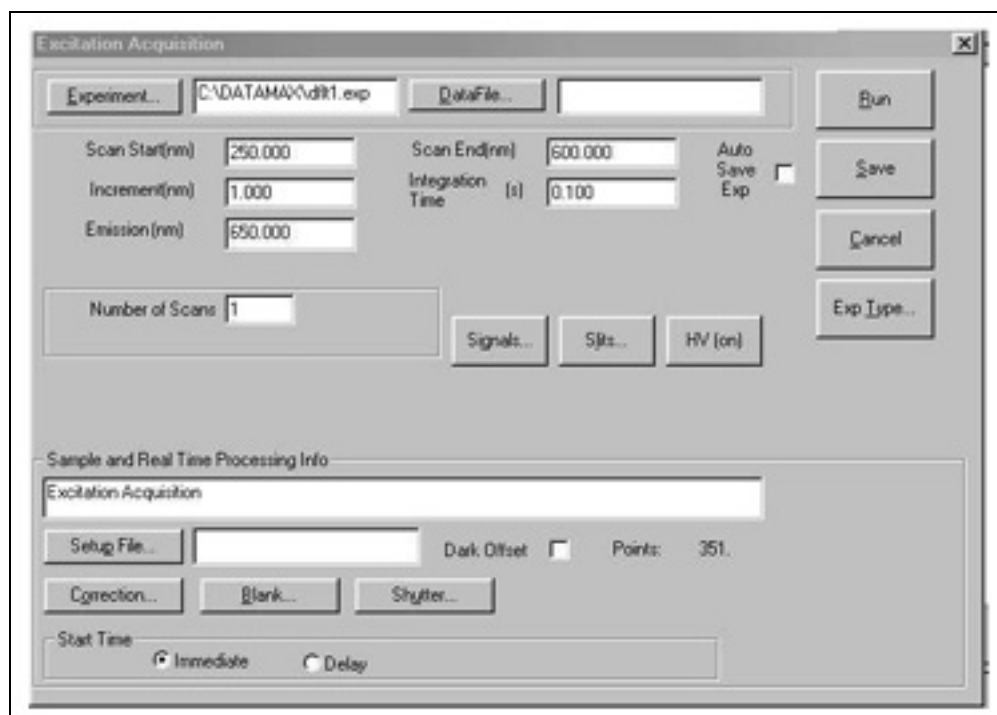


Figure 71. DataMax Excitation Acquisition dialog box.

- Step 7 Enter the parameters and hardware settings from Table 18 below into the dialog box. The acquisition mode setting is set under the Signals button.

Table 18. Excitation calibration parameters.

Hardware Settings	
Slits	0.5 mm
High Voltage (Signal)	950 V
Parameters	
Type of Experiment	Excitation Acquisition
Number of Scans	1
Start Wavelength	250 nm
End Wavelength	600 nm
Integration Time	1 ms
Increment	1 nm
Emission Monochromator Position	650 nm
Acquisition Mode	S

Step 8 Enter a name for the data file. The default directory is C:\Datamax\data.

Step 9 Click on the Run button to start the scan.

Step 10 When the scan is complete, your spectrum should look like Figure 72 below. If the maximum peak is at 467 ± 0.5 nm (the FL3-22 is accurate to within 0.5 nm), the excitation monochromator is calibrated and you can skip to step # 16 for calibration of the emission monochromator.

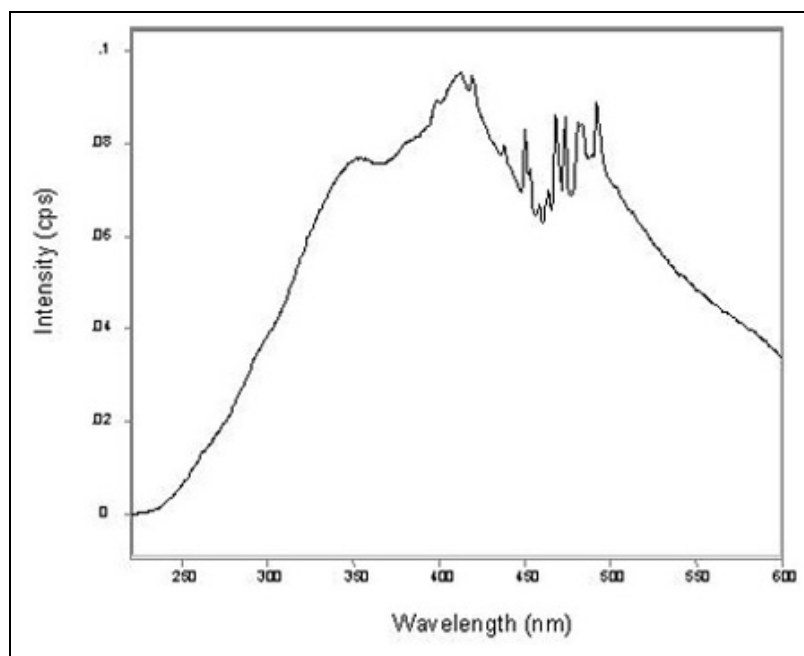


Figure 72. Xenon lamp spectrum.

- Step 11 Write down the wavelength of the most intense peak and click on the RTD button of the Instrument Control Center.
- Step 12 Reposition the excitation monochromator to the wavelength indicated by the peak of the xenon lamp scan by entering the observed peak position in the Monox dialog box on the RTD Control Panel. Close the RTD application.
- Step 13 Access the Visual Setup application through the Instrument Control Center. Click on the excitation monochromator Grating image (see Figure 73 below).

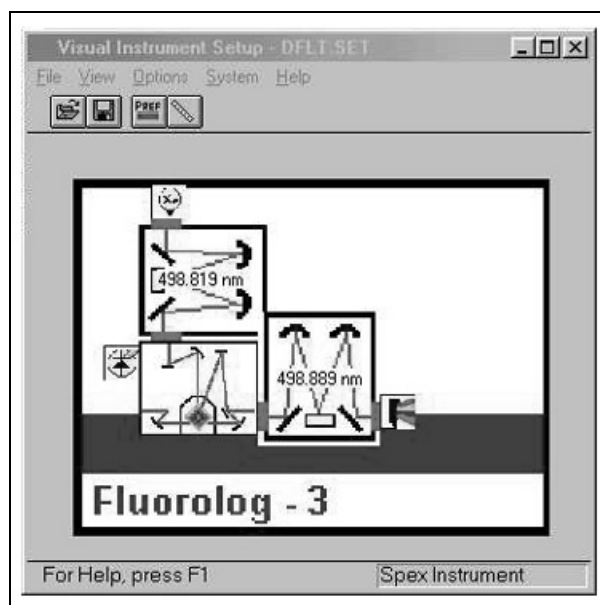


Figure 73. DataMax Visual Setup screen.

Step 14 Click on the calibrate button and enter the actual xenon lamp scan peak (see Figure 74 below) of 467.1 nm and click OK.

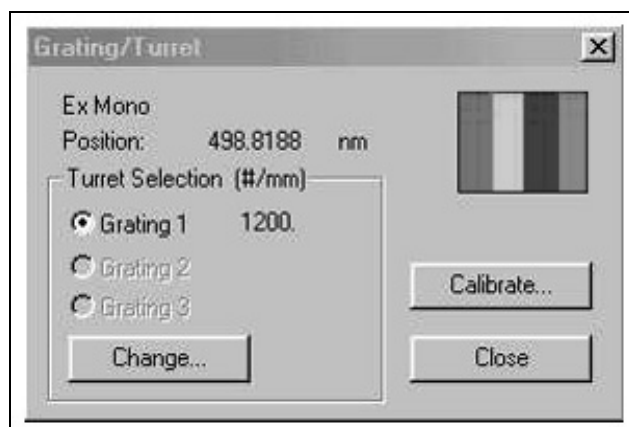


Figure 74. Grating calibration dialog box.

- Step 15 Click OK to close the Grating/Turret dialog box. Close the Setup application. Run another lamp scan following the same steps to confirm that the xenon lamp peak is now at 467 ± 0.5 nm.
- Step 16 Install the standard single holder in the sample chamber and set the selection knob on top of the sample chamber to RA (right angle).
- Step 17 Insert a cuvette filled with distilled water into the standard single sample holder. To minimize the background signal, use double distilled water if available.
- Step 18 From the main menu of the Experiment/Processing application, select Collect/Experiment. Click on the Exp Type button and select the Emission Acquisition experiment type. An Emission Acquisition dialog box (see Figure 75 below) should open on the screen.

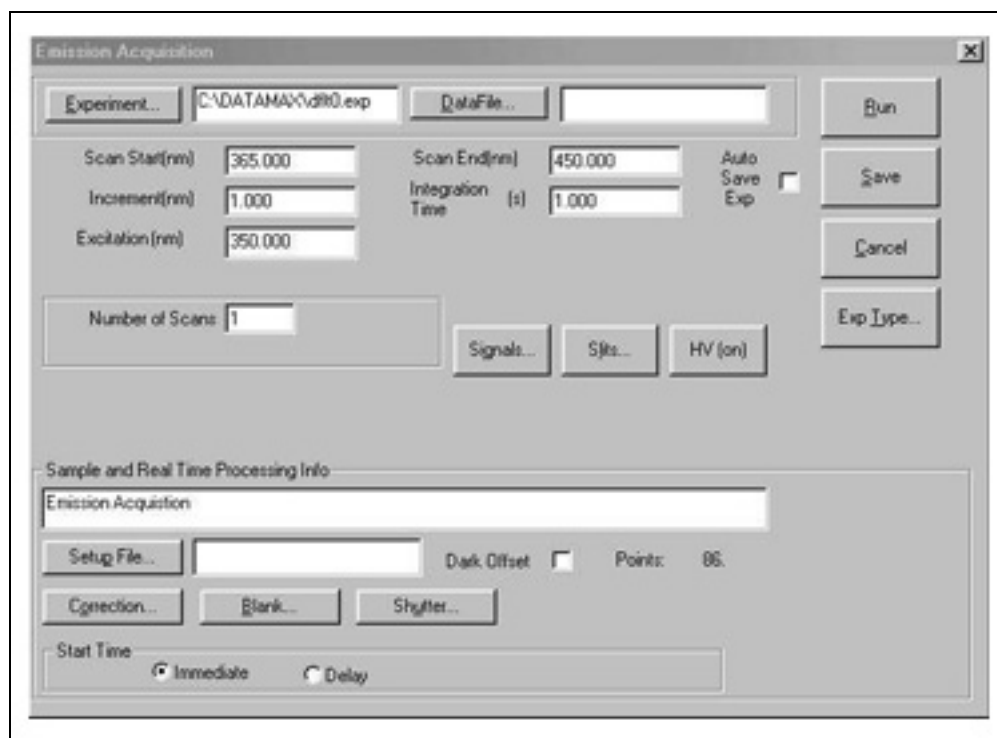


Figure 75. DataMax Emission Acquisition dialog box.

Step 19 Enter the hardware and parameter settings from Table 19 below into the dialog box.

Table 19. Settings for emission monochromator calibration.

Hardware Settings	
Slits (excitation and emission)	2.50 mm
High Voltage	950 V
Parameters	
Excitation Monochromator	350 nm
Emission Monochromator	365 nm to 450 nm
Increment	0.5 nm
Acquisition Mode	S
Integration time	0.5 sec
Total Time	N/A

- Step 20 Enter a name for the data file.
- Step 21 Click the Run button to start the scan. The expected peak is at 397 ± 1 nm and the minimum expected intensity is 450,000 CPS (counts per second).
- Step 22 The spectra should look like Figure 76 below. If the maximum peak is 397 ± 1 nm, run another water Raman spectrum using the FF (front face) setting. The front face should produce a spectra with the peak at the same wavelength but with a much more intense signal. If the peak for the FF is 397 ± 1 nm, the emission monochromator is calibrated and you may ignore the rest of this section.

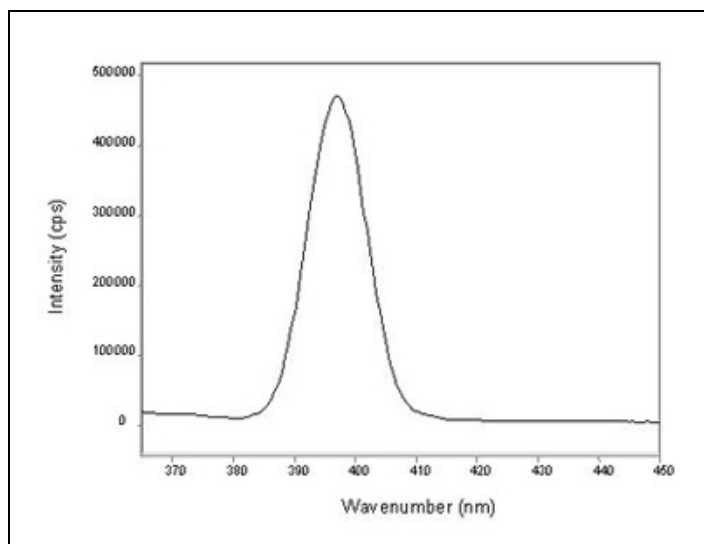


Figure 76. Water Raman spectrum.

- Step 23 If the water Raman peak is not acceptable (more than 1 nm away from the correct wavelength), make a note of the wavelength indicated and click on the RTD button on the Instrument Control Center.
- Step 24 Reposition the emission monochromator to the wavelength indicated by the peak of the water Raman scan by entering the observed peak position in the Monos dialog box on the RTD Control Panel. Close the RTD application.
- Step 25 Click on the Setup button on the Instrument Control Center and click on the emission monochromator Grating image (see Figure 73 above).
- Step 26 Click on the calibrate button and enter the actual peak of the water Raman scan (397 nm) and click OK. Click OK on the Grating/Turret dialog box and close the Setup application.
- Step 27 Run a second RA Raman scan to verify the corrected peak location.
- Step 28 Run a FF water Raman scan. The peak should happen at the correct wavelength but with a greater intensity. The FL3-22 is now fully calibrated and ready for your experiments.

G-2. Sample runs

This section provides the settings and procedures to record phosphorescence spectra on a uranium oxide sample. Most of the FL3-22 parameters and settings were obtained from the work done by 1LT Rand [Rand, 1999] and MAJ Schueneman [Schueneman, 2001] and from the FL3-22 Operators Manual (Jobin Yvon-SPEX, 1996).

This section assumes that you have performed a calibration and have installed the flash lamp and phosphorimeter.

The xenon flash lamp was inspected every other day to check for signs of degradation. The glass walls of the lamp will turn black shortly before the end of the lamp's life. The xenon lamp must be replaced before it fails in order to prevent severe damage to the focusing mirror and optical located inside the lamp housing. For the UO_2 experiment, the number of flashes used in the emission scan from 470 nm to 660 nm was reduced from 500 flashes per data point to 200 flashes per data point in order to extend the life of the xenon lamp.

The emission, excitation, and lifetime experiment set-up files (see Table 20 below) are stored on the system computer in the directory C:\Datamax\data.

Table 20. Photoluminescence experiment file names.

Sample	Experiment Type	File Name
UO_2	Emission Scan	uo2m.exp
	Excitation Scan	uo2x.exp
	Lifetime Scan	uo2lt.exp
UO_3	Emission Scan	uo3m.exp
	Excitation Scan	uo3x.exp
	Lifetime Scan	uo3lt.exp

Step 1 Put a sample in the Hansen cell following the procedures in Appendix F and remove the Hansen cell from the glove box following the procedures in Appendix E.

- Step 2 Attach the Hansen cell to the vacuum system and temperature controller and then place the Hansen cell in the custom holder inside the FL3-22 sample chamber. Hang the “RADIOACTIVE MATERIALS PRESENT” sign face out on the vacuum system cart and display the appropriate signs on the door to the lab.
- Step 3 Establish a vacuum (10^{-5} torr) around the uranium oxide sample following the procedures in Appendix D.
- Step 4 Run the initial scan (emission, excitation, or lifetime). For emission scans, enter the values from Table 20 into the Emission Acquisition dialog screen (see Figure 77 below).

Phosphorimeter Emission Acquisition

Experiment... c:\datamax\uo3m.exp DataFile... t:\amax\data\uo3m1223c.spc Run

Scan Start(nm) 470.000 Scan End(nm) 600.000 Auto Save Exp ☐ Save

Increment(nm) 1.0000

Excitation(nm) 425.000 Cancel

Number of Scans 1 Exp Type...

Signals... S/its... HV (on)

Phosphorimeter

Sample Window (ms) 3.000 Delay After Flash (ms) 0.100 Time Per Flash (ms) 40.00 Num Flashes 100

Sample and Real Time Processing Info

lamp corr FF scan of T101G; 70C and 760 torr O2 t=24hr (1600)

Setup File... Dark Offset ☐ Points: 131.

Correction... Blank... Shutter...

Start Time ☐ Immediate ☒ Delay Hr Min

Figure 77. DataMax phosphorimeter emission acquisition dialog screen.

Table 21. Parameters for uranium oxide photoluminescence measurements.

Parameter	Emission Scan	Excitation Scan	Lifetime Scan
Emission monochromator	470 to 600 nm	514 nm	514 nm
Emission monochromator increment	1 nm	N/A	N/A
Excitation monochromator	425 nm	400 to 480 nm	421 nm
Excitation monochromator increment	N/A	1 nm	N/A
Sample window	3 msec	3 msec	3 msec
Delay time	0.10 msec	0.10 msec	0.10 msec
Delay time increment	N/A	N/A	0.05 msec
Time per flash	40 msec	40 msec	40 msec
Number of flashes per data point	500	100	100
Signal	Sc	Sc	Sc
Excitation slit widths	14.7 mm	14.7 mm	14.7 mm
Emission slit widths	14.7 mm	14.7 mm	14.7 mm
PMT cooling temp	10 °C	10 °C	10 °C
Number of flashes per scan	65,500	8100	5800
Est. time for scan	45 min	9 min	5 min

- Step 5 For the oxidation experiments, introduce the desired partial pressure of oxygen into the Hansen cell following the procedures in Appendix D.
- Step 6 Take a spectra once the partial pressure is set (initial scan) and a spectra after the oxidation time is complete (final scan).
- Step 7 Return the Hansen cell to the glove box and repeat the process for the next sample. Remember to turn over the “RADIOACTIVE MATERIALS PRESENT” sign when the Hansen cell is not in the sample chamber. If no other sources are in the room, change the signs of the lab door as well.

Appendix H. Procedures for Introducing Water Vapor

Water vapor was used in conjunction with research grade oxygen in this experiment to simulate the natural atmosphere found in the environment, only for this research, under strict control and at known quantities. The figure below shows the equipment used for this portion of the experiment. Distilled water measured at 18 M Ω -cm was used to minimize contamination to the uranium oxide samples and the weathering system.



Figure 78. Apparatus used to introduce water vapor into the weathering system.

This appendix contains the methods used to introduce water vapor into the weathering system used in this research. These procedures allowed me to expose the uranium oxide samples to known quantities of oxygen pressure at known values for relative humidity.

- Step 1 Clean flask, stopper, petcock valve, tubing, and connectors in methanol. Allow items to dry in the nitrogen purged glove box for a minimum of two hours. This is done to prevent other compounds or complexes from adsorbing on the equipment surfaces prior to use.
- Step 2 Install the petcock valve and seal the valve (clockwise to tighten, counter-clockwise to loosen). Introduce distilled water into the flask and seal with the stopper. Connect the tubing to the petcock valve.
- Step 3 Place the flask of distilled water over the hot-plate and heat the water to approximately 70° C. Connect the tubing to the roughing pump used for the glove box (a special fitting is used to connect the flask to the vacuum pump).
- Step 4 After heating the water to 70° C, turn on the vacuum pump and then open the petcock valve to expose the heated water to the reduced pressure. The reduced pressure will cause the heated water to boil. Allow the water to boil at this pressure for one minute.
- Step 5 Repeat Step 4, two more times. This should effectively remove all but the smallest fraction of other gases present in the flask, leaving only pure water vapor.
- Step 6 Remove the flask from the hot-plate and allow to cool for approximately 30-minutes.
- Step 7 Disconnect the flask tubing from the vacuum pump and seal the tube with a cleaned stopper. Move flask to the weathering system and remove the

temporary stopper. Connect the flask tubing to valve #2 of the weathering system.

- Step 8 Apply 70° C from the hot-plate to the flask of distilled water as shown in the diagram. This is done to increase the water vapor pressure in the flask prior to introducing it into the weathering system.
- Step 9 Allow the water vapor system to stabilize at these conditions for 20-minutes. While this is happening, the weathering system needs to be evacuated to below 1.0×10^{-3} torr following the procedures outlined in Appendix D.
- Step 10 Turn on the MKS Baratron Pressure instrument and allow to warm up. The MKS Baratron was used for all high-pressure readings conducted during this research.
- Step 11 Open the flask petcock valve, allowing water vapor to fill the tubing then open Valve #2 as shown in the weathering system schematic shown in Appendix D. This will introduce the high-pressure water vapor into the low pressure weathering system. Once the desired water vapor pressure has been introduced, as measured with the MKS Baratron, close Valve #2 and close the flask petcock valve. Turn off hot-plate.
- Step 12 If continuous water vapor is desired to circulate throughout the weathering system, leave Valve #2 and the flask petcock valves open and leave the temperature of the hot-plate at 70° C.

Appendix I. Procedures for Surface Analysis Measurements

This appendix contains the steps, procedures, and settings used to collect the uranium oxide particle surface analysis measurements using the NOVA-1000 High Speed Gas Sorption Analyzer (see Figure 79 below) used in this research. The complete operating instructions are contained in the Owners/Operators Manual. The NOVA-1000 was in storage for approximately seven years. Before using the equipment for surface analysis measurements, a complete calibration was conducted.

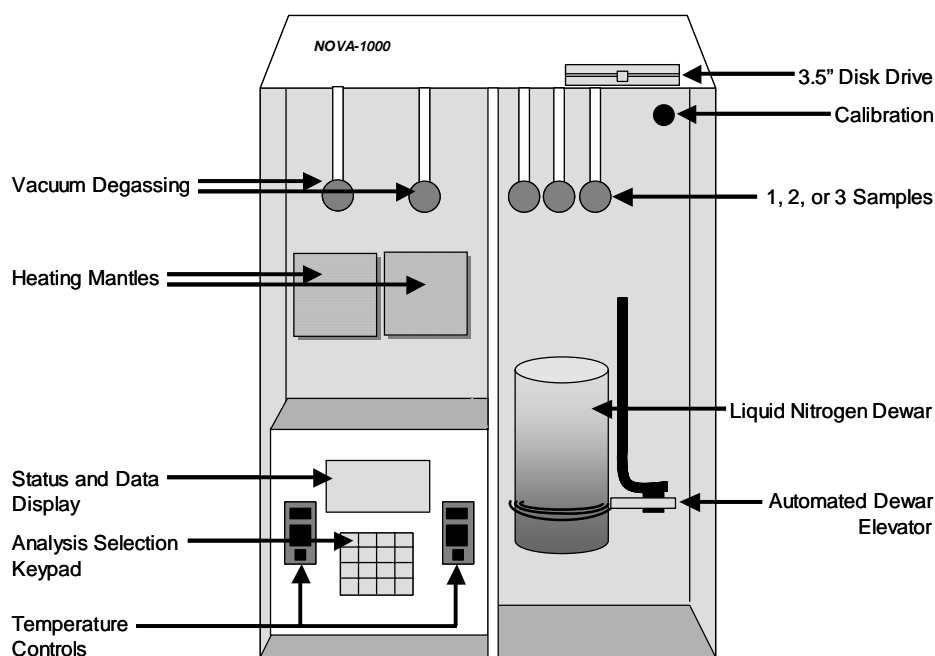


Figure 79. Schematic of NOVA-1000, High Speed Gas Sorption Analyzer.

Note: The NOVA-1000 will not operate without the system disk installed.

The NOVA-1000 is very sensitive. Clean the sample cell and filler rod thoroughly with methanol prior to use.

I-1. Calibration

- Step 1 Disconnect ultra-high purity (UHP) nitrogen from the quick disconnect device located in the rear of the device.
- Step 2 Connect the NOVA-1000 to the vacuum pump and turn on.
- Step 3 Turn on the NOVA-1000. Press <0> to get to the Main Menu.
- Step 4 Select <6>, Options and then select <6>, Purge to purge the system after initial start-up. Follow instructions on screen.
- Step 5 After purge is complete, re-connect N₂ gas line and press <0> to return to the main menu.
- Step 6 Select <3>, Outgas Station to outgas the sample cell prior to use.
- Step 7 Select <1>, Load Outgasser and then select <1>, Vacuum Outgas, follow screen.
- Step 8 Place a sample cell (size 12 mm was used in this research) in the outgas station and outgas at 300°C for five minutes. Remove plastic filler tube before heating.
- Step 9 Select <2>, Unload Outgasser and follow instructions on screen. Turn off heating mantle. Press <0> to return to the Main Menu.
- Step 10 Select <5>, Calibration, then <2>, Manifold to begin calibration of the system.
- Step 11 Follow instructions on screen. The manifold volume will be displayed. The operator can <0>, Abort, <1>, Accept, <2>, Retry, or <3>, Enter.
- Step 12 Select <5>, Calibration, then <1>, Sample Cell to calibrate the sample cell.
- Step 13 Enter a Sample Cell Number. Record.
- Step 14 Replace plastic filler rod and place sample cell in Analysis Station 1. Fill dewar with liquid nitrogen.

Step 15 Select <2>, Full Calibration. Follow instructions on screen. Calibration data will be stored on the 3.5" disk.

I-2. Analysis Set-up

An analysis must be set-up and stored before a sample can be tested.

Step 1 From the Main Menu, select <1>, Analysis Set-up. Now select <1>, Adsorption for particle size measurement.

Step 2 From the BET Set-up window; for a linear spread enter 0.0386, 2×0.0386, 3×0.0386 ... 25×0.0386. Press <0> to exit the BET Set-up page.

Step 3 From the Adsorption Set-up window, select <99> for a linear spread.

Step 4 Enter an Equilibrium Tolerance of 0.1.

Step 5 Enter an Equilibrium Time Tolerance of 60.

Step 6 Enter a Maximum Equilibrium Dwell Time of 120. After these parameters have been set, you will be returned back to the Analysis Set-up Window. Press <0> to return to the Main Menu.

Introduce the sample cell without filler rod into the Glove Box in accordance with Appendix B. Weigh the sample cell empty. Fill the sample cell approximately 3/4 full of uranium oxide and weigh again. Record the sample weight in your lab notebook. Ensure your face-mask is in place when handling loose uranium oxide powder. Cover the sample cell with X-Ray Mylar and secure for removal from the Glove Box. When the

sample cell with uranium oxide is in the NOVA-1000, hang a sign that states “RADIOACTIVE MATERIAL PRESENT” and close the lab. Outgas the sample cell with uranium oxide as described above. Replace the filler rod in the sample cell and place it in Analysis Station 1.

I-3. Sample Analysis

A sample cannot be analyzed until a sample cell set and an analysis set-up have been defined.

Step 1 From the Main Menu, select <2>, Analyze Sample. The system will prompt the user to place the sample cell in the analysis station. Ensure the liquid N₂ level is topped off. Follow instruction on the screen.

Step 2 Enter the sample weight in grams.

Step 3 Enter the density of the material or press <0> and the NOVA-1000 will calculate the density. The dewar flask will raise and cover the sample cell.

Step 4 The system will begin taking data points. The measurement process will take from 45-minutes to an hour to complete.

Step 5 The results of the 25-Point BET Measurement will be displayed on the screen and all the data will also be saved on the 3.5” disk.

Step 6 Take the disk from the NOVA-1000 and place it in the Computer. Open the NOVA Data Reduction Program (DRP) by double-clicking its icon on the

desktop. From the File Menu, select Open, Drive:\A. The file names generated by the NOVA-1000 are discussed below.

I-4. File Names

At the completion of an analysis, the data are stored in an incremented, data coded file in the DATA subdirectory on the user disk. The file name is displayed at the time the file is saved.

An example of how a typical NOVA-1000 data file name is generated is shown below. For example, the data file named N4C3001.DAT was created by the following method:

N represents NOVA

4 represents the year, 4 for 2004, etc.

C represents the month (1–9 for January through September, A–C for October through December)

30 represents the day of the month

01 represents the first analysis of the day

Bibliography

- Allen, Geoffrey C. and Holmes, Nigel R., *Surface Characterization of α -, β -, γ -, and δ - UO_3 Using X-ray Photoelectron Spectroscopy*. Great Britain: Berkeley Nuclear Laboratories, Berkeley, Gloucestershire, 1987.
- Anderson, J.S., Harper, E.A., Moorbath, S., and Roberts, L.E.J., *The Properties and Microstructure of Uranium Dioxide; Their Dependence Upon the Mode of Preparation*. Harwell, UK: Ministry of Supply, 1952.
- Benedict, M., Pigford, T. H., and Levi, H. W., *Nuclear Chemical Engineering* (Second Edition). McGraw-Hill, 1981.
- Blackburn, Paul E., Weissbart, Joseph, and Gulbransen, Earl A., *Oxidation of Uranium Dioxide*, Journal of Physical Chemistry, Vol. 62, pp. 902-908, Aug 1958
- Brown, Theodore L., Lemay, H. Eugene, and Bursten, Bruce, E. *Chemistry, the Central Science* (Seventh Edition). Prentice-Hall, Inc. 1997.
- Colmenares, C., *Oxidation Mechanisms and Catalytic Properties of the Actinides*, Progress in Solid State Chemistry, Vol. 15, pp. 276-364, 1984.
- CRC Handbook of Chemistry and Physics* (61st Edition), Edited by Weast, Robert A., CRC Press, Inc. 1981.
- Guilbault, G. *Practical Fluorescence* (Second Edition). Marcel Dekker, Inc. 1990.
- Hanchar, John M., *Spectroscopic Techniques Applied to Uranium in Metals*, Reviews in Mineralogy, Vol. 38, pp. 499-520, 1999.
- Hoekstra, H.R., Santoro, A., and Siegel, S., *The Low Temperature Oxidation of UO_2 and U_4O_9* . Journal of Inorganic Nuclear Chemistry, Vol. 18, pp. 166-178, 1961.
- Holmes, Nigel Richard, *The Characterisation of Uranium-Oxide Surfaces*. Great Britain: Berkeley Nuclear Laboratories, Berkeley, Gloucestershire, 1998.
- Katz, Joseph J., Seaborg, G.T., and Morss, L.R., *The Chemistry of the Actinide Elements* (Second Edition), Volume 1, Chapman and Hall Ltd, 1986.
- Katz, Joseph J. and Rabinowitch, Eugene. *The Chemistry of Uranium* (Part I). McGraw-Hill Book Company, Inc. 1951.
- Kingery, W., Bowen, H., and Uhlmann, D. *Introduction to Ceramics* (Second Edition). John Wiley and Sons, Inc. 1976.

Knief, Ronald A., *Nuclear Engineering: Theory and Technology of Commercial Nuclear Power* (Second Edition). Taylor and Francis. 1992.

Levine, Ira N. *Physical Chemistry* (Fifth Edition). McGraw-Hill. 2002.

NOVA – 1000, *Gas Sorption Analyzer*, Version 3.10 (Operations Manual). Quantachrome Corporation. 1994.

McEachern, R.J. and Taylor, P., *A Review of the Oxidation of Uranium Dioxide at Temperatures below 400° C*. Journal of Nuclear Materials, Vol. 254. pp. 87-121, 1998.

<http://www.psigate.ac.uk>, Zero-Order Rate Law, Chemistry Gateway, 2005.

Quantachrome Corporation, “NOVA Series”. Technical information provided on Quantachrome website. http://www.quantachrome.com/PDF_Brochures/NOVABro.pdf. Dec 2004.

Rand, Dennis S. *Characterization of Weathering in Uranium Oxide Particles by Raman, Photoluminescence, and Infrared Spectroscopy*. Masters Thesis AFIT/GAP/ENP/99M-08, Air Force Institute of Technology, 1999.

Schueneman, Richard A. *Oxidation at Surfaces of Uranium Oxide Particles*. Masters Thesis AFIT/GNE/ENP/01M-05, Air Force Institute of Technology, 2001.

Schueneman, R. A., Khaskelis, A. I., Eastwood, D., Van Ooij, W. J., Burggraf, L. W. *Uranium Oxide Weathering: Spectroscopy and Kinetics*. Journal of Nuclear Materials 323 (2003) 8-17, Elsevier, B. V., 2003.

Skoog, Douglas A., F. James Holler, and Timothy A. Neiman. *Principles of Instrumental Analysis*. Philadelphia: Harcourt Brace College Publishers, 1998.

Swissa, Eli, Shamir, Noah, Mintz, Moshe H., and Bolch, Joseph. *Heat-Induced Redistribution of Surface Oxide in Uranium*. Journal of Nuclear Materials 173 (1990) 87-97, Elsevier, B. V., 1990.

Taylor, Peter, Lemire, Robert J., and Wood, Donald D., *The Influence of Moisture on Air Oxidation of UO₂: Calculations and Observations*. Nuclear Technology, Vol. 104, pp. 164-170, Nov 1993.

Turner, James E. *Atoms, Radiation, and Radiation Protection* (Second Edition). New York: John Wiley & Sons, Inc., 1995.

Warner, H and Forest, I. *Chemical Thermodynamics of Uranium* (Volume 1). North-Holland Elsevier Science Publishers, 1992.

Watkins, Thayer. "Derivation of Kelvin's Equation". Technical information provided on the 'applet-magic.com', Silicon Valley, website. <http://www.applet-magic.com/Kelvin2.htm>. Dec 2004.

West, Anthony R. *Solid State Chemistry and its Applications*. John Wiley and Sons Ltd. 1984.

Willard, H., Merritt, L., Dean, J., and Settle, F. *Instrumental Methods of Analysis* (7th Edition). Wadsworth Publishing Company, 1988.

Zickafoose, Matthew S. *Analysis of Uranium Oxide Weathering by Molecular Spectroscopy*. Masters Thesis AFIT/GAP/ENG/97D-10, Air Force Institute of Technology, 1997.

REPORT DOCUMENTATION PAGE				Form Approved OMB No. 074-0188	
<p>The public reporting burden for this collection of information is estimated to average 1 hour per response, including the time for reviewing instructions, searching existing data sources, gathering and maintaining the data needed, and completing and reviewing the collection of information. Send comments regarding this burden estimate or any other aspect of the collection of information, including suggestions for reducing this burden to Department of Defense, Washington Headquarters Services, Directorate for Information Operations and Reports (0704-0188), 1215 Jefferson Davis Highway, Suite 1204, Arlington, VA 22202-4302. Respondents should be aware that notwithstanding any other provision of law, no person shall be subject to a penalty for failing to comply with a collection of information if it does not display a currently valid OMB control number.</p> <p>PLEASE DO NOT RETURN YOUR FORM TO THE ABOVE ADDRESS.</p>					
1. REPORT DATE (DD-MM-YYYY) March 2005		2. REPORT TYPE Master's Thesis		3. DATES COVERED (From - To) Jun 2004 - Mar 2005	
4. TITLE AND SUBTITLE SURFACE OXIDATION STUDY OF URANIUM DIOXIDE UNDER WET AND DRY CONDITIONS				5a. CONTRACT NUMBER	
				5b. GRANT NUMBER DEA10702ID1382	
				5c. PROGRAM ELEMENT NUMBER	
6. AUTHOR(S) Brett, Gary T., Major, USA				5d. PROJECT NUMBER	
				5e. TASK NUMBER	
				5f. WORK UNIT NUMBER	
7. PERFORMING ORGANIZATION NAMES(S) AND ADDRESS(S) Air Force Institute of Technology Graduate School of Engineering and Management (AFIT/EN) 2950 Hobson Way, Building 640 WPAFB OH 45433-8865				8. PERFORMING ORGANIZATION REPORT NUMBER AFIT/GNE/ENP/05-01	
9. SPONSORING/MONITORING AGENCY NAME(S) AND ADDRESS(ES) Dr. Kathy McCarthy DOE - NEER Technical Program Manager Idaho National Environmental & Engineering Laboratory PO Box 1625 Idaho Falls, ID 83415-2208				10. SPONSOR/MONITOR'S ACRONYM(S) DOE - NEER	
				11. SPONSOR/MONITOR'S REPORT NUMBER(S)	
12. DISTRIBUTION/AVAILABILITY STATEMENT APPROVED FOR PUBLIC RELEASE; DISTRIBUTION UNLIMITED.					
13. SUPPLEMENTARY NOTES					
14. ABSTRACT <p>The surface oxidation of pressed uranium dioxide (UO₂) powder under controlled environmental conditions and the oxidation and reduction of pressed uranium trioxide (UO₃) powder are presented.</p> <p>This is a continuing research project in the investigation of the oxidation of UO₂ powder using Photoluminescence (PL) Spectroscopy. UO₂ particles exposed to the ambient atmosphere will oxidize into a number of chemical complexes (specifically hydrates, hydroxides, and carbonates). During certain of these oxidation processes, the uranium ion can lose two of its electrons and change from uranous (U^{IV+}) to uranyl (U^{VI+}). This research is an attempt to monitor and control the oxidation of UO₂ as well as the development of the uranyl ion from the uranous ion and model their behavior under both wet and dry atmospheric conditions.</p> <p>Two UO₂ samples were created by pressing UO₂ powder into a tungsten screen and were then subjected to a pure, dry oxygen environment and a wet oxygen environment at temperatures below 200°C. The UO₂ oxidation was periodically monitored with <i>in-situ</i> PL spectroscopy. Using this analysis method, I was not able to successfully distinguish between the different uranium oxide compounds as they were formed under the different weathering conditions enforced at this temperature.</p>					
15. SUBJECT TERMS Uranium Dioxide, Uranium Trioxide, Photoluminescence, Oxidation					
16. SECURITY CLASSIFICATION OF:			17. LIMITATION OF ABSTRACT	18. NUMBER OF PAGES	19a. NAME OF RESPONSIBLE PERSON
a. REPORT	b. ABSTRACT	c. THIS PAGE			Larry W. Burggraf, PhD, ENP
U	U	U	UU	168	19b. TELEPHONE NUMBER (Include area code) (937) 255-6565, ext 4507 (Larry.Burggraf@afit.edu)

